The role of cytotoxic necrotizing factor 1-induced activation of RhoG during uropathogenic *Escherichia coli* infections

DISSERTATION

zur Erlangung der Würde des Doktors
der Naturwissenschaften des Fachbereichs Biologie,
der Fakultät für Mathematik, Informatik und
Naturwissenschaften, der Universität Hamburg

vorgelegt von

KERSTIN LARDONG

Hamburg, Juni 2014

Die vorliegende Arbeit wurde am Institut für Medizinische Mikrobiologie, Virologie und Hygiene am Universitätsklinikum Hamburg-Eppendorf angefertigt.

Gutachter der Dissertation:

1. Gutachter: Prof. Dr. Martin Aepfelbacher
2. Gutachter: PD Dr. Andreas Pommerening-Röser
3. Gutachter: Prof. Dr. Iris Bruchhaus
4. Gutachter: Prof. Dr. Harald Genth

Danksagung

Ich danke Prof. Martin Aepfelbacher, dass ich die Möglichkeit hatte, meine Doktorarbeit in seinem Institut durchführen zu können.

Vielen Dank auch an meine weiteren Gutachter für die Dissertation, Dr. Andreas Pommerening-Röser und Prof. Iris Bruchhaus sowie meiner Prüfungskommission, Prof. Hans-Peter Mühlbach, Prof. Julia Kehr und Prof. Iris Bruchhaus. Besonderen Dank an Dr. Andreas Pommerening-Röser für die Wahrnehmung seiner Funktion als zweiter Betreuer.

Für die Einführung in das Thema, weitere Unterstützung und das Vertrauen in meine wissenschaftliche Arbeit danke ich meiner Betreuerin Dr. Erin Boyle. Vielen Dank für das kritische Korrekturlesen dieser Arbeit.

Außerdem großen Dank an Dr. Fritz Buck für seine Hilfe bei der Massenspektrometrie und seine vielzähligen Erläuterungen und Hilfestellungen bei auftauchenden Fragen.

Der gesamten Arbeitsgruppe Aepfelbacher einen herzlichen Dank für ein angenehmes Arbeitsklima, ihre stetige Hilfsbereitschaft und vor allem für ein humorvolles Miteinander. Ebenfalls danke ich allen anderen Kollegen aus dem Institut, die mich mit fachlichem oder auch mit nicht-fachlichem Rat unterstützt haben während der letzten 3 Jahre.

Ich danke den Organisatoren Dr. Irm Hermanns-Borgmeyer und Dr. Sabine Hoffmeister-Ullerich für ihren Einsatz im Aufbaustudium Molekularbiologie am ZMNH. Außerdem danke ich meinen Mitstreitern für tolle Stunden auch außerhalb der Vorlesungen.

Meine "Grundausbildung" im Labor fand schon viel früher statt, mein Dank geht daher auch an Dr. Uwe Bertsch, Prof. Andreas Winterpacht, Dr. Irm Hermanns-Borgmeyer und Prof. Matthias Kneussel und ihren Mitarbeitern für lehrreiche Zeiten und frühzeitige Förderung.

Ein ganz herzliches Dankeschön an meine Freunde, die mich auf diesem Weg in den letzten Jahren immer großartig unterstützt haben. Nicht zu vergessen sind so viele tolle musikalische Momente, die ohne euch nur halb so schön gewesen wären!

Ein großer Dank geht schließlich an Norman. Danke für viele schöne gemeinsame Jahre und ein großartiges Repertoir an Vertrauen und Unterstützung, das mir vor allem in letzter Zeit eine zuverlässige Hilfe war.

Zusammenfassung

Pathogene Bakterien müssen schützende epitheliale und endotheliale Barrieren überwinden, um in den Wirt einzudringen und eine Infektion hervorrufen zu können. Durch eine Vielzahl von Virulenzfaktoren sind die Erreger in der Lage, die entscheidenden Schritte während der Kolonisation des Wirtes zu bewältigen. Zu diesen Schritten gehören die initiale Adhärenz, die anschließende Aufnahme in die eukaryotische Zelle, die erfolgreiche Unterlaufung der spezifischen Immunabwehr und schließlich die Etablierung einer intrazellulären Nische für die Replikation.

Uropathogene *Escherichia coli* (UPEC), die häufigste Ursache für Harnwegsinfektionen, kodieren eine Vielzahl von Virulenzfaktoren, die den Bakterien das Überleben in den Harnwegen in Gegenwart sehr wirksamer Abwehrmechanismen des Wirts ermöglichen. Dadurch kann der Krankheitsverlauf komplizierter oder chronisch werden. Weiterhin führt diese Persistenz zu intrazellulären Bakterienreservoiren, die eine Ursache von rezidivierenden Infektionen bilden können. Wiederkehrende Harnwegsinfektionen sind antibiotisch therapierbar, allerdings erhöhen sich dadurch die medizinischen Kosten und die Gefahr von Resistenzentwicklung.

Der Virulenzfaktor zytotoxischer nekrotisierender Faktor 1 (CNF1) ist ein Toxin, das von vielen Stämmen der extraintestinalen *E. coli* (ExPEC) exprimiert wird. CNF1 gehört zu einer Gruppe von Toxinen, die die Rho GTPasen des Wirts kovalent modifizieren können. Rho GTPasen sind molekulare Schalter, die an der Regulation zahlreicher zellulärer Prozesse, vor allem an der Umstrukturierung des Aktin-Zytoskeletts, beteiligt sind. CNF1 ist dafür bekannt, die Rho GTPasen Rac1, RhoA und Cdc42 durch Deamidierung des konservierten Glutamins 61/63 zu aktivieren. Die Aktivierung der Rho-Proteine ist nur transient, da die CNF1-modifizierten Proteine Ubiquitin-Proteasom-abhängig degradiert werden. Durch die Expression von CNF1 wird vor allem die Internalisierung der Pathogene erhöht und häufig werden auch wirtsspezifische Immunantworten zu Gunsten des Erregers reguliert.

In dieser Arbeit wurde gezeigt, dass auch die Rho GTPase RhoG durch CNF1 aktiviert und im Anschluss degradiert wird. Die Intoxikation mit dem eng verwandten Toxin CNFy von *Yersinia pseudotuberculosis* führte hingegen nicht zur Aktivierung von RhoG. Mittels Massenspektrometrie konnte außerdem gezeigt werden, dass CNF1 das konservierte Glutamin an Position 61 von RhoG deamidiert. Weitere Untersuchungen zur Identifizierung einer funktionellen Rolle für CNF1-aktiviertes RhoG während der UPEC Infektion ergaben, dass RhoG keine Rolle in CNF1-induzierten proinflammatorischen Signalwegen spielt. Jedoch konnte festgestellt werden, dass CNF1-aktiviertes RhoG eine funktionelle Rolle als negativer Regulator der Rac1-vermittelten Invasion von UPEC hat. Aufgrund der Rac1-Abhängigkeit der zellulären Aufnahme von UPEC wurden mögliche Interaktionen zwischen RhoG und Rac1 untersucht. Jedoch zeigte RhoG weder auf die Aktivierung, subzelluläre Lokalisation noch auf die Degradation von Rac1 einen negativen Effekt. Zusammenfassend wurde RhoG als neues Substrat von CNF1 identifiziert und eine regulatorische Funktion von CNF1-aktiviertem RhoG in der bakteriellen Invasion gefunden.

Abstract

Virulence factors enable the pathogen to overcome host barriers, facilitating many steps during the infection process, ranging from adherence, uptake into host cells, and evasion from the immune system to finally establishing a niche for replication. Uropathogenic *Escherichia coli* (UPEC) encode a variety of virulence factors allowing the bacteria to persist in the urinary tract in the face of host defenses. In addition to antibiotic resistance mechanisms, many UPEC virulence factors make infections refractory to medical treatment. Therefore, it is of great interest to understand underlying pathogenic mechanisms of UPEC infections.

The virulence factor cytotoxic necrotizing factor 1 (CNF1) is a toxin expressed by many extraintestinal pathogenic *E. coli* (ExPEC) strains. It belongs to a group of toxins that manipulate several host functions by covalent modification of Rho GTPases. Rho GTPases are molecular switches that regulate many important cellular processes, most prominent of which are the rearrangements of the actin cytoskeleton. Through its ability to modulate Rho GTPases, CNF1 facilitates bacterial internalization and is implicated in regulation of host immune responses. CNF1 has previously been shown to activate the Rho GTPases Rac1, RhoA and Cdc42 by deamidation of the conserved glutamine 61/63. The abundance of activated Rho GTPases is subsequently attenuated by ubiquitin-mediated proteasomal degradation.

This study demonstrates that the less studied Rho GTPase RhoG is strongly, but transiently activated upon intoxication with CNF1 but not upon intoxication with the closely related CNFy toxin from *Yersinia pseudotuberculosis*. Using mass spectrometry, it was shown that CNF1 deamidates glutamine at position 61 of RhoG. Investigation of the functional role of CNF1-activated RhoG during UPEC infection revealed that RhoG is not responsible for the induction of CNF1-induced proinflammatory signaling pathways. Instead, RhoG was found to be strongly recruited to sites of UPEC infection where it had an inhibitory effect on invasion. Invasion of UPEC is primarily Rac1-dependent, and therefore, possible crosstalk between RhoG and Rac1 was explored. However, CNF1-activated RhoG did not reduce Rac1 activation or change the subcellular localization of Rac1 or the rate of Rac1 degradation.

In conclusion, these data demonstrate that RhoG is a novel target of CNF1 and implicate CNF1-induced activation of RhoG in bacterial invasion. This study enhances our understanding of host-pathogen interactions during UPEC infection as well as sheds light on the dynamic crosstalk between Rho GTPases.

Table of contents

List of figures

List of tables

List of abbreviations

α	alpha, anti
Abi-1	Abelson interactor protein 1
ADP	adenosine diphosphate
ANOVA	analysis of variance
AP-1	activator-protein 1
APS	ammonium persulfate
Arp2/3	actin-related protein 2/3
β	beta
Bcl-2	B-cell lymphoma 2
BSA	bovine serum albumin
°C	degree Celsius
CA	constitutively active
Cdc42	cell division cycle 42 GTP binding protein
CGT	*Clostridium* glycosylating toxin
cm	centimeter
cm^2	square centimeter
cAMP	cyclic adenosine monophosphate
CEACAM	carcinoembryonic antigen-related cell adhesion molecule
CFU	colony forming units
CNF	cytotoxic necrotizing factor
CR3	complement receptor 3
CRIB	Cdc42/Rac interactive binding
Da	Dalton
DAPI	4',6-diamidino-2-phenylindole
dd	double distilled
DMEM	Dulbecco's Modified Eagle's Medium
DMSO	dimethyl sulfoxide
DN	dominant negative
DNA	deoxyribonucleic acid
Dnt	dermonecrotizing toxin
Dock180	Dedicator of cytokinesis 180
DTT	dithiothreitol
EDTA	ethylenediamine tetraacetic acid
EGFP	enhanced green fluorescent protein
EGFR	epidermal growth factor receptor
EIC	extracted ion chromatogram
ELISA	Enzyme-linked immunosorbent assay
ELMO	Engulfment and Cell Motility
et al.	and others (et alii)
ER	endoplasmic reticulum
ExPEC	extraintestinal pathogenic E. coli
F-actin	filamentous actin
FAK	focal adhesion kinase
FBS	fetal bovine serum
fil	filopodia
FRET	Fluorescence resonance energy transfer
γ	gamma
g	gram
g	relative centrifugal force
G-actin	globular actin
GAP	GTPase activating protein
GDP	guanine diphosphate
GDI	guanine nucleotide dissociation inhibitors
GEF	guanine nucleotide exchange factor
GFP	green fluorescent protein
Gln	glutamine
GPI	glycophosphatidylinositol
GST	glutathione-S-transferase
GTP	guanine triphosphate
h, hrs	hour, hours
H_2O	water
HA	hemagglutinin
HACE1	HECT domain and ankyrin repeat-containing E3 ligase 1
HECT	homologous to the E6-AP carboxyl terminus
HeLa	cervix carcinoma cell line, isolated from Henrietta Lacks
HEPES	(4-(2-hydroxyethyl-)piperazine-1-ethanesulfonic acid
HGF	hepatocyte growth factor
HPLC	high-performance liquid chromatography
HRP	horseradish peroxidase
HSPC	hematopoietic stem progenitor cell 300
HSPG	heparansulfate proteoglycan
IBC	intracellular bacterial communities
IbpA	immunoglobulin-binding protein A
ICAM	intercellular adhesion molecule
IF	immunofluorescence
IFN	interferon
Ig	immunoglobulin
IL	interleukin
IPEC	intestinal pathogenic *E. coli*
Ipg	invasion plasmid gene
IPTG	isopropyl β-D-1-thiogalactopyranoside
IRSp5	insulin receptor tyrosine kinase substrate
JNK	cJun N-terminal kinase
kDa	kilo Dalton
kV	kilo volt
l	liter
lam	lamellipodia
LB	Luria-Bertani
LC	liquid chromatography
LMK	LIM kinases
LPA	Lysophosphatidic acid
LPS	lipopolysaccharide

M	molar
m^2	squaremeter
mA	milliampere
mant	*N*-methylanthraniloyl
MAP	mitogen-activated protein
mDia	mammalian homologue of the *Drosophila* gene diaphanous
MS	mass spectrometry
m/z	mass/charge
µg	microgram
mg	milligram
min	minute
µl	microliter
ml	milliliter
MLC	myosin light chain II
MLCP	myosin light chain phosphatase
µm	micrometer
µM	micromolar
mM	millimolar
MOI	multiplicity of infection
MOPS	3-(N-morpholino) propanesulfonic acid
mruf	membrane ruffles
ms	millisecond
MTOC	microtubule organization center
n	number
NADPH	nicotinamide adenine dinucleotide phosphate
Nap1	Nck-associated protein 1
NF-κB	nuclear factor 'kappa-light-chain-enhancer' of activated B-cells
ng	nanogram
NGS	normal goat serum
NPF	nucleation promoting factor
ns	not significant
nt	non-targeting
N-WASP	Neural Wiskott-Aldrich Syndrome Protein
OD	optical density
OMV	outer membrane vesicles
O/N	overnight
p	plasmide, probability
PAGE	polyacrylamide gel electrophoresis
PAI	pathogenicity island
PAK	p21-activated kinase
PAMP	pathogen-associated molecular pattern
PBS	phosphate buffered saline
p-cJun	phosphorylated cJun
PD	pulldown
PFA	paraformaldehyde
PI3K	phosphoinositide 3-kinase
PIP	phosphotidylinositides
PKA	protein kinase
PLEKHG6	pleckstrin homology domain containing family G member 6
PMN	polymorphonuclear leukocyte
PMSF	phenylmethanosulfonylfluoride
PVDF	polyvinylidede fluoride
QIR	quiescent intracellular reservoir
Rac	Ras-related C3 botulinum toxin substrate
RCB	Rac binding motive
RNA	ribonucleic acid
rpm	rounds per minute
Rho	Ras homolog gene family
RING	really interesting new gene
ROCK	Rho-associated protein kinase
ROS	reactive oxygen species
RT	room temperature
s/sec	second
SAPK	stress-activated kinase
SDS	sodium dodecylsulfate
SEM	standard error of the mean
SGEF	Src homology 3-containing guanine nucleotide exchange factor
SH3	Src homology domain 3
siRNA	small interfering RNA
SILAC	stable isotope labeling by amino acids in cell culture
Smurf	SMAD specific E3 ubiquitin protein ligase
Sop	*Salmonella* outer protein
Sra1	specifically Rac-associated protein 1
strf	stress fibers
SUMO	small ubiquitin-like modifier
TAE	Tris-acetate-EDTA
TBS	Tris buffered saline
TEMED	N,N,N',N'-tetramethylethylenediamine
THP	Tamm-Horsfall protein
TLR	Toll-like receptor
TMB	tetramethylbenzidine
TNFα	tumor necrosis factor α
TrioD1	Trio NH_2-terminal exchange domain
Tris	Tris-(hydroxymethyl)-aminomethane
UP1a	uroplakin 1a
UPEC	uropathogenic *E. coli*
UTI	urinary tract infections
V	volt
Vop	*Vibrio* outer protein
v/v	volume/volume
WASP	Wiskott-Aldrich syndrome protein
WAVE	WASP family Verprolin-homologous protein
WB	Western blot
WCL	whole cell lysate
WRC	WAVE reaction complex
w/v	weight/volume
Yop	*Yersinia* outer protein

1 Introduction

1.1 The host's actin cytoskeleton: structure and function

The actin cytoskeleton is a dynamic network that is essential for cell shape, cell-cell interactions and such cellular processes as movement, endocytosis, exocytosis, phagocytosis, and cytokinesis. Additionally, the cytoskeleton forms an association between the cellular periphery and the cytoplasm, which is constructed on the one hand by several membrane proteins (e.g. integrins, adhesins) and actin-associated proteins (e.g. talin, vinculin, actinin) on the other hand, converting extracellular signals into cytoskeletal changes (de Curtis and Meldolesi, 2012). These functions require a constant process of assembly and disassembly of actin filaments in order to react to different cellular stimuli. Under physiological conditions, actin filaments underlie a steady-state control during the assembly process. In the cytosol, actin exists in two different forms. Monomeric globular (G-) actin is polymerized to filamentous (F-) actin. G-actin monomers are preferentially added to a filament's fast-growing (+)-end - called the barbed end - and simultaneously, F-actin monomers disassemble at the slow-growing (-)-end, the pointed end. This process of actin filament formation is known as "treadmilling" (Carlier, 1998). Spontaneous actin polymerization is a slow process and rather requires nucleation factors such as actin-related protein (Arp) 2/3 complex and formins. Activation of the Arp2/3 complex is indirectly mediated via nucleation promoting factors (NPFs) such as Wiskott-Aldrich syndrome protein (WASP) and WASP family Verprolin-homologous protein (WAVE) (Millard et al., 2004). Actin-binding proteins like profilin and cofilin further control assembly and disassembly, respectively (Mazur et al., 2010).

The most prominent changes in cell shape driven by the actin cytoskeleton are stress fibers, lamellipodia and filopodia (Figure 1.1).

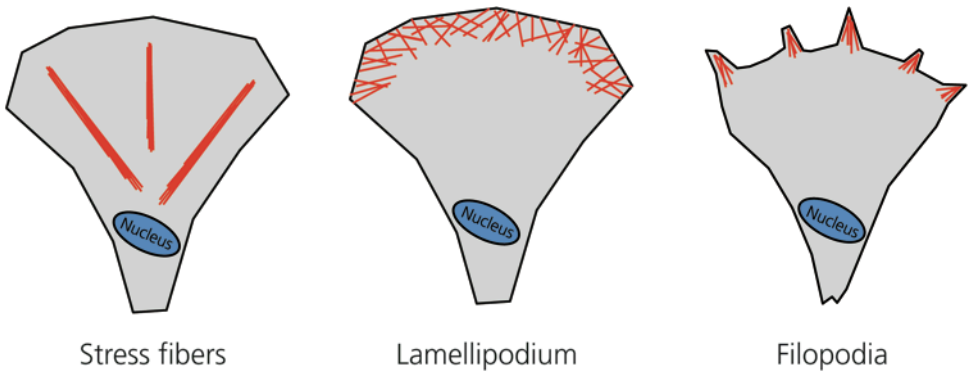

Figure 1.1: Distribution of actin structures within a cell.

Stress fibers are thick, parallel bundles composed of actin and myosin that give the cell its contractibility. At the leading edge of a cell, a thin membrane sheet built up by a branched actin network called a lamellipodium plays a crucial role in cell motility. Filopodia are thin, rod-shaped membrane protrusions that sense the extracellular environment.

Stress fibers are composed of parallel actomyosin bundles and serve as the major contractile structures within a cell, where they are involved in adhesion, motility and morphogenesis. Around 10 – 30 actin filaments form a bundle and are cross-linked by α-actinin. Additionally, stress fibers are often associated with focal adhesions, protein assemblies that connect the cytoskeleton to the extracellular matrix (Pellegrin and Meller, 2007; Naumanen et al., 2008).

Lamellipodia are thin membrane sheets built up of a branched network of actin filaments at the leading edge of motile cells. These structures display a high motility due to a dynamic actin turnover. Thus, broad membrane protrusions are promoted in a process known as ruffling. Lamellipodia have functions in migration, exocytosis and chemotaxis (Small et al., 2002).

Filopodia are thin, rod-shaped plasma membrane protrusions composed of linear actin filaments bundled by actin-binding proteins (e.g. fascin, fimbrin). They are often located beyond the leading edge of a lamellipodium. However, it remains unclear whether they necessarily require the presence of a lamellipodium. Cells sense their environment through filopodia, and thus these actin structures are implicated in migration, neurite outgrowth and wound healing (Rottner and Stradal, 2011; Mattila and Lappalainen, 2008; Hanein et al., 1997).

1.1.1 Rho GTPases: master regulators of the actin cytoskeleton

GTPases are hydrolase enzymes that cycle between an active and an inactive state depending on their binding or hydrolysis of guanosine triphosphate (GTP). They control various cellular processes including signal transduction, cytoskeletal organization and intracellular trafficking (Bourne et al., 1990). Small GTPases - also called Ras superfamily of GTPases – can be further divided into 5 subfamilies, namely Ras, Rho, Rab, Arf and Ran. The family of Rho (Ras homologous) GTPases contains 26 proteins (20 - 40 kDa) and is further classified into 6 subfamilies according to their homology at the amino acid sequence: Rho, Rac, Cdc42, Rnd, RhoBTB and RhoT/Miro (Wennerberg et al., 2005). Rho GTPases differ from other small GTPases by the presence of a Rho-specific insert domain (Valencia et al., 1991). Common to all Rho proteins is the possession of a N-terminal, highly conserved domain for GTP/GDP (guanosine diphosphate) binding, named the G-domain, reflecting their function as "molecular switches"- being active when GTP-bound and inactive when GDP-bound (Figure 1.2A). The transition between activation and inactivation is based on a conformational change in two regions of the G-domain named switch I and switch II (Figure 1.2B). The switch regions are located in the nucleotide-binding pocket and are the sites of selective interaction with downstream effector proteins. Upon binding to GTP, the structure of the G-domain changes, thus providing access for effector proteins to bind and consequently initiate divers signaling pathways (Vetter and Wittinghofer, 2001).

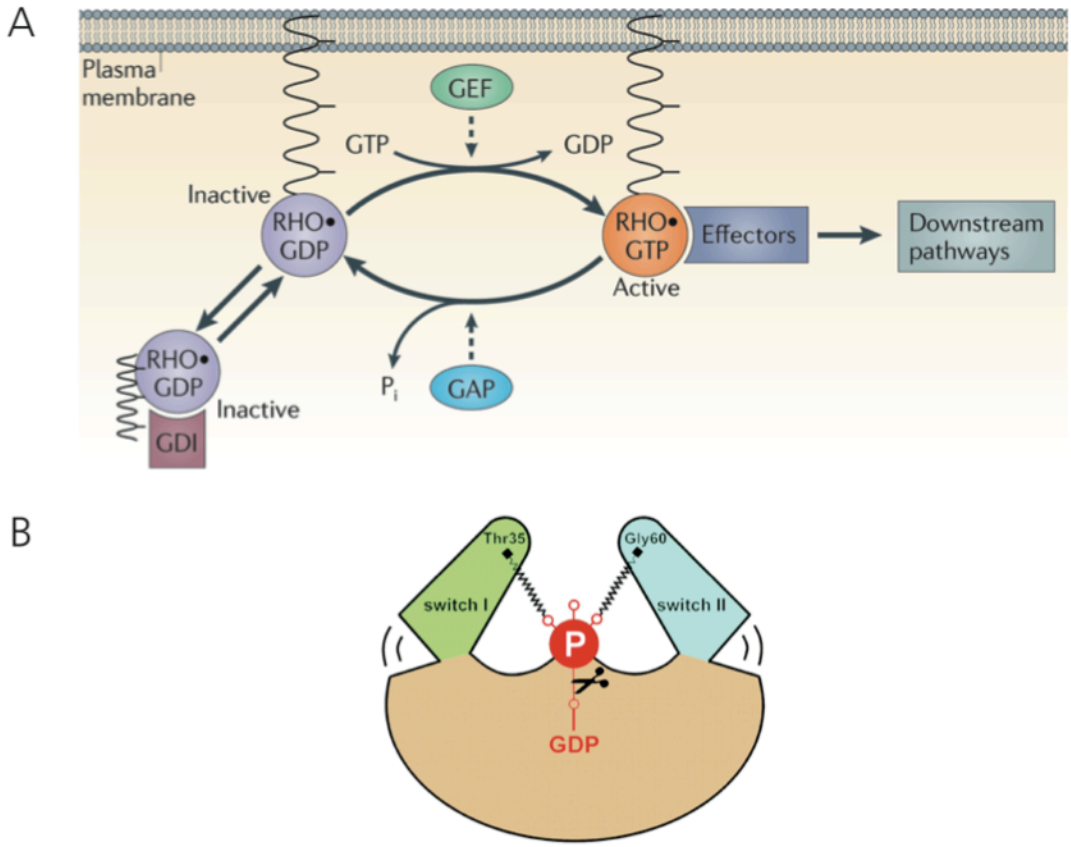

Figure 1.2: Molecular switch of Rho GTPases.

(A) Rho GTPases cycle between an inactive, GDP-bound and an active, GTP-bound state. The switch is mainly regulated by guanine exchange factors (GEFs), GTPase-activating proteins (GAPs) and guanine dissociation inhibitors (GDIs). By binding to their specific downstream effectors, active Rho GTPases influence various cellular effects (modified from Aktories, 2011). **(B)** Schematic view of the switch mechanism. Switch I and II of the G-domain are bound to the γ–phosphate of GTP. Hydrolysis of GTP brings the switch regions into a relaxed conformation (modified from Vetter and Wittinghofer, 2001).

Different types of proteins regulate the molecular switch. Guanine nucleotide exchange factors (GEFs) catalyze the exchange of GDP for GTP molecules, thus promoting activation, while GTPase-activating proteins (GAPs) stimulate GTP-hydrolysis resulting in inactivation of the Rho GTPase. Another class of regulators is guanine nucleotide dissociation inhibitors (GDIs). Inactive Rho proteins are associated with GDIs, which divert the GDP-bound form to the cytosol to prevent GDP release and to protect them from misfolding or degradation (Garcia-Mata et al., 2011; Hakoshima et al., 2003). In resting cells, Rho GTPases are GDI-bound in their inactive state and localized in the cytosol. Upon stimulation, the GDI is released by different means of dissociation such as phosphorylation, protein-protein interactions or phospholipids (Dovan and Couchman, 2005). The released Rho GTPase binds to the plasma membrane, where it interacts with membrane-associated GEFs that accelerate GTP binding. Due to the conformational change in the switch regions of Rho GTPases, they are transformed into their active form and can interact with specific effectors. The dissociation of the effectors is facilitated by

GTP-hydrolysis promoted by GAPs. Specific Rho GDIs extract inactive Rho proteins from the membrane and return them to the cytosol (Olofsson, 1999).

Notably, there are more than 70 GEFs, 80 GAPs and 3 GDIs identified so far, highlighting the importance of Rho GTPase regulation and suggesting that the same Rho GTPase can be modulated by different GEFs and GAPs (Garcia-Mata and Burridge, 2007).

By binding to their specific downstream effectors, including serine/threonine kinases, lipases, oxidases and scaffold proteins, active Rho GTPases play a role in a variety of cellular processes that are dependent (e.g. cytokinesis, phagocytosis, migration) or independent (e.g. regulation of nuclear factor 'kappa-light-chain-enhancer' of activated B-cells (NF-κB) transcription factor, cJun-N-terminal kinase (JNK) pathway, nicotinamide adenine dinucleotide phosphate (NADPH) oxidase complex, secretion) on the actin cytoskeleton (Bishop and Hall, 2000).

1.1.2 Signaling of Rho GTPases RhoA, Rac1 and Cdc42

RhoA (Ras homolog gene family, member A), Rac1 (Ras-related C3 botulinum toxin substrate 1) and Cdc42 (cell division control protein 42 homolog) are the members of the Rho GTPase family that are most prominent and best studied for their role in regulating the actin cytoskeleton and other cell functions. Many studies employ the use of constitutively active (CA) and dominant negative (DN) mutants as well as modifying toxins to investigate the biological function of Rho GTPases. Substitutions of specific amino acids (valine for glycine 12, leucine for glutamine 61) generate constitutively active mutants by preventing intrinsic and GAP-induced GTP hydrolysis, thus locking the Rho GTPase in an active state. Dominant negative mutants are achieved by substitution of asparagine for threonine17, whereby they then compete with the endogenous GTPase for binding to GEFs. This complex does not generate a functional downstream response (Bishop and Hall, 2000; Feig, 1999).

RhoA activation leads to the assembly of actin stress fibers and focal adhesions mediated by the Rho kinase (ROCK) pathway. This serine/threonine kinase inactivates myosin light chain phosphatase (MLCP) leading to increased phosphorylation of myosin light chain II (MLC). Alternatively, MLC can directly be phosphorylated by ROCK. This promotes the formation of actin bundles by myosin II. ROCK-mediated phosphorylation of LIM kinases (LIMKs) results in phosphorylation of the actin-binding protein cofilin, thereby inhibiting cofilin-mediated actin-disassembly (Riento and Ridley, 2003). Another crucial downstream effector of RhoA is the formin family of proteins that produce straight, unbranched actin filaments, typically evident in actin stress fibers, filopodia or actin cables (Goode and Eck, 2007).

Activation of Rac1 promotes actin polymerization to form lamellipodia and membrane ruffles. By binding to WAVE, Rac1 regulates these actin structures via the Arp2/3 complex. It has been reported that the interaction between Rac1 and WAVE is indirect through binding to the adaptor molecule insulin receptor tyrosine kinase substrate (IRSp5). IRSp5 binds to Rac1 with a N-terminal Rac binding motive (RCB), whereas the C-terminal Src-homology-3 (SH3) domain contacts the polyprolin region of WAVE2 leading to the formation of a trimolecular complex (Miki et al., 2000). However, due to controversial

observations the precise function of IRSp5 in the regulation of actin organization still remains unclear. Another concept regards WAVE proteins as part of a complex containing additionally Nck-associated protein 1 (Nap1), specifically Rac-associated protein 1 (Sra1), Abelson interactor protein 1 (Abi-1) and hematopoietic stem progenitor cell 300 (HSPC300) (Eden et al., 2002). The nature of this complex is stable, but inactive towards Arp2/3 complex, until stimulatory signals lead to its activation (Ismail et al., 2009). The subunit Sra1 binds to Rac1 and this interaction is crucial for the recruitment and activation of the WAVE complex leading to actin polymerization (Stradal and Scita, 2006). Additionally, Rac1 was reported to regulate actin turnover by activation of p21-activated serine/threonine kinase (PAK). PAK activates LIM kinases, thus actin filaments are stabilized as depolymerizing cofilin is inhibited (Jaffe and Hall, 2005; Yang et al., 1998).

Activated Cdc42 stimulates the formation of filopodia. Indeed, several downstream effectors for active Cdc42 have been implicated in filopodia formation. Cdc42 induces actin polymerization via the Arp2/3 complex by binding to WASP or insulin receptor substrate 53 (IRSp53). Additionally, the formin mDia2 (mammalian homologue of the *Drosophila* gene diaphanous) is targeted by Cdc42 and contributes to filopodia assembly (Peng et al., 2003; Disanza et al., 2006).

Figure 1.3 displays changes of actin cytoskeleton induced by RhoA, Rac1 and Cdc42 activation.

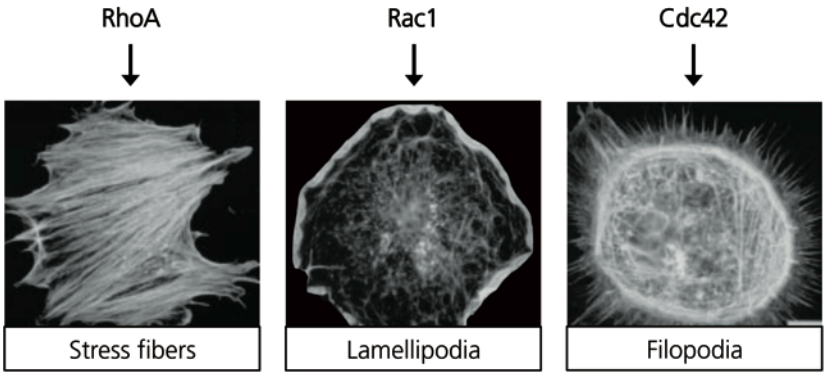

Figure 1.3: Actin phenotypes induced by different Rho GTPases.

Immunofluorescent staining of F-actin reveals morphological changes of the actin cytoskeleton induced upon activation of various Rho GTPases. RhoA induces stress fibers, whereas Rac1 induces lamellipodia and Cdc42 filopodia (modified from A. Hall, 1998).

In addition to their broad actions in actin remodeling, Rho GTPases influence almost all levels of cellular functions. RhoA stimulates downstream signaling pathways affecting endosomal trafficking, cytokinesis and other aspects of cell cycle progression as well as stabilization of microtubules via binding to formins. Rac1 regulates the activation of NADPH oxidase system and production of reactive oxygen species (ROS). Thereby, the activation of NF-κB-dependent gene expression, such as inflammatory cytokines, is mediated. Rac1 is also involved in activator-protein 1 (AP-1) dependent gene expression by stimulating the JNK or p38 mitogen-activated protein (MAP) kinase pathway. Additional

effects of Rac1 are cell cycle progression, migration and cell-cell adhesion. Cdc42 has a crucial role in the establishment and maintenance of cell polarity, regulating microtubule organization centers (MTOCs) and tight junction formation. Other important roles of Cdc42 signaling include vesicle trafficking, gene transcription, T-cell differentiation and apoptosis of immune cells and neuronal cells (Jaffe and Hall, 2005; Schwartz, 2004).

Many cellular functions are orchestrated by interplay of different Rho GTPases and Table 1.1 gives an overview about the variety of Rho GTPase signaling (Jaffe and Hall, 2005).

Table 1.1: Actin-independent functions of Rho GTPases.

Cellular function	Rho GTPase
Microtubule dynamics	RhoA, Rac1, Cdc42
Activation of serum response factor	RhoA
JNK and p38 MAP kinase pathway	RhoA, Rac1, Cdc42
NF-κB pathway	RhoA, Rac1, Cdc42
ROS production	Rac1, Cdc42
Cytokine production	RhoA, Rac1, Cdc42
Lipid metabolism	RhoA, Rac1, Cdc42
Cell cycle	RhoA, Rac1, Cdc42
Cell morphogenesis	RhoA, Rac1, Cdc42
Migration	RhoA, Rac1
Directional sensing	Cdc42

1.1.3 Rho GTPase RhoG

Identified in 1992 during a screen for growth factors, RhoG (Ras homolog gene family, member G, 21 kDa) is a relatively new member of the Rho GTPase family and remains one of the least characterized Rho proteins (Vincent et al., 1992). Ubiquitously expressed, RhoG is most homologous to Rac1 (72 %) and shares overlapping functions with Rac1 due to binding of some common effector proteins (Wennerberg et al., 2002). Knowledge of RhoG upstream and downstream signaling is still lacking with only a few GEFs (Trio NH_2-terminal exchange domain 1 = TrioD1, Src homology 3-containing guanine nucleotide exchange factor = SGEF, members of the Vav family, pleckstrin homology domain containing family G member 6 = PLEKHG6 and kalirin) and no GAPs having been described (Blangy et al., 2000; Ellerbroek et al., 2004). Additionally, only 3 surface receptors were reported to influence RhoG activity upon binding: epidermal growth factor receptor (EGFR), intercellular adhesion molecule 1 (ICAM-1) and syndecan-4 (Samson et al., 2010; van Buul et al., 2007; Elfenbein et al., 2009). With regard to downstream signaling, to date there are only a few effectors identified, including ELMO (Engulfment

and Cell Motility), phosphoinositide 3-kinase (PI3K), phospholipase D1 and kinectin (Katoh et al., 2000; Vignal et al., 2001; Wennerberg et al., 2002; Yamaki et al., 2007).

Although Wennerberg and colleagues reported that Rac1 and RhoG may signal in parallel, another study presented a model in which RhoG acts upstream of Rac1 activation (Wennerberg et al., 2002; Katoh and Negishi, 2003). Activation of Rac1 by RhoG occurs via the ELMO-Dock180 pathway and results in changes in the actin cytoskeleton and other downstream effects like cell proliferation. RhoG interacts with the N-terminus of its specific effector ELMO. Together with the unconventional Rac1-specific GEF Dock180 (dedicator of cytokinesis), they form a ternary complex that is translocated from the cytoplasm to the plasma membrane, where it can activate Rac1 (Katoh and Negishi, 2003). Due to their close structural relationship in the switch regions (switch I 92%, switch II 89,5%) it seems likely that RhoG and Rac1 signal through the same pathways, thus RhoG functions can be explained by activation of Rac1. However, despite their similarity, RhoG also regulates cellular processes independently on Rac1.

RhoG has been shown to be involved in various cellular functions by regulating cytoskeletal reorganization in different cell types, including regulation of neurite outgrowth, migration, membrane ruffling, macropinocytosis and phagocytosis of apoptotic cells (Katoh et al., 2000, Katoh et al., 2006, Gauthier-Rouvier et al., 1998; Ellerbroek et al., 2004; deBakker et al., 2004). However, it still remains controversial whether RhoG-induced effects on the cytoskeleton are dependent on Rac1 (Wennerberg et al., 2002; Meller et al., 2008). In addition, RhoG regulates neutrophil NADPH oxidase, gene transcription, the microtubule system, trans-epithelial migration of lymphocytes, T-cell receptor internalization, and glioblastoma invasion (Condliffe et al., 2006; Murga et al., 2002; Vignal et al., 2001; van Buul et al., 2007; Martinez-Martin et al., 2011; Kwiatkowska et al., 2012).

Rac1-independent signaling was described for neural progenitor cell proliferation, migration, cell survival and aniokis, intracellular vesicle trafficking as well as Fcγ- and complement receptor 3 (CR3)-mediated phagocytosis (Fujimoto et al., 2009; Meller et al., 2008; Yamaki et al., 2007; Prieto-Sanchez et al., 2006; Tzircotis et al., 2011).

Recently, a study reported for the first time that RhoG acts as a negative regulator in neuronal processes. It was found to inhibit axonal branching via the ELMO-Dock180-Rac1 signaling pathway and in turn is regulated by the microRNA miR-124 (Franke et al., 2012).

1.1.4 Alternative and crosstalk regulation of Rho GTPases

The regulation of RhoGTPases cannot totally be explained by the exclusive action of GEFs and GAPs. Indeed, there are alternative mechanisms reported that complement the GEF-/GAP-mediated regulation of Rho proteins including posttranslational modifications, subcellular localization, local degradation and crosstalk between Rho GTPases.

Posttranslational modification of Rho proteins is one of the most common alternative mechanisms of regulation and can be triggered endogenously or stimulated by pathogens during infection (Boquet and Lemichez, 2003). Rho GTPases are isoprenylated at the C-terminus during their postsynthesis maturation leading to the addition of hydrophobic

molecules to the protein. This leads to endoplasmic reticulum (ER) membrane translocation where the Rho GTPase is cleaved and methylated resulting into a fully mature protein. After release into the cytosol, the Rho GTPase can associate with RhoGDIs or be shuttled to cell membranes. Isoprenylation thereby regulates the intracellular localization of Rho proteins, which itself modulates Rho GTPase activation (Boulter et al., 2012). The main dogma is that inactive, GDP-bound Rho proteins rest in the cytosol, while active, GTP-bound Rho GTPases translocate to the plasma membrane. However, it was shown that Rho GTPases do not necessarily need to be membrane bound for biochemical activation, but instead, membrane localization of the activated Rho GTPase is required for appropriate signaling (del Pozo et al., 2004). Additional modifications like polybasic sequences or palmitoyl modifications are required for sufficient recruitment of the Rho proteins to the membrane (Hancock et al., 1990). Another mechanism found to regulate Rho GTPase activation is phosphorylation, although this is only reported for a few Rho proteins, namely RhoA, RhoG and Cdc42. Phosphorylation may be important for association of Rho GTPases with RhoGDIs, thus regulating their localization and activation (Lang et al., 1996). Recently it was shown that the activity of RhoA at the leading edge of migrating cells is controlled by the cyclic adenosine monophosphate (cAMP)-activated protein kinase (PKA). Phosphorylation of RhoA (serine 188) by PKA increased the interaction between RhoA and RhoGDI1, thus RhoA was extracted from the plasma membrane (Tkachenko et al., 2011). Other posttranslational modifications influence the activation of Rho GTPases directly, including redox-mediated oxidation of cysteine residues. This alteration stimulates in some Rho proteins the nucleotide exchange in the absence of GEFs. Stimulated by physiological amounts of oxidative substances like ROS, cysteine 20 can be oxidized as shown for RhoA and Rac1 (Heo and Campbell, 2005). Thereby, the nucleotide-binding pocket changes in conformation and releases the nucleotide. Due to the intrinsically higher cytosolic concentration of GTP than GDP, GTP binds in the pocket, leading to activation of the Rho protein. Recently, Rac1 was reported to be SUMOylated (small ubiquitin-like modifier) upon hepatocyte growth factor (HGF) stimulation (Castillo-Lluva et al., 2010). This modification was found to stabilize Rac1 activation, however the underlying mechanism has not yet been revealed.

Protein expression and stability is another means by which Rho GTPases can be regulated. The expression level of Rho GTPases themselves regulates their activation state. The observation that activated Rho GTPases are regulated by degradation processes was first found in 2001 when ROS was found to trigger Rac1 degradation via the proteasome (Kovacic et al., 2001). Further studies revealed that the bacterial toxin cytotoxic necrotizing factor 1 (CNF1) was able to degrade activated RhoA, Rac1 and Cdc42 (Doye et al., 2002; Lerm et al., 2002). The expression level of Rho GDIs is also a limiting factor that can control the activity of Rho GTPases. Rho GDIs function to stabilize inactive Rho GTPases and protect them from degradation (Boulter et al., 2010). Within a cell the amount of ubiquitous Rho GDI1 is more or less equal to the total amount of Rho GTPases (Michaelson et al., 2001), implicating that Rho GTPases compete for this limiting factor. Thus, an altered RhoGDI1 binding affinity of a Rho GTPase unbalances the resting inactive Rho GTPases and also influences the activation of the displaced Rho GTPase (Boulter et al., 2010, Rolli-Derkinderen et al., 2010).

The complexity of regulation of Rho GTPases becomes even more apparent when one considers the fact that many Rho proteins control several cellular functions in cooperative or antagonistic manners. Ridley and colleagues first reported in 1992 that Rac1 was capable of inducing RhoA-like stress fibers upon stimulation with growth factors, suggesting interaction of Rac1 and RhoA (Ridley et al., 1992). Since then, numerous studies have revealed crosstalk between Rho GTPases occurs at different levels to regulate cellular functions. Most crosstalk regulation is described at the level of GEFs and GAPs, affecting the activation of Rho GTPases. Since many GEFs are able to activate divers Rho GTPases, the possibility that different Rho GTPases are activated in the same pathway is relatively high. But in many pathways the activation of the Rho GTPases is temporally-spatially orchestrated leading to separated activation or inhibition of individual Rho GTPases. Rac1 and RhoA for instance often display a reciprocal balance of their activities, as it was shown that Rac1 decreased RhoA activation, thereby determining cell morphology and migration in mouse embryonic fibroblasts (Sander et al., 1999). Less is known about the crosstalk at the level of downstream signaling. This crosstalk is mediated by the ability of Rho GTPases to share downstream effectors or molecular targets, resulting in coordinate organization of cellular tasks. RhoG, for example, by signaling via ELMO-Dock180 activates Rac1 and thus affects many cell functions due to Rac1 activation. However, despite these Rac1-dependent signaling pathways and sharing of some effectors with Rac1, RhoG can also act without interaction with Rac1 (Wennerberg et al., 2002; Samson et al., 2010).

1.1.5 Modulation of Rho GTPases by pathogens

Due to its importance in the structure and function of a cell, the actin cytoskeleton is also vulnerable, making it a potent target for pathogens that usurp the cytoskeleton for their own benefit. The cytoskeleton is fundamental for establishing and maintaining the barrier function of epithelial and endothelial monolayers, thereby limiting the invasion of pathogens. Pathogens, however, often need to breach barriers within the host in order to cause disease. Thus, pathogens have established many ways to modulate the actin cytoskeleton for their survival and fitness benefit. The production of effector molecules or cytotoxins can either affect the actin cytoskeleton directly as shown for *Clostridium botulinum* toxin C2 (Aktories et al., 1986), but more often Rho GTPases are targeted. Many secreted bacterial effector molecules modulate Rho GTPases by mimicking or inhibiting the action of GEFs or GAPs. On the other hand, released cytotoxins often modify the Rho GTPases covalently, thereby targeting the Rho switch and resulting in changes in signaling pathways of the host. Corresponding to their mode of action towards the targeted protein, those toxins are grouped into inhibitors or activators. The underlying mechanisms for the modifications include adenosine diphosphate (ADP)-ribosylation, glycosylation, adenylation or proteolysis for inhibiting toxins and ADP-ribosylation, deamidation and transglutamination for activating toxins (Figure 1.4, Aktories, 2011).

The C3 toxin from *C. botulinum* was the first toxin identified to modify Rho GTPases (Rubin et al., 1988). Containing ADP-ribosyltransferase activity, it modifies Rho GTPases at asparagine 41 causing tight binding to RhoGDIs and thereby prevents Rho activation by

GEFs. This modification inhibits downstream signaling (Genth et al., 2003; Sehr et al., 1998). Blockade of downstream signaling is also achieved by glycosylation. *Clostridium* glycosylating toxins (CGTs) form a large group of Rho GTPase inhibiting toxins, with the most prominent members being *C. difficile* toxins A and B. Glycosylation of conserved threonine residues leads to the inability of GTPases to be activated by GEFs and to bind GAPs, thus the GTPases do not switch into their activated conformation and downstream signaling is prevented (Sehr et al., 1998; Just et al., 1995; Genth et al., 1999). The same effect is achieved by adenylylation, a modification used by *Vibrio parahaemolyticus* outer protein S (VopS) or *Histophilus somni* immunoglobulin-binding protein A (IbpA). Toxins from *Yersinia* spp. and *Photorhabdus luminescence*, *Yersinia* outer protein T (YopT) and LopT (YopT-like from *P. luminescence*), respectively, are cysteine proteases that target the isoprenylated cysteine at the C-terminus of the Rho GTPase, releasing the protein from the membrane inactivated (Yarbrough et al., 2009; Worby et al., 2009).

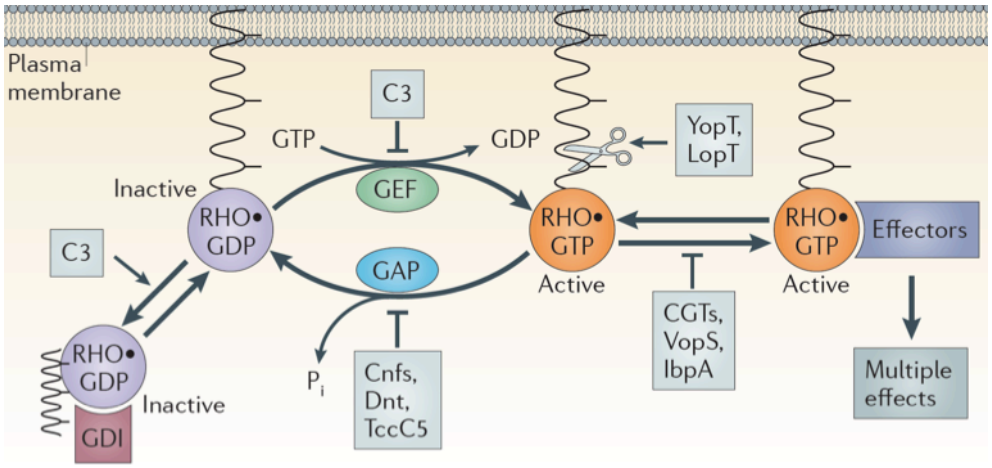

Figure 1.4: Modifications of Rho GTPases by bacterial toxins.

Bacterial toxins modify Rho GTPases covalently at various steps of the Rho switch. Inhibition of Rho GTPases is caused by ADP-ribosylation by C3 toxin from *Clostridium botulinum*. Other toxins like YopT from *Yersinia* spp. and LopT from *Photorhabdus luminescens* act as proteases and thus lead to inactivation. Glycosylation by *Clostridium* glycosylating toxins (CGTs) and adenylylation by VopS *Vibrio parahaemolyticus* from or IbpA from *Histophilus somni* result in the inability of Rho proteins to interact with their effectors. Toxins that activate Rho GTPases are cytotoxic necrotizing factors (CNFs) from *E. coli* and dermonecrotizing toxins (Dnts) from *Bordetella* spp. They cause deamidation and transglutamination. The TccC5 toxin from *P. luminescens* activates Rho GTPases by the attachment of an ADP-ribosyl moiety (Modified from Aktories, 2011).

Very few bacterial toxins modify Rho GTPases by activation. ADP-ribosylation of glutamine 61/63 by toxin TccC5 from *P. luminescence* leads to activation of Rho GTPases by blocking the intrinsic and the GAP-induced GTP hydrolysis, thereby causing permanent activation (Scheffzek et al., 1998). The same residue is modified for Rho activation through transglutamination or deamidation by *Bordetella parapertussis* and *B. bronchoseptica* dermonecrotizing toxins (Dnts) and *Escherichia coli* and *Y. pseudotuberculosis* cytotoxic necrotizing factors (CNFs). Dnt and CNFs are related and share 30 % homology at the C-terminal catalytic domain. Dnt acts as transglutaminase and deamidase at glutamine 61/63, whereas CNFs preferentially deamidate glutamine 61/63 (Masuda et al., 2000). Deamidation of glutamine 61/63 results into an amino acid change to glutamic acid,

which blocks GTP hydrolysis, locking the Rho GTPase in their activated state (Flatau et al., 1997).

1.1.6 RhoG and its role during infection

Recent research has shown that several pathogens modulate or mimic RhoG activity as a means of promoting internalization into non-phagocytic host cells or subverting the host immune response. For example, *Salmonella enterica* uses a set of bacterial effector proteins secreted into the host cytosol to usurp host Rho GTPases. The effector *Salmonella* outer protein B (SopB) is a phosphoinositide phosphatase that indirectly activates RhoG via its GEF SGEF, thereby inducing cytoskeletal rearrangements that lead to *Salmonella* invasion (Patel and Galan, 2006).

The effector protein IpgB1 (invasion plasmid gene) delivered into the host cytosol by *Shigella* binds to ELMO and thereby directly activates the ELMO-Dock180 pathway to induce Rac1 activation. In this case, IpgB1 mimics the role of RhoG, thereby promoting membrane ruffling and subsequent bacterial invasion (Handa et al., 2007).

Another mode of RhoG modulation by a pathogen was reported for *Y. enterocolitica*. In order to invade the cell, RhoG is activated upon invasin-mediated integrin binding leading to Rac1 activation via the ELMO-Dock180 pathway. In a later phase of infection, injected effector protein YopE acts as a Rho GAP resulting into inactivation of RhoG and Rac1 (Roppenser at al., 2009).

YopE effector produced by *Y. pseudotuberculosis* also targets RhoG. In addition to the GAP-function of YopE, another effector, YopT, is secreted to modulate RhoG. Acting as a protease, YopT cleaves and mislocates RhoG, which may function to dampen immune responses (Mohammadi and Isberg, 2009).

These examples illustrate RhoG plays an important role in the virulence strategy of certain pathogens. It is likely that other pathogens have evolved additional means of interfering with RhoG due to its central role in phagocytosis, macropinocytosis and host immune responses.

1.2 Bacterial toxin CNF1: the pathogen's tool to establish infection

1.2.1 Urinary tract infection

Found in 1885 by Theodor Escherich the bacterial strain *Escherichia coli* was regarded for many years as a commensal organism of the mammalian colon. Indeed, the Gram-negative, motile *E. coli* belongs to the normal flora of the gut, exchanging mutual benefits with its host. However, due to evolutionary acquisition of genes encoding for various virulence factors, *E. coli* are comprised also of pathogenic strains that cause disease inside or outside of the gastrointestinal system. Regarding these sites of infection, the group of intestinal pathogenic *E. coli* (IPEC) is distinguished from extraintestinal pathogenic *E. coli* (ExPEC). ExPEC may originate within the gut and are able to exist within the gastrointestinal tract without causing disease. However, due to their ability to disseminate

and colonize other niches within the host, ExPEC cause disease outside of the gastrointestinal tract (Wiles et al., 2008). The most common infections caused by ExPEC are urinary tract infections (UTIs), and additionally this *E. coli* group causes sepsis and neonatal meningitis (Karper et al., 2004). Despite a high level of hygiene standard and the broad use of antibiotics, UTIs remain to be among the most common and troublesome bacterial infections in developed countries (Foxman et al., 2000; Bower et al., 2005). Uncomplicated infections can progress into upper parts of the urinary tract and lead to pyelonephritis or cystitis (Foxman, 2002). Women are mostly affected by UTIs and about 25 % of them sustain recurrent infections from the initial strain, causing additional high medical costs and bearing an increased risk to develop bladder cancer (Russo et al., 1995; Yamamoto et al., 1992). A number of pathogens are able to cause UTIs, including *Klebsiella* spp, *Proteus* spp., *Enterobacter* spp., *Staphylococcus aureus* and strains of uropathogenic *E. coli* (UPEC).

1.2.2 Uropathogenic *Escherichia coli*

UTIs are primarily (up to 95 %) caused by uropathogenic *E. coli* (UPEC), a subpopulation of ExPEC that have developed mechanisms to invade the host cells, thereby evading antibiotic treatment and host responses (Dhakal et al., 2008). The primary source of UPEC isolates is the human intestinal tract, however sometimes a clonal group of UPEC may disperse infection via contaminated food or other consumables (Russo et al., 1995; Manges et al., 2001). In comparison to commensal *E. coli* the genomes of UPEC isolates are larger due to the possession of distinct genetic elements referred to as pathogenicity islands (PAIs). The PAIs are acquired through horizontal gene transfer and carry genes encoding for divers virulence factors. The expression of a variety of virulence factors facilitates UPEC to colonize the urinary tract, to evade the host's immune response, to internalize the host cells and also to obtain nutrients from the host, thus enhancing the pathogenicity of UPEC (Johnson, 1991; Wiles et al., 2008).

Pili or fimbriae and adhesins are virulence factors that mediate adherence and colonization of the urothelium. Common of these adhesive organelles expressed by UPEC are type 1, P, S and F1C pili encoded by *fim*, *pap*, *fsa* and *foc* operons, respectively. Regulatory interactions between the operons lead to phase variable and coordinated expression of pilus genes, enhancing the possibility to colonize different niches within the urinary tract (Holden and Gally, 2004; Snyder et al., 2005). Specific adhesin proteins mostly localized at the distal tip of pili enable the bacteria to attach to and sometimes to invade the host tissue. Interactions between adhesins and host cell receptors target the bacteria to specific host niches, dictating the tissue tropism (Mulvey et al., 2000). Type 1 pili carry the adhesin FimH, which binds mannose-containing glycoprotein receptors expressed by a number of different cell types. The adhesin of P-pili PapG recognizes glycolipid receptors expressed by kidney cells and erythrocytes, thus P-pili are associated with *E. coli* strains causing pyelonephritis (Roberts et al., 1994). S/F1C pili harbor the adhesins SfaS and SfaA mediating binding to sialic-acid residues on receptors expressed by kidney epithelial and endothelial cells and glycolipids in endothelial cells and plasminogen, respectively (Morschhauser et al., 1990; Parkkinen et al., 1991; Prasadarao et al., 1993). The family of Dr adhesins includes the fimbrial Dr adhesin and afimbrial members like the Afa adhesins

(Nowicki et al., 2001). These adhesins adhere to epithelial cells by binding to decay-accelerating factor (DAF/CD55) and carcinoembryonic antigen (CEA)-related cell surface proteins (Korotkova et al., 2006).

Secreted toxins are virulence factors that enable UPEC to influence host cell signaling pathways, to control immune responses and to cause cell death. The pore-forming toxin α-Hemolysin (HlyA) is encoded by ≈ 50 % of UPEC isolates and is capable to cause lysis of a variety of cells, including monocytes, erythrocytes and macrophages, thus facilitating the release of nutrients and other factors (e.g. iron) (Johnson, 1991). Cell lysis occurs at higher concentrations of HlyA, whereas sublytic levels of HlyA rather stimulate host signaling pathways levels that degrade structural cell components, promote host cell death and compromise host inflammatory responses, leading to severe tissue damage within the urinary tract (Dhakal and Mulvey et al., 2012). Other toxins secreted by UPEC belong to the group of autotransporters, namely vacuolating autotransporter toxin (Vat) and secreted autotransporter toxin (Sat). These toxins provoke different cytopathic effects in host cells, for example vacuolation and swelling (Wiles et al., 2008). The toxin cytotoxic necrotizing factor 1 encoded by many UPEC isolates facilitates bacterial internalization and evasion of the host immune response by direct modification of Rho GTPases. Many CNF1-mediated effects may help UPEC to disseminate and persist in the urinary tract (Bower et al., 2005).

Iron is an essential factor for many prokaryotic and eukaryotic cell functions. Limitation of free available iron is a host defense mechanism against invading bacteria, but many pathogens, including UPEC, have evolved strategies to exploit divers iron resources. Iron-acquisition systems are virulence factors that help the pathogen to achieve the required iron concentration by scavenging iron from the host and concentrating it in the bacterial cytosol (Skaar, 2010). UPEC express different iron-chelating molecules, namely siderophores, to sequester iron with high affinity and transport it into the bacterial cytosol.

Finally, the expression of flagella enables the bacteria to ascend to the upper urinary tract, i.e. from the bladder to the kidney and disseminate within the host (Lane et al., 2007). Interestingly, the expression of flagella is reduced when UPEC initially establish infection and in presence of type 1 pili on the bacterial surface, suggesting a reciprocal balance between adherence and motility (Lane et al., 2007). However, despite their contribution to bacterial motility, flagella have also been reported to be involved in adherence to epithelial cells due to the adhesive nature of some flagellin subunits (Erdem et al., 2007).

The urinary tract is a hostile environment for many microbes. However, due to the complex interplay of several virulence factors UPEC are able to colonize and breach the uroepithelium, thus contributing to the successful establishment of a UTI. The capacity of UPEC to colonize the urinary tract and to invade host cells is mainly mediated by the toxin CNF1 and two groups of adhesins (Dr/Afa family adhesin and type 1 pilus adhesin FimH) (Bower et al., 2005). Within the preferentially colonized bladder epithelial cells, the pathogen is confined within late endosomal-lysosomal like compartments and, depending on the differentiation state of the host cell, UPEC either escape the vacuole and rapidly replicate to form large intracellular bacterial communities (IBC) or follows a more quiescent fate (Eto et al., 2006). IBC formation mainly occurs within the differentiated

superficial facet cells, in which the actin network is sparse and UPEC can break into the host cytosol. Bladder cells comprising a large number of UPEC will detach and exfoliate, thus infected cells can subsequently be cleared from the urinary tract. Consequently, UPEC need to escape from infected cells. This efflux is observed during the exfoliation complex and triggered by the production of second messenger cyclic adenosine monophosphate (CAMP). Cell exfoliation allows the bacteria to invade underlying layers of immature bladder cells. Within these cells UPEC persist enmeshed within a dense network of actin fibers as quiescent intracellular reservoirs (QIRs). In this status UPEC replication is reduced, thus UPEC may resist antibiotic treatment and host immune responses. The ability of UPEC to enter, colonize and re-emerge from epithelial cells contributes to the recurrence of UTIs (Mulvey et al., 1998; Eto et al., 2006; Dhakal et al., 2008). Figure 1.5 summarizes the infection stages of UPEC.

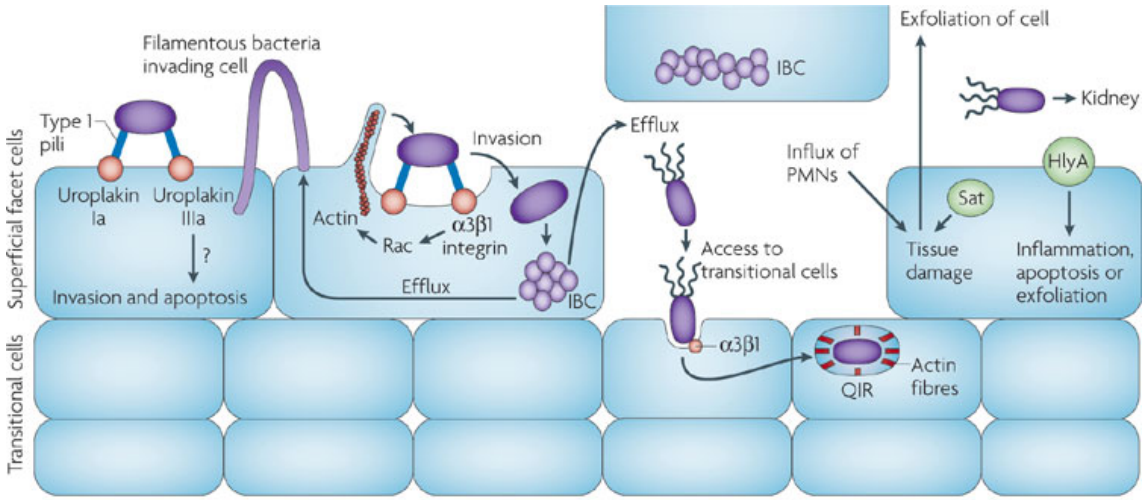

Figure 1.5: Infection stages of uropathogenic *E. coli*.

Type 1 pili from uropathogenic *E. coli* (UPEC) bind to the host receptors, i.e. uroplakins. Underlying mechanisms how this receptor binding triggers signaling pathways remain unclear. However, binding to α3β1 integrins mediates bacterial uptake by activating signal cascades that promote actin rearrangements. UPEC are able to establish intracellular bacterial communities (IBC) in order to replicate rapidly. Exfoliation of host cells eliminates infected cells, but also allows the bacteria to invade deeper layers of the infected tissue, where the bacteria can reside as quiescent intracellular reservoirs (QIRs) that may be involved in recurrent infections (modified from Croxen and Finlay, 2010).

1.2.3 Type 1 pilus-mediated invasion

Type 1 pili are complex peritrichous organelles that are found on almost all UPEC isolates and represent one of the most important virulence factor involved in adherence (Buchanan et al., 1985). A promoter called the *fim* switch controls the expression of type 1 pili. Bacteria switch between phase-on and type 1 pili are expressed, while expression is lost in phase-off. This phenomenon is known as phase variation (Abraham et al., 1985). The adhesive structures are assembled via a chaperone-usher pathway and are composed of a helical rod of repeating FimA subunits that are attached to adaptor proteins, FimF and FimG, and the adhesin FimH (Remaut et al., 2008; Jones et al., 1995). The carbohydrate-

binding pocket of FimH preferentially binds mannose-containing glycoproteins, thus type 1 pili mediate bacterial adherence to various mannose-containing host epithelial receptors (Hung et al., 2002). FimH has been shown to interact with uroplakin 1a (UP1a), type I and type IV collagens, laminin, fibronectin, glycophosphatidylinositol (GPI)-anchored protein CD48, carcinoembryonic antigen-related cell adhesion molecule (CEACAM) members, Tamm-Horsfall protein (THP), α3 and β1 integrin subunits (Zhou et al., 2001; Eto et al., 2007; Smith et al., 2006; Baorto et al., 1997; Leuch et al., 1991; Pouttu et al., 1999; Kukkonen et al., 1993; Sokurenko et al., 1992). Binding of FimH to these proteins does not necessarily lead to bacterial uptake into host cells. Studies with UPEC strains lacking FimH (type 1 pili^{+}, FimH^{-}) and FimH-coated beads revealed that FimH is sufficient to mediate bacterial internalization and that this uptake requires localized host actin rearrangements to induce a zipper-like uptake of adherent bacteria (Martinez et al., 2000). Given its wide distribution within the urinary tract UP1a was considered to be a good candidate for the FimH-dependent invasion receptor, however it failed to mediate FimH-mediated invasion (Zhou et al., 2001). Further work focused on integrins, which are transmembrane receptors linking the extracellular matrix with the actin cytoskeleton (Arnaout et al., 2005). The interaction between FimH and α3β1 integrin was found to be capable of promoting type 1 pili invasion by activating signal cascades that result into actin rearrangements.

Host factors that are recruited and involved in integrin-mediated FimH-dependent invasion include focal adhesion kinase (FAK), tyrosine kinase Src, phosphoinoside 3 (PI 3)-kinase, phosphotidylinositides (PIPs), actinin and vinculin as well as Rho GTPases like Rac1 (Martinez et al., 2000, 2002; Eto et al., 2007). Despite that fact that α3β1 integrin are expressed throughout the urothelium and therefore best situated to act as key receptors mediating UPEC internalization, the broad variety of host receptors able to bind FimH, suggests that additional uptake pathways may be involved (Dhakal et al., 2008).

1.2.4 Virulence factor cytotoxic necrotizing factor 1

The family of cytotoxic necrotizing factors includes CNF1, 2, 3 expressed by pathogenic *E. coli* and CNFy produced by *Yersinia pseudotuberculosis*. While CNF1 originates from human and animal *E. coli* isolates, CNF2 has been found in pathogenic *E. coli* isolated from calf and piglet with diarrhea and the recently discovered CNF3 was found in sheep and goat necrotoxigenic *E. coli* pathotypes (NTEC) (Blanco et al., 1992; Orden et al., 2007). All CNFs are highly homologous, sharing identities between 60 and 80 % (Landraud et al., 2000; De Rycke et al., 1999; Orden et al., 2007). Closely related CNFy is 65 % identical to CNF1 (Lockmann et al., 2002). Whereas CNF1 and CNF3 are chromosomally encoded, CNF2 localizes on a transmissible plasmid (Oswald et al., 1990). All CNFs belong to a family of deamidating toxins. Rho GTPases are constitutively activated via deamidation, but the activity of Rho GTPases is restricted due to degradation processes.

Although CNF1 is an important virulence factor for UPEC, it is not exclusively associated with uropathogenic *E. coli*. It was also isolated from *E. coli* infected skin and soft tissue (Petkovsek et al., 2009). Moreover, other ExPEC strains were also shown to produce CNF1.

In particular, meningitis causing *E. coli* strain K1 produces CNF1 as contributor to invasion of brain microvascular endothelial cells (BMECs), thus penetrating the central nerve system via the blood-brain-barrier (Khan et al., 2002). A study with 60 isolates of sepsis-associated *E. coli* strains (SEPEC) revealed that 20% of this ExPEC group encoded for CNF1 (Ananias and Yano, 2008).

CNF1 was identified in 1983 and named based on its multinucleating and necrotizing effect on cultured cells or rabbit skin, respectively (Caprioli et al., 1983). It is a 114 kDa single chain AB-toxin encoded chromosomally within pathogenicity islands. It contains on its N-terminus a receptor-binding domain that is connected via a translocation domain to a C-terminal catalytic domain (Figure 1.6A) (Fabro et al., 1993; Lemichez et al., 1997).

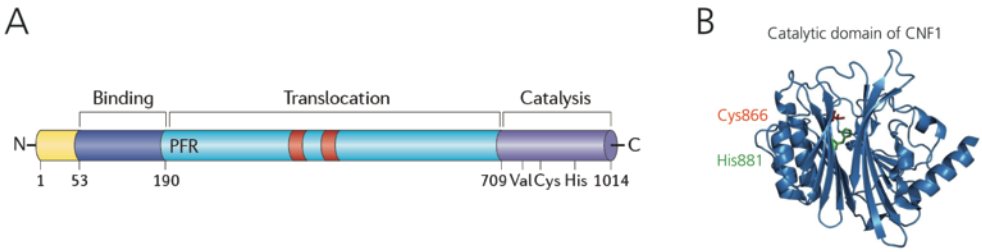

Figure 1.6: Structure of cytotoxic necrotizing factor 1.

(A) CNF1 is a 114 kDa protein containing an N-terminal host receptor binding domain and a C-terminal catalytic domain that is cleaved and reaches the cytosol during after internalization. A translocation domain connects both domains. The catalytic triade of CNF1 is composed of Val833, Cys866 and His881. **(B)** Crystal structure of the catalytic domain in a ribbon presentation (aa 710 – 1014) with Cys866 and His881 highlighted in red and green, respectively (modified from Aktories, 2011; Knust and Schmidt, 2010).

Structural analysis of the catalytic domain of CNF1 revealed a highly conserved catalytic triade of valine (Val833), cysteine (Cys866) and histidine (His881), in which Cys866 and His881 are responsible for deamidase activity towards Rho GTPases (Figure 1.6B) (Buetow et al., 2001). Exactly how CNF1 is secreted from bacteria is somewhat unclear, the sequence of CNF1 reveals no typical signal peptide. However it was observed that active CNF1 associates with outer membrane vesicles (OMV) released by the bacteria (Kouokam et al., 2006). These CNF1-containing vesicles transfer biologically active toxin to target cells (Davis et al., 2006). Recently, a study revealed that ferredoxin is involved in the secretion of CNF1 across the membrane of meningitis-causing *E. coli* K1 (Yu and Kim, 2010). Once secreted, CNF1 was shown to bind the 37 kDa laminin receptor precursor (p37 LRP) using yeast two-hybrid assays (Chung et al., 2003). Some years later, CNF1 was found to interact with the mature 67 kDa laminin receptor on human brain microvascular endothelial cells (Kim et al., 2005). Additionally, competition studies with CNFy proposed that heparansulfate proteoglycan (HSPG) functions as a coreceptor for CNF1 (Blumenthal et al., 2007).

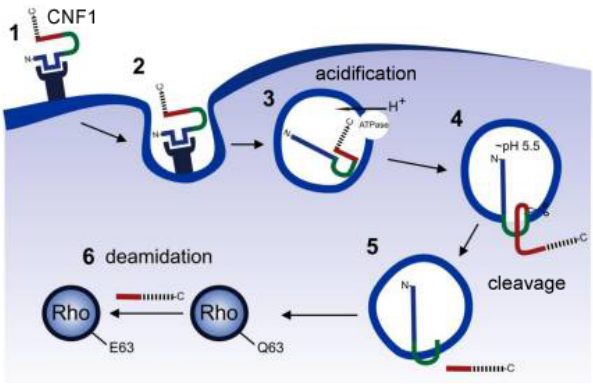

Figure 1.7: Cellular uptake of CNF1.

Bacterially secreted CNF1 binds to the laminin receptor via its N-terminal binding domain and uptake via receptor-mediated endocytosis independent of clathrin and calveolin. Embedded into late endosomal-like compartments, the toxin is translocated into the membrane upon acidification of the vesicle. The catalytic domain of CNF1 is cleaved off and reaches the cytosol where it targets Rho GTPases. Rho GTPases are deamidated by CNF1 leading to their activation (modified from Knust and Schmidt, 2010).

Uptake of CNF1 into the host cell follows a receptor-mediated endocytosis pathway independent of clathrin and calveolin (Figure 1.7). Subsequently, CNF1 is embedded into late endosomal like compartments, where acidification leads to transport of the C-terminus into the cytosol. Upon cleavage a 55 kDa fragment containing the catalytic domain, CNF1 reaches the cytosol (Contamin et al., 2000; Knust et al., 2009). Within the host cytosol, CNF1 targets Rho GTPases and modifies the members RhoA, Rac1 and Cdc42 via its deamidase activity. This posttranslational modification leads to an amino acid change at glutamine 63 (RhoA) or 61 (Rac1, Cdc42) to glutamic acid (Flatau et al., 1997, Schmidt et al., 1997), which blocks the intrinsic and the GAP-catalyzed GTP-hydrolytic activity of the Rho GTPase, keeping it in its activated form. Notably, CNF1-induced deamidation is targeted to a 20 amino acid region of the switch II region of Rho GTPases (Lerm et al., 1999). Within the catalytic triade of CNF1 Cys866 is supposed to form a transient complex with glutamine on the target Rho GTPase, leading to glutamic acid upon hydrolysis. CNF1 also possesses weak transglutaminase activity towards Rho GTPases, but however this does not seem to play a role in CNF1 activation as CNF1 preferentially acts as deamidase *in vivo* (Schmidt et al., 1998).

In 2002 it was observed in two studies that the CNF1-induced activation is only transient. CNF1-activated Rho GTPases are sensitized to ubiquitin-mediated proteasomal degradation (Figure 1.8) (Doye et al., 2002; Lerm et al., 2002).

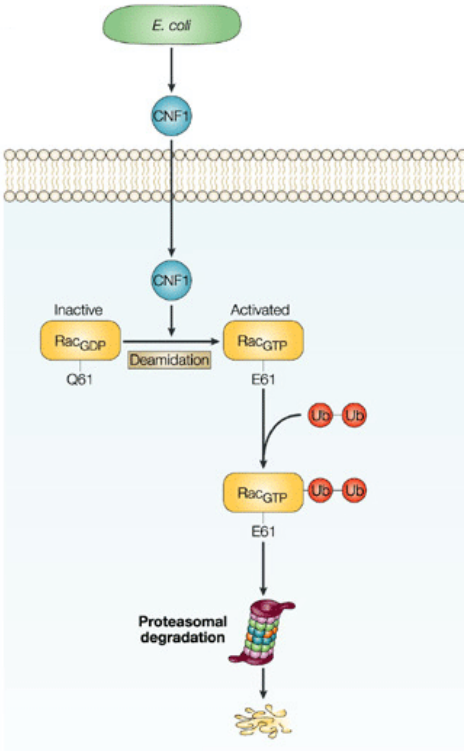

Figure 1.8: CNF1-activated Rho GTPases are sensitized to ubiquitin-mediated proteasomal degradation.

Once inside the host cytosol, CNF1 deamidates Rho GTPases, i.e. Rac1 at Gln61 (Q61) resulting in an amino acid change into Glu61 (E61). Thereby, Rho GTPases are locked in their active state and subsequently sensitized to ubiquitin-mediated protein degradation (modified from Boyer and Lemichez, 2004).

Degradation via the proteasomal pathway requires an initial modification of the targeted protein by conjugation of ubiquitin to lysine residues. The eukaryotic 26S-proteasome is a proteolytic complex in the cytosol and nuclear compartment that recognizes proteins tagged with polyubiquitin. Ubiquitination is a complex multistep process performed by different ubiquitin-carrier proteins. The ubiquitin-ligase E3 specifically targets protein substrates for degradation and catalyzes the attachment of ubiquitin (Weissman, 2001). The E3-ligases can be divided into 2 groups: RING (really interesting new gene) E3 ligases and HECT (homologous to the E6-AP carboxyl terminus) E3 ligases (Nethe and Hordijk, 2010). CNF1-activated Rac1 was shown to be targeted by the HECT E3 ligase HACE1 (HECT domain and ankyrin repeat-containing E3 ubiquitin-protein ligase 1) for ubiquitin-mediated proteasomal degradation (Torrino et al., 2011). Additionally, SMAD specific E3 ubiquitin protein ligase 1 (Smurf1), another HECT E3 ligase, was reported to promote ubiquitination and degradation of activated RhoA. Using $Smurf^{-/-}$ cells it was demonstrated that CNF1-induced proteasomal depletion of activated RhoA requires Smurf1 (Boyer et al., 2006).

Interestingly, this transient activation of Rho GTPases was reported to be necessary for CNF1-induced invasion and has been suggested to play a role in dampening the host immune responses (Doye 2002; Munro et al., 2004).

As Rho GTPases regulate so many different cellular processes, toxin-induced activation of Rho GTPases is a powerful strategy for bacterial manipulation of the host.

1.2.5 CNF1 in bacterial pathogenesis

Due to the activation of actin-regulating Rho GTPases, CNF1 induces prominent morphological changes in the host cytoskeleton. The toxin induces actin stress fibers, lamellipodia and membrane ruffling, and filopodia according to the activation of RhoA, Rac1 and Cdc42, respectively (Lerm et al., 1999). As part of pathogenesis, modulation of the host cytoskeleton by CNF1 affords pathogenic *E. coli* control over many cellular functions. Most of the CNF1-induced cellular effects can be explained by the implication of Rho GTPases, but often it remains unclear how these effects may fit into the virulence strategy of the pathogen. Furthermore, recent studies revealed that CNF1-induced activation of Rho GTPases is only transient, providing the pathogen with the ability to modulate cellular functions depending on the needs of the pathogen (Doye et al., 2002). Using UPEC lacking CNF1 in a mouse UTI model, it was demonstrated that CNF1 plays an important role in virulence (Rippere-Lampe et al., 2001). Additionally, this study showed that infection with the CNF1-positive strain increased neutrophil influx into the bladder, but at the same time neutrophils were less effective in bacterial killing, suggesting that CNF1 stimulates inflammation but also protects UPEC from killing via phagocytosis. In line with these findings, CNF1 is described to enhance polymorphonuclear leukocytes (PMNs) adherence to the epithelium and oxidative burst but decreases the phagocytic function of PMNs (Hofmann et al., 2000). Falzano and colleagues further investigated the contribution of CNF1 to inflammatory host responses. They showed that CNF1 triggers the release of proinflammatory cytokines such as tumor necrosis factor α (TNF-α), interferon γ (IFN-γ), interleukin 6 (IL-6) and IL-8 (Falzano et al., 2003). Moreover, T-lymphocytes are activated and display cytotoxicity against intestinal epithelium upon CNF1 stimulation (Brest et al., 2003). CNF1 interferes with signaling pathways like the stress-activated protein kinase (SAPK) pathways that lead to specific gene expression of e.g. pro-inflammatory cytokines (Munro et al., 2004). Inflammation processes involve recruitment of immune cells to sites of infection, production of reactive oxygen species and proinflammatory cytokines resulting in epithelial necrosis and tissue damage. The ability of CNF1 to manipulate these host defense mechanisms could benefit UPEC, allowing the pathogen to reach deeper tissue layers in order to find its intracellular niche. Indeed, CNF1 is responsible for tissue damage and decreased barrier function analyzed by transepithelial resistance in uroepithelial cells (Hopkins et al., 2003). CNF1 is capable of inducing phagocytic behavior of non-phagocytic cells, thereby enabling UPEC to invade epithelial cells (Falzano et al., 2003). For meningitis-causing *E. coli* strain K1 it was described that CNF1 increases invasion into brain microvascular endothelial cells, thus facilitating crossing of the pathogen across the blood brain barrier (Khan et al., 2002). Besides increasing the invasiveness of the pathogen, CNF1 also contributes to cell-cell junction disruption (Doye et al., 2002). This ability may promote spreading of the bacterium within the infected tissue, but it has also been linked to favor cancer progression. Indeed, some CNF1-induced cellular effects reflect carcinogenic properties of the toxin suggesting that UPEC infections may contribute to tumor development. CNF1 inhibits cytokinesis thereby leading to

multinucleation of cells (Malorni and Fiorentini, 2006). Additionally, CNF1 plays a role in anti-apoptotic signaling pathways. CNF1 protects cells from apoptotic cell death by activating transcription factor NF-κB, an accepted marker for tumor cells (Boyer et al., 2004). Furthermore, NF-κB controls gene expression involved in different inflammation processes, including antiapoptotic Bcl-2 (B-cell lymphoma 2) (Ghosh et al., 1998). In contrast, CNF1 has also been reported to induce apoptotic cell death of uroepithelial cells resulting in an exfoliation process that allows UPEC to reach deeper layers of the tissue (Mills et al., 2000). A clearer picture of the role of CNF1 in the pathogenesis of *E. coli* infections is emerging; however, more research into the molecular mechanisms is needed.

1.2.6 Host responses during UPEC infection

Being confronted with UPEC infection, the host tissue mobilizes different defense mechanisms to oppose bacterial colonization in the bladder. The first line of defense is the urothelium itself. Glycosaminoglycans and proteoglycans localized on the luminal surface of the bladder function to prevent bacterial adherence and secreted antimicrobial peptides like human beta-defensin or cathelicidin act by disrupting bacterial membranes (Hurst, 1994; Valore et al., 1998; Chromek et al., 2006). Once bladder cells are infected by UPEC, exfoliation of superficial cell layers eliminates infected cells from the host with the flow of urine (Mulvey et al., 1998). This host response follows an apoptosis pathway by down regulation of NF-κB (Klumpp et al., 2001). However, in order to balance tissue-disruption, epithelial cells start to differentiate and proliferate rapidly preventing further barrier dysfunction (Mysorekar et al., 2002). UPEC infection triggers innate and adaptive host immune responses. Innate responses include activation of Toll-like receptors (TLRs) that are widely expressed by epithelial and immune cells in the urothelium (Schilling et al., 2003). TLR4 and TLR11 were shown to play a role in innate host defenses against UPEC. Due to its high prevalence to be expressed in kidney and bladder cells, TLR11 was long regarded to be highly specific to UPEC (Zhang et al., 2004). However, recently it was found to respond to other microbes as well including *Salmonella* species (Mathur et al., 2012). TLR4 plays a major role in the inflammatory responses against UPEC, with TLR4-deficient mice unable to produce efficient immune responses towards UPEC infiltration (Haraoka et al., 1999). Upon TLR stimulation, pro-inflammatory cytokines like IL-8 are secreted that in turn attract neutrophils to the site of infection (Agace et al., 2003). Neutrophils are rapidly recruited to kill bacteria in a phagocytic-manner and produce reactive oxygen species and antimicrobial peptides. Additionally, UPEC infection also triggers the migration of cells of the adaptive immune system. It was reported that B- and T-lymphocytes infiltrate the infected bladder. The presence of subsets of $CD4^+$ and $CD8^+$ T-lymphocytes contributes to the clearance of infection (Thumbikat et al., 2006).

1.3 Aim of the study

UPEC are the primary cause of urinary tract infections with over 3 million cases in Germany each year. UPEC possess mechanisms to evade host responses and resist antibiotic treatment. Consequently, recurrent infections are commonplace and contribute to antibiotic resistance and increase the risk of bladder cancer. Therefore it is of great

interest to identify and analyze the interaction of pathogen and host factors that promote UTIs in order to develop more efficient therapies.

This study focused on the function of the UPEC virulence factor CNF1, which activates host cell Rho GTPases thereby facilitating actin-dependent bacterial invasion, and manipulation of proinflammatory signaling pathways. The Rho GTPases Rac1, RhoA and Cdc42 are well-established targets of CNF1 and have well-studied roles in host-pathogen interactions, however, much less is known about RhoG as a potential target of CNF1. A few pathogens have been reported to manipulate RhoG, however, it is not known whether UPEC are able to utilize RhoG as part of their virulence strategy. First, this project asked whether CNF1 intoxication led to activation of RhoG, and if so, whether this occurred via deamidation. The second part of the thesis explored the functional role of CNF1-induced RhoG activation during UPEC pathogenesis. We determined whether CNF1-activated RhoG played a role in proinflammatory signaling during UPEC infection or whether it was important during the invasion process. Finally, the interplay between CNF1-activated Rac1 and RhoG was examined.

These studies will enhance the understanding of host-pathogen interaction and the molecular events leading to disease.

2 Materials and methods

2.1 MATERIALS

2.1.1 Devices

Balances	440-47N/ACS 120-4 (Kern & Sohn GmbH, Balingen-Frommern, G)
Benches	HERAsafe KSP (Thermo Fisher Scientific, Rockford, IL, USA)
	HERAsafe HS15 (Kendro Instruments, Hanau, G)
Centrifuges	5417R, 5810R (Eppendorf, Hamburg, G)
	Sigma 3-18KS (Sigma, Osterode, G)
	Sorvall RC-5B Superspeed (Thermo Fisher Scientific, Rockford, IL, USA)
CO_2 incubator	CB 53 series (Binder, Tuttlingen, G)
Confocal Laser Scanning Microscope	DM IRE2 and TCS SP5 II (Leica, Wetzlar, G)
Cryocontainer	Mr. Frosty Freezing Container (Thermo Fisher Scientific, Rockford, IL, USA)
Developer (X-ray film)	Curix 60 (Agfa, Mortsel, B)
Bacterial electroporator	Gene Pulser II + Pulse Controller (Bio-Rad, Munich, G)
Cell electroporator	NEON® Transfection System (Invitrogen, Darmstadt, G)
Gel dryer	Gel dryer 543 (Bio-Rad, Munich, G)
Gel electrophoresis (SDS-PAGE)	Mini-Protean II (Bio-Rad, Munich, G)
Heater	Dri-block® DB-3 (Techne, Staffordshire, UK)
HPLC	nanoACQUITY™ Ultra Performance LC® (Waters, Eschborn, G)
Incubation shaker	CERTOMAT® BS-1 Incubation-Shaking Cabinet (Sartorius, Göttingen, G)
Bacterial incubator	Heraeus B 5090 E (Kendro Instruments, Hanau, G)
Magnetic stirrer	RCT basic IKAMAG® (IKA®, Staufen, G)
Mass spectrometer	Quadropol-Tof-Tandem-MS: Q-Tof Premier™ (Waters, Eschborn, G)

Microplate reader	Infinite M200 (Tecan, Männedorf, G)
Nanodrop	Nanodrop2000 (Thermo Fisher Scientific, Rockford, IL, USA)
pH-Meter	SevenEasy™ pH (Mettler-Toledo, Gießen, G)
Photometer	Ultrospec3100 pro (GE Healthcare Europe, Freiburg, G)
Pipettes	Pipetman (Gilson, Limburg-Offheim, G)
Pipette controller	accu-jet® pro (Brand, Wertheim, G)
Power supply	PowerPac™ HV High Voltage Power Supply (Bio-Rad, Munich, G)
Sonifier	Digital Ultrasonic Disruptor S-250D (Branson, Danbury, CT, USA)
Thermomixer	Thermomixer compact (Eppendorf, Hamburg, G)
Tilt shaker	WS-10 (Edmund Bühler GmbH, Hechlingen, G)
Transmitted Light Microscope	Eclipse TS100 provided with digital SLR camera D5000 (Nikon, Tokyo, J)
Vortex	Vortex-Genie 2 (Scientific Industries, Bohemia, NY, USA)
Water bath	GFL Typ1013 (GFL, Burgwedel, G)
Western blot apparatus	OWL Hep-2 (Thermo Fisher Scientific, Rockford, IL, USA)

2.1.2 Chemicals, enzymes, antibiotics

All chemicals used in this thesis were level of purity "for analysis" or of highest possible purity and obtained from following companies: AppliChem (Darmstadt, G), Invitrogen (Darmstadt, G), Promega (Mannheim, G), Roche (Mannheim, G), Sigma-Aldrich (Taufkirchen, G), Roth (Karlsruhe, G), and Merck (Darmstadt, G).

Trypsin (0,05 %, Ethylenediaminetetraacetic acid (EDTA)) was purchased from Invitrogen/Life Technologies GmbH (Darmstadt, G).

Antibiotics were used in following concentrations.

Table 2.1: Antibiotics.

Antibiotic	Dissolved in	Final concentration (µg/ml)
Ampicillin	ddH_20	100
Carbencillin	ddH_20	100
Chloramphenicol	70% ethanol	30
Kanamycin	ddH_20	50
Gentamicin	ddH_20	50

2.1.3 Kits

- ZR Plasmid Miniprep™ – Classic (Zymo Research Corporation, Irvine, CA, USA)
- NucleoBond® Xtra Maxi EF (Macherey-Nagel Inc., Düren, G)
- NEON® transfection system (Invitrogen/Life Technologies GmbH, Darmstadt, G)
- Lipofectamine® LTX with Plus™ Reagent (Invitrogen/Life Technologies GmbH, Darmstadt, G)
- Lipofectamine® RNAiMAX Transfection Reagent (Invitrogen/Life Technologies GmbH, Darmstadt, G)
- SuperSignal West Femto Chemiluminescence Substrate (Thermo Fisher Scientific Inc., Rockford, IL, USA)
- Bio-Rad Protein Assay (Bio-Rad Laboratories GmbH, München, G)
- Complete Protease Inhibitor Cocktail Tablets (Roche Diagnostics GmbH, Mannheim, G)
- BD OptEIA™ Human IL-8 ELISA Set (BD Biosciences Europe, Heidelberg, G)

2.1.4 Buffers, solutions, media

For all media, buffers and solutions „aqua bidest" was used. Buffers and solutions were sterilized by autoclaving (121 °C, 20 min) or by sterile filtering (0,2 µm pore size). Media for cell culture were purchased from Invitrogen/Life Technologies GmbH, Darmstadt, G.

Blocking buffer *(Immunodetection)*	5 % (w/v) milk powder in PBST or TBST
Cell lysis buffer *(Cell lysates)*	50 mM Tris-HCl, pH 7,4 1 % (v/v) Triton X-100 1x protease inhibitor cocktail

CNF1 buffer (10x)	500 mM Tris-HCl, pH 7,4 100 mM $MgCl_2$ 10 mM EDTA before use: 10 mM DTT
Coomassie staining	0,1 % (w/v) Coomassie Brilliant Blue R-250 25 % (v/v) methanol 10 % (v/v) glacial acetic acid
Destain solution *(Coomassie staining)*	25 % (v/v) methanol 10 % (v/v) glacial acetic acid
Elution buffer *(Protein purification)*	10 mM reduced glutathione 50 mM Tris-HCl, pH 8 100 mM NaCl
LB agar *(Bacterial culture medium)*	LB broth 1,5 % (w/v) agar
LB broth *(Bacterial culture medium)*	10 g trypton 5 g yeast extract 10 g NaCl bring up to 1000 ml with ddH_20; pH7,0 ± 0,2
Lysis buffer *(Gentamicin assay)*	PBS (+ Ca^{2+}/Mg^{2+}) 1 % (v/v) Triton X-100 0,1 % (w/v) SDS sterile filter
Lysis buffer *(Protein purification)*	20 mM Tris-HCl, pH 7,4 10 mM NaCl 5 mM $MgCl_2$ 1 % (v/v) Triton X-100 before use: 5 mM DTT, 1x protease inhibitor cocktail
Lysis buffer (Rac1) *(Cell lysates)*	50 mM Tris-HCl, pH7,4 2 mM $MgCl_2$ 1 % (w/v) NP-40 10 % (v/v) glycerol 100 mM NaCl 1x protease inhibitor cocktail

Lysis buffer (RhoG) *(Cell lysates)*	20 mM Tris-HCl, pH 7,4 150 mM NaCl 5 mM $MgCl_2$ 0,5 % (v/v) Triton X-100 1 mM DTT 1x protease inhibitor cocktail
PBS (10x)	1,37 M NaCl 26,5 mM KCl 0,1 M Na_2HPO_4 17,6 mM KH_2PO_4 adjust to pH 7,4
PBST *(Immunodetection)*	1x PBS 0,05 % (v/v) Tween®20
Resolving buffer *(SDS-PAGE)*	1,5 M Tris Base 0,004 % (w/v) SDS adjust to pH 8,8
SDS-running buffer (10x) *(SDS-PAGE)*	0,025 M Tris Base 0,192 M glycine 0,1 % (w/v) SDS
SDS-sample buffer (3x) *(SDS-PAGE)*	6 % (w/v) SDS 30 % (v/v) glycerol 187,5 mM Tris-HCl, pH 6,8 0,015 % (w/v) bromophenol blue before use: 15 % (v/v) ß-mercaptoethanol
Stacking buffer *(SDS-PAGE)*	0,5 M Tris Base 0,004 % (w/v) SDS adjust to pH 6,8
TBS (10x)	20 mM Tris Base 150 mM NaCl adjust to pH 7,4
TBST *(Immunodetection)*	1x TBS 0,1 % (v/v) Tween®20

TFB 1 *(Chemically competent cells)*	100 mM RbCl 50 mM $MnCl_2$ 30 mM potassium acetate 10 mM $CaCl_2$ 15 % (v/v) glycerol adjust to pH 5,8 with acetic acid, sterile filter
TFB 2 *(Chemically competent cells)*	10 mM MOPS 10 mM RbCl 75 mM $CaCl_2$ 15 % (v/v) glycerol adjust to pH 8,0 with NaOH, sterile filter
Transfer buffer (10x) *(Western blot)*	1,5 M Tris Base 250 mM glycine add 20 % (v/v) methanol for 1x transfer buffer
Wash buffer *(Protein purification)*	50 mM HEPES, pH 7,4 150 mM NaCl 2 mM $MgCl_2$

2.1.5 Vectors and constructs

Table 2.2: Vectors and constructs.

Name	Source or reference	Application
Bacterial expression		
pGEX4T-2-GST	Group Aepfelbacher, UKE (Hamburg, G)	Expression of GST in prokaryotic cells
pGEX2T-GST-CNF1	Essler et al., 2003	Expression of GST-tagged CNF1 in prokaryotic cells
pGEX4T-2-GST-CNFy	Group Aepfelbacher, UKE (Hamburg, G)	Expression of GST-tagged CNFy in prokaryotic cells
pGEX4T-2-GST-ELMO2NT	Group Aepfelbacher, UKE (Hamburg, G)	Expression of GST-tagged ELMO2 (N-terminal region) in prokaryotic cells
pGEX4T-2-GST-PAK-CRIB	Sander et al., 1998	Expression of GST-tagged PAK-CRIB in prokaryotic cells

pGEX4T-2-GST-RhoA	L. Feig, Tufts University (Boston, MA, USA)	Expression of GST-tagged RhoA in prokaryotic cells
pGEX4T-2-GST-RhoG	Group Aepfelbacher, UKE (Hamburg, G)	Expression of GST-tagged RhoG in prokaryotic cells
Mammalian expression		
pCMV-HA	Clontech (Saint-Germain-en-Laye, F)	Expression of HA-tagged proteins in eukaryotic cells
pCMV-Myc	Clontech (Saint-Germain-en-Laye, F)	Expression of myc-tagged proteins in eukaryotic cells
pEGFP-C1	Clontech (Saint-Germain-en-Laye, F)	Expression of N-terminal marked EGFP-fusion proteins in eukaryotic cells
pEGFP-LifeAct	AG Linder, UKE (Hamburg, G)	Expression of EGFP-fused F-actin marker in eukaryotic cells
pEGFP-Rac1	K. Giehl, University of Ulm (Ulm, G)	Expression of EGFP-fused Rac1 in eukaryotic cells
pEGFP-RhoG	A. Blangy, CRBM (Montpellier, F)	Expression of EGFP-fused RhoG in eukaryotic cells
pEGFP-RhoGV12	A. Blangy, CRBM (Montpellier, F)	Expression of EGFP-fused constitutively active RhoG in eukaryotic cells
pRK5-myc-Rac1L61	P. Aspenström, Uppsala University (Uppsala, S)	Expression of constitutively-active myc-tagged Rac1 in eukaryotic cells
pRK5-myc-RhoGV12	P. Aspenström, Uppsala University (Uppsala, S)	Expression of constitutively-active myc-tagged RhoG in eukaryotic cells
pXJ-HA-Rac1E61	A. Doye, INSERM (Nice, F)	Expression of constitutively active HA-tagged Rac1

2.1.6 Eukaryotic cell lines and bacterial strains

Eukaryotic cell lines

- **HeLa cells** = Human cervix carcinoma cell line. Epithelial cell line.
  Cultured in DMEM + GlutaMAX™, 4,5 g/L D-glucose, 1 mM pyruvate, 10 % FBS, 1 % non-essential amino acids.

– **MEFs** = Mouse embryonic fibroblasts.
Cultured in DMEM + GlutaMAX™, 4,5 g/L D-glucose, 1 mM pyruvate, 10 % FBS, 1 % non-essential amino acids.
Rac1-deficient ($Rac1^{-/-}$) and wildtype Rac1 ($Rac1^{+/+}$) MEFs are described elsewhere (Steffen et al., 2013). Kindly provided by Klemens Rottner, Bonn, G.

E. coli strains

– **TOP10**: F- mcrA Δ(*mrr-hsd*RMS-*mcr*BC) φ80*lac*ZΔM15 Δ*lac*X74 *nup*G *rec*A1 *ara*D139 Δ(*ara-leu*)7697 *gal*E15 *gal*K16 *rps*L(StrR) *end*A1 λ-
(Invitrogen, Darmstadt, G)
– **BL21**: F– *omp*T *gal dcm lon hsd*SB(rB- mB-) λ(DE3)
(Invitrogen, Darmstadt, G)
– **UTI89:** Cystitis isolate, serotype O18:K1:H7 (Mulvey, M. et al., 2001)
Kindly provided by Matthew Mulvey, Salt Lake City, UT, USA.

2.1.7 Oligonucleotides

Predesigned sets of siRNA from Dharmacon/Thermo Fisher Scientific were used for knockdown experiments as described in 3.2.3.3. siRNA targeting Rac1 or RhoG were used as siGenome SMARTpools (set of 4 siRNA). Control experiments were performed with non-targeting siRNA against firefly luciferase.

Table 2.3: siRNA sequences.

Gene target	siRNA set	Target sequence
Human Rac1	siGenome SMARTpool	#1 UAAGGAGAUUGGUGCUGUA
		#2 UAAAGACACGAUCGAGAAA
		#3 CGGCACCACUGUCCCAACA
		#4 AUGAAAGUGUCACGGGUAA
Human RhoG	siGenome SMARTpool	#1 CUACACAACUAACGCUUUC
		#2 CCAGUCCGCCGUCCUAUGA
		#3 GCAACAGGAUGGUGUCAAG
		#4 CGUCAUCUGUUUCUCCAUU
Firefly Luciferase	siGenome SMARTpool	unspecified

2.1.8 Ladders

PageRuler Prestained Protein Ladder (Thermo Fisher Scientific, Rockford, IL, USA)

PageRuler Plus Prestained Protein Ladder (Thermo Fisher Scientific, Rockford, IL, USA)

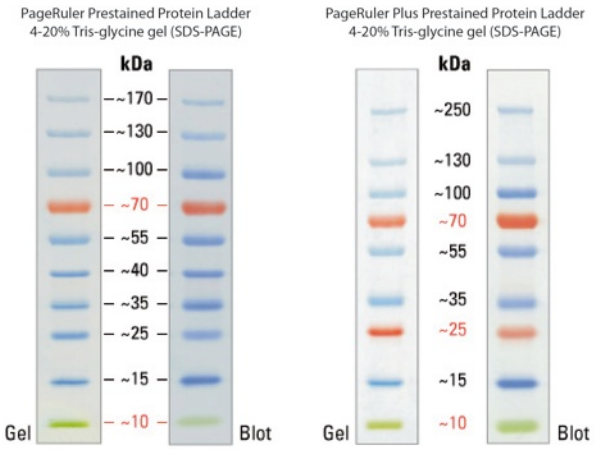

Figure 2.1: Protein ladders.

2.1.9 Antibodies

Table 2.4: Primary antibodies.

Antibody	Working concentration	Company
Mouse-α-actin, monoclonal	1:5000 (WB)	Millipore
Rabbit-α-Calnexin, polyclonal	1:3000 (WB)	Enzo Life Science
Mouse-α-GFP, monoclonal	1:5000 (WB)	Clontech
Rabbit-α-GST, polyclonal	1:2000 (WB)	Invitrogen
Rat-α-HA, monoclonal	1:1500 (WB), 1:100 (IF)	Roche
Mouse-α-myc, monoclonal	1:5000 (WB)	Cell Signaling
Rabbit-α-p-cJun, monoclonal	1:1000 (WB), 1:100 (IF)	Cell Signaling
Mouse-α-Rac1, monoclonal	1:5000 (WB)	Millipore
Mouse-α-RhoG, monoclonal	1:3000 (WB)	Millipore
Rabbit-α-*E.coli* O18, monospecific serum	1:25 (IF)	Sifin

Table 2.5: Secondary antibodies.

Antibody	Working concentration	Company
Alexa Flour® 488 Goat Anti-Mouse IgG	1:200 (IF)	Invitrogen
Alexa Flour® 568 Goat Anti-Mouse IgG	1:200 (IF)	Invitrogen
Alexa Flour® 488 Goat Anti-Rabbit IgG	1:200 (IF)	Invitrogen
Alexa Flour® 568 Goat Anti-Rabbit IgG	1:200 (IF)	Invitrogen
Cy5® Goat Anti-Rabbit IgG	1:200 (IF)	Invitrogen
Anti-Mouse IgG, HRP-conjugated	1:10.000 (WB)	GE Healthcare
Anti-Rabbit IgG, HRP-conjugated	1:10.000 (WB)	GE Healthcare
Anti-Rat IgG, HRP-conjugated	1:10.000 (WB)	GE Healthcare

F-actin was stained with Alexa Flour® 488/568 conjugated phalloidin (1:50) and cell nuclei were stained with DAPI (300 nM) or TO-PRO®-3 (1:500), all from Invitrogen.

2.2 METHODS

2.2.1 Molecular biology methods

2.2.1.1 Isolation of plasmid-DNA (mini and maxi preparation)

Plasmid DNA preparation was performed in accordance with the manufacturer's instructions. For mini preparations the kit "ZR Plasmid Miniprep™ - Classic" from Zymo Research was used, whereas for maxi preparations the kit "Nucleo Bond® Xtra Maxi EF" from Macherey-Nagel was used. Preparations are based on alkaline lysis method (Birnboim and Doly, 1979) and purification was carried out by anion-exchange columns. Plasmid DNA was eluted in endotoxin-free H_20.

2.2.1.2 Determination of nucleic acid concentration

Concentrations of DNA or RNA were determined using a microvolume spectrophotometer NanoDrop 2000. At a wavelength of 260 nm - the absorbance maximum of nucleic acids – the optical density (OD_{260}) was directly measured in 2 µl sample volumes. Using the NanoDrop 2000 software, concentration and purity of samples were determined. OD_{260} of 1 equals 50 µg/ml double stranded DNA or 40 µg/ml RNA. Pure nucleic acid solutions have a value of OD_{260}/OD_{280} = 1,8 – 2,0. Lower values suggest protein contamination.

2.2.1.3 Preparation of chemically competent bacteria

50 ml LB broth were inoculated with bacteria and incubated shaking at 37 °C until OD_{600} = 0,5. The bacterial culture was then placed on ice and centrifuged for 10 min at 4 °C (6000 rpm, Sorvall SS34). After resuspension of the pellet in 10 ml pre-cooled TFB1 buffer, the suspension was incubated on ice for 90 min. Following centrifugation (10 min, 4 °C,

6000 rpm) the pellet was resuspended in 1 ml pre-cooled TFB 2 buffer. 100 µl aliquots were shock-frozen in liquid nitrogen and stored at - 80 °C.

2.2.1.4 Preparation of electrocompetent bacteria

10 ml of an overnight (O/N) starter culture were inoculated with a single colony of bacteria and grown at 37 °C shaking. The next day, 100 ml LB broth were inoculated with 1 ml O/N culture and incubated at 37 °C shaking until OD_{600} = 0,6. Cells were put on ice and centrifuged at 4 °C for 10 min (7000 rpm, Sigma 19776). Supernatant was carefully discarded and the pellet was resuspended in 20 ml ice-cold dH_2O. Centrifugation, resuspension and centrifugation steps were repeated. Next, the pellet was resuspended into 10 ml dH_2O + 10 % glycerol, centrifuged and finally resuspended into 600 µl dH_2O + 10 % glycerol. 60 µl aliquots were shock-frozen in liquid nitrogen and stored at - 80 °C.

2.2.1.5 Transformation of chemically competent bacteria

Chemically competent bacteria (100 µl) were thawed on ice. Plasmid-DNA (100 ng) was added to the bacterial suspension and incubated on ice for 30 min. Afterwards, a heat shock followed for 90 sec at 42 °C. The bacteria were placed on ice for 2 min and, after addition of 1 ml LB broth, incubated for 45 min at 37 °C shaking. Transformed bacteria were selected onto LB agar plates containing antibiotics.

2.2.1.6 Transformation of electrocompetent bacteria

Electrocompetent bacteria were thawed on ice. Bacteria and added DNA (100 ng) were transferred into ice-cold cuvettes. Electroporation was performed with following settings: 2,0 kV, 200 Ω low range, 25 µF. Bacteria suspension was quickly transferred into tubes with 900 µl LB broth and incubated for 45 min at 37 °C shaking. Plating onto LB agar plates containing antibiotics selected transformed bacteria.

2.2.2 Biochemical methods

2.2.2.1 Protein expression and purification

Glutathione-*S*-transferase (GST) fusion proteins were expressed in *E.coli* transformed with expression vectors pGEX-4T harboring the gene of interest. O/N bacterial cultures were diluted 1:40 in 1 liter LB broth containing selective antibiotics and incubated at 37 °C shaking until $OD_{600} \approx 0,7$. Protein expression was induced by addition of 1 mM isopropyl-β-D-thiogalactopyranoside (IPTG). Culture was incubated for 3 hrs at 37 °C with shaking and then centrifuged (6000 rpm, 4 °C, 15 min). The pellet was resuspended in 10 ml cold lysis buffer and the suspension was sonicated on ice 10 times for 10 sec with 17 % amplitude. The lysate was centrifuged (20.000 g, 4 °C, 15 min), the supernatant mixed with washed 1 ml glutathione sepharose 4B beads and incubated for 1 h at 4 °C rotating end over end. Using a column, unbound proteins were removed by addition of cold washing buffer. GST-fused proteins were eluted by adding 0,5 ml cold elution buffer. When necessary, protein samples were dialyzed against 50 mM Tris-HCl (pH 7,4), 10 mM $MgCl_2$ at 4 °C O/N.

2.2.2.2 Determination of protein concentration

Total protein concentration in samples was measured using the Bradford method based Protein Assay (Bio-Rad) according to the manufacturer's protocol. This colorimetric protein assay is based on an absorbance shift due to protein binding of the dye Coomassie Brilliant Blue G-250. Absorbance was measured at 595 nm.

2.2.2.3 SDS-polyacrylamide gel electrophoresis (SDS-PAGE)

Separation of proteins according to their molecular weight was carried out with denaturing SDS-PAGE. Electrophoresis was performed with mini gels (6 x 9 cm) in a Mini Protean II apparatus. Preparation of resolving and stacking gels is described in Table 2.6. Protein samples for analysis were mixed with 3x SDS-sample buffer and heat-denatured for 10 min at 95 °C. Gels were run at a constant voltage of 120 V in 1x SDS-running buffer. Prestained protein ladder was used for protein weight standard. After electrophoresis proteins were either visualized using Coomassie staining (2.2.2.4) or transferred onto polyvinylidene difluoride (PVDF) membranes (2.2.2.5).

Table 2.6: Preparation of polyacrylamide gels.

	Resolving, 10 ml		Stacking, 3 ml
	10 %	**12 %**	**5 %**
ddH_20	4 ml	3,3 ml	2,1 ml
Acrylamide (30%)	3,3 ml	4,0 ml	0,5 ml
Resolving buffer	2,6 ml	2,6 ml	-
Stacking buffer	-	-	0,41 ml
10% Ammonium persulfate (APS)	0,1 ml	0,1 ml	0,03 ml
Tetramethylethylenediamine (TEMED)	0,004 ml	0,004 ml	0,003 ml

2.2.2.4 Coomassie staining

To visualize proteins after electrophoresis (2.2.2.3), the gel was rinsed in ddH_20 before being soaked in Coomassie staining solution for 3-16 hrs. After staining, the gel was destained by periodic exchange of spent destaining solution with either destaining solution or ddH_20 until protein bands became clearly visible.

2.2.2.5 Western blot

For specific analysis of proteins by immunodetection proteins were transferred onto a PVDF membrane after electrophoresis (2.2.2.3). PVDF membrane was activated in methanol before being soaked in transfer buffer. Six Whatman filter papers were also soaked in transfer buffer. The blot was assembled from cathode to anode: 3 Whatman

filter papers, gel, membrane, and 3 Whatman filter papers. Transfer was carried out in a semi-dry blotting apparatus at constant current of 2 mA/cm^2 for 1 h.

2.2.2.6 Immunodetection

To detect proteins that were immobilized on PVDF membranes with specific antibodies the membrane was initially incubated in blocking buffer for 1 h at room temperature (RT). Binding of the primary antibody was carried out in blocking buffer (Table 2.4) at 4 °C overnight under gentle agitation. After 3 washing steps for 5-10 min with PBST or TBST the membrane was incubated with horseradish peroxidase (HRP)-conjugated secondary antibody (Table 2.5) for 1 h at RT under gentle agitation. After 3 additional washing steps for 5-10 min each with PBST or TBST detection was performed using chemiluminescence-based SuperSignal West Femto substrate according to the manufacturer's protocol. For documentation, light sensitive X-ray films were used.

2.2.2.7 Enzyme-linked immunosorbent assay (ELISA)

To detect production of human interleukin 8 (IL-8) by CNF1-intoxicated HeLa cells, ELISA was performed in accordance with the manufacturer's instructions (BD OptEIA, BD Bioscience). Briefly, cells were intoxicated with CNF1 (300 ng/ml) for indicated time points at 37 °C. Culture medium was collected and centrifuged (10.000 g, 5 min, 4 °C). Supernatants were added to a 96-well plate coated with anti-human IL-8 antibody. For detection of captured IL-8, biotinylated detection antibody and streptavidin-conjugated horseradish peroxidase conjugate were used. Captured IL-8 was visualized using a tetramethylbenzidine (TMB) substrate reagent set and absorbance was read at 450 nm in a microplate reader. Recombinant human IL-8 was used as a standard. IL-8 levels were determined by interpolation from the standard curve.

2.2.2.8 Whole cell lysates

Cells were washed 2x with ice-cold PBS (+ Ca^{2+}/Mg^{2+}) and scraped off in cold cell lysis buffer. Cell lysates were centrifuged (20.000 g, 20 min, 4 °C) and supernatants were collected for analysis.

2.2.2.9 Rho GTPase activation pulldown

Activation of Rho GTPases can be analyzed and quantified in cell lysates with pulldown assays. Specific effector proteins of the active form of the Rho GTPase are used as GST-fusion proteins. The GST-fusion proteins were recombinantly expressed and purified from *E. coli* (2.2.2.1). To analyze active Rac1, GST-PAK-CRIB was used whereas GST-ELMO-2NT was used to pull down active RhoG. Glutathione sepharose 4B beads (100 µl) were washed 3 times by centrifugation (510 g, 3 min, 4 °C) with cold PBS containing 100 µM phenylmethylsulfonylfluorid (PMSF) followed by incubation with GST-fusion proteins for 1 h at 4 °C rotating. Beads coupled with GST-fusion proteins were washed three times with cold PBS/PMSF and incubated with cell lysates (2.2.2.8) for 2 hrs at 4 °C rotating. After 4 washing steps with cold PBS/PMSF, remaining buffer was completely removed from beads and proteins were released with 3x SDS-sample buffer. Beads were incubated with 30 µl

3x SDS-sample buffer for 10 min at 95 °C and the supernatant was transferred into a new tube.

2.2.2.10 Nucleotide binding assay

Fluorescent nucleotide analogs incorporating *N*-methylanthraniloyl (mant) fluorophore were used to analyze functional GDP-binding ability of recombinant Rho GTPases. The fluorescence intensity of GTPase-bound mant-GDP is higher compared to free mant-GDP and therefore nucleotide-protein interactions are detectable. The fluorescence of baseline mant-GDP (0,5 µM final concentration) in CNF1 buffer was monitored with excitation at 350 nm and emission at 448 nm. Measurements were taken every 30 sec. After the addition of 1 µM Rho GTPase, the increase in fluorescence intensity was recorded. Relative fluorescence intensity was calculated as the fluorescence signal of GTPase-bound mant-GDP divided by fluorescence signal of baseline mant-GDP.

2.2.2.11 *In vitro* modification of recombinant Rho GTPases by CNF1

For analysis of Rho GTPase deamidation, recombinant proteins of GST-CNF1 and GST-Rho GTPase (RhoG, RhoA) were incubated for 4 hrs at 37 °C in CNF1 buffer. The ratio of CNF1:GTPase (molar masses) varied between 5-20:1. After incubation, samples were supplied with 3x SDS-sample buffer and proceeded for SDS-PAGE.

2.2.2.12 Proteolytic digestion for mass spectrometric analysis

The gel was stained with colloidal Coomassie, the bands were cut out, the proteins were reduced with 10 mM DTT at 56 °C for 30 min, the cysteine residues were modified with 55 mM iodacetamid for 20 min in the dark and the proteins were in-gel digested with 5 ng/µl trypsin in 50 mM NH_4HCO_3 at 37 °C for 16 hrs. After digestion, the gel pieces were repeatedly extracted (50 % acetonitrile/5 % formic acid), the combined extracts dried down in a vacuum concentrator and redissolved in 20 µl formic acid (0,1 %).

2.2.2.13 Mass spectrometry

Liquid chromatography/mass spectrometry (LC/MS) runs were done on a Quadropol-Tof-Tandem mass spectrometer equipped with Ultra Performance LC® (Waters, Eschborn, G). Samples were applied onto a trapping column, washed for 10 min (flow: 5 µl/min) with 5 % acetonitrile, 0,1 % formic acid and then eluted onto the separation column with following gradient: A = 0,1 % formic acid and B = 0,1 % formic acid in acetonitrile, 5 – 50 % B in 120 min.

In order to identify and label-free quantify the proteins, the MS^E technique according to Silva et al. (2005) was applied: alternating scans (0,95 sec; 0,05 sec interscan delay) with low (4 eV) and high (ramp from 20-35 eV) collision energies were recorded. The data were evaluated with the software package Protein Lynx Global Server 2.3 (Waters, Eschborn, G).

2.2.3 Cell culture and cell imaging

Mammalian cell lines were grown as subconfluent monolayers and cultured in a humified atmosphere (37 °C, 5 % CO_2). Work with cell culture was performed under a sterile workbench and with sterile equipment.

2.2.3.1 Passaging of cells

Cells were passaged every 2-3 days. After washing with PBS, cells were trypsinized (trypsin, EDTA) for 3 minutes. Detached cells were split and seeded in fresh medium.

2.2.3.2 Freezing and thawing of cells

Confluent monolayers of cells were washed with PBS, detached by trypsin/EDTA and centrifuged (200 g, 5 min). Cells were resuspended in DMEM (+ 10 % FBS), dropwise mixed with an equal volume of DMEM (+ 10 % FBS, + 20 % DMSO) and aliquots were transferred into cryovials. Cryovials were placed into a "Mr. Frosty" cryocontainer overnight at - 80 °C and put into liquid nitrogen the next day for long time storage.

Cryoconserved cells were quickly thawed at 37 °C and transferred into 15 ml prewarmed culture medium. After centrifugation (200 g, 5 min) cells were resuspended in 10 ml culture medium.

2.2.3.3 Transfection of mammalian cells (siRNA, DNA)

Reverse siRNA transfection was performed according to the manufacturer's protocol (RNAiMax, Invitrogen). Briefly, 10-20 nM siRNA and 4 µl transfection reagent were mixed in 500 µl OptiMEM and added to one well of a 6 well plate. The mixture was incubated for 15 minutes at RT and then 250.000 cells in 2,5 ml culture medium were seeded per well. Medium was changed after 24 hrs and transfected cells were cultured for 72 hrs.

DNA transfection was performed using either a NEON® electrotransfection kit (Invitrogen) or LTX Lipofectamine® (Invitrogen) in accordance with the manufacturers' instructions. Settings for NEON® electrotransfection of HeLa cells were 1005 Volt, 35 ms and 2 pulses. For transfection with LTX Lipofectamine®, 5 x 10^4 cells per well were seeded into 24 well plates. After 24 hrs, culture medium was renewed and DNA-Lipofectamine® LTX complexes (1 µl LTX per 0,5 µg DNA in 100 µl Opti-MEM®) were added. Cells were incubated at 37 °C 18-24 hrs post-transfection.

2.2.3.4 Bacterial infection of eukaryotic cells

24 hrs before infection cells were seeded into 24 well plates with or without coverslips at a density of 1 x 10^5 cells/ml. Bacteria were grown O/N in LB broth at 37 °C under static conditions. On the day of infection bacteria were statically subcultured (1:10) for 3,5 hrs and adjusted to OD_{600} = 0,6. Bacteria were centrifuged (6000 rpm), washed and finally resuspended in PBS (+ Ca^{2+}/Mg^{2+}). Cells were infected for 1 h at 37 °C with a multiplicity of infection (MOI) of ≈ 100. CNF1-intoxicated cells were pre-incubated 2 hrs before infection with 300 ng/ml CNF1.

2.2.3.5 Gentamicin protection assay

For quantification of intracellular bacteria gentamicin protection assay was performed (Figure 2.2A). Gentamicin is an antibiotic that cannot penetrate eukaryotic cells, therefore internalized bacteria are protected during gentamicin treatment.

After infection, cells were washed 3 times with PBS (+ Ca^{2+}/Mg^{2+}) and culture medium was replaced by culture medium containing 100 µg/ml gentamicin. After incubation of an additional 1 h at 37 °C, cells were washed 4 times with PBS and lysed in 500 µl lysis buffer. Lysates were plated in different dilutions onto LB agar plates. Bacterial colony forming units (CFU) were counted the next day.

2.2.3.6 Adherence assay

For quantification of adherent bacteria, bacterial infection procedure was performed as described in 2.2.3.5, yet after infection cells were washed 4 times with PBS (+ Ca^{2+}/Mg^{2+}) and lysed in 500 µl lysis buffer. Lysates were plated in different dilutions onto LB agar plates. Bacterial colony forming units (CFU) were counted the next day. Quantifications in this assay include intracellular and cell-associated bacteria.

2.2.3.7 Agglutination of yeast cells

The presence of adhesin FimH expressing bacteria was assayed by their ability to agglutinate yeast (*Saccharomyces cerevisiae*) cells on glass sides. An aliquot of washed bacterial suspension at OD_{600} = 0,6 was mixed with commercial available yeast (1 % in PBS, + Ca^{2+}/Mg^{2+}) and agglutination monitored visually.

2.2.3.8 Immunfluorescent staining of eukaryotic cells

Cells were washed 3 times with PBS (+ Ca^{2+}/Mg^{2+}) and fixed with 2,5 % paraformaldehyde (PFA) for 25 min at RT. After fixation, cells were permeabilized and unspecific binding sites blocked at once with 0,1 % Triton X-100 and 10 % normal goat serum (NGS) in PBS for 30 min. Primary antibodies were diluted in blocking/permeabilizing solution as listed in Table 2.4 and incubated for 45 min. After 3 washing steps with PBS, cells were incubated with Alexa or Cy5 dye-coupled secondary antibodies (Table 2.5) diluted in blocking/permeabilizing solution followed for 45 min in the dark. Samples were washed 3 times with PBS and mounted on glass slides in Mowiol. Analysis of the fluorescent immunostaining was performed with a confocal laser microscope DM IRE2 or TCS SP5 (Leica, Wetzlar, G) and software LAS AF (Leica, Wetzlar, G).

2.2.3.9 Inside/outside immunostaining

To quantify adherent and intracellular bacteria, inside/outside immunostaining was used (Figure 2.2B). After infection cells were washed 3 times with PBS (+ Ca^{2+}/Mg^{2+}), fixed with 2,5 % PFA and blocked in 10 % NGS in PBS. To label adherent bacteria, cells were probed with anti-*E.coli* (O:18) antiserum for 45 min in blocking solution, washed with PBS and incubated with Alexa 568-conjugated goat anti-rabbit antibody for 45 min in the dark. Following 3 washing steps with PBS, cells were permeabilized and blocked with 0,1 % Triton X-100 and 10 % NGS for 30 min. Cells were probed with anti-*E.coli* (O:18)

antiserum, washed with PBS and incubated with Cy5-conjugated goat anti-rabbit antibody to label intracellular bacteria. Samples were washed and mounted in Mowiol. Analysis of the fluorescent inside/outside immunostaining was performed with a confocal laser microscope DM IRE2 or TCS SP5 (Leica, Wetzlar, G) and software LAS AF (Leica, Wetzlar, G). For each experiment at least 100 cells were imaged and analyzed.

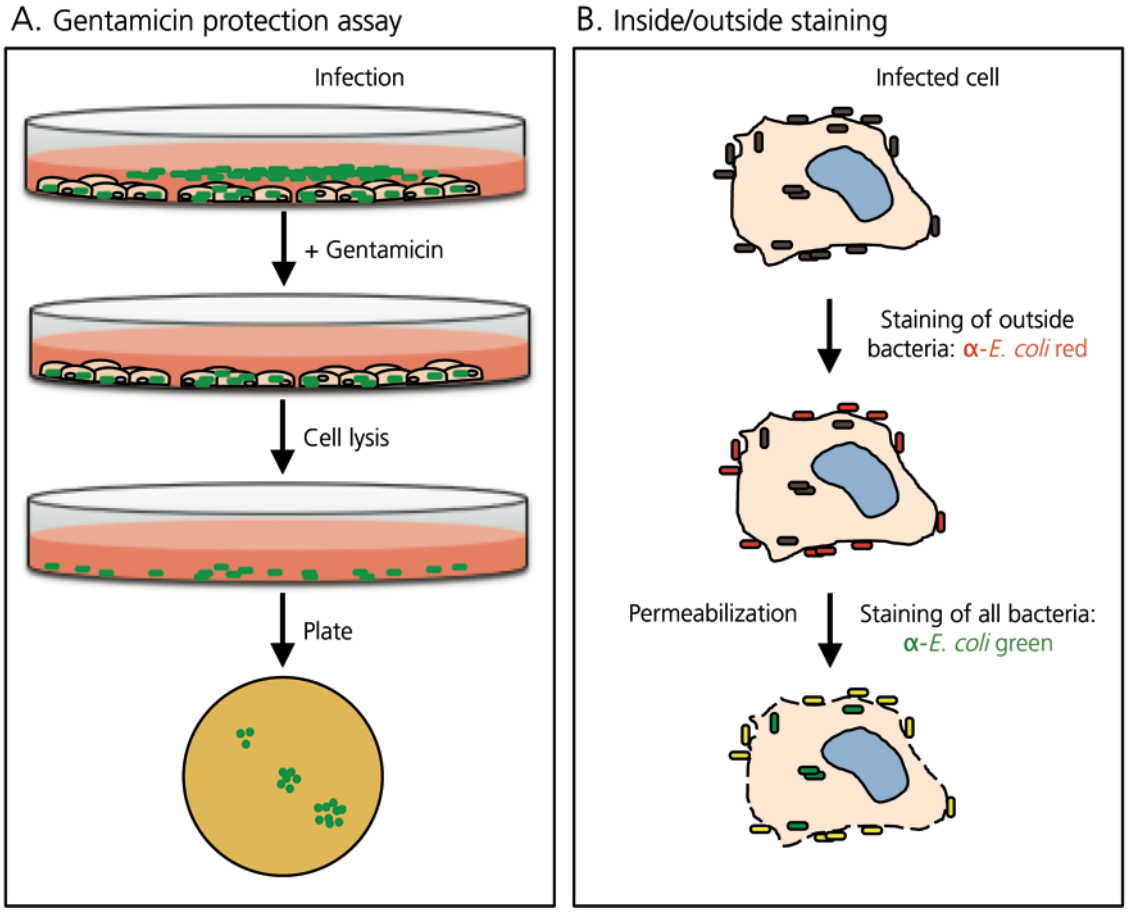

Figure 2.2: Schematic view of gentamicin protection assay and inside/outside staining to quantify intracellular bacteria.

(A) Gentamicin protection assay is based on the ability of pathogens to invade host cells. Application of antibiotic gentamicin to culture medium of infected cells kills all extracellular bacteria while successfully invaded bacteria are protected. Lysis of eukaryotic cells releases intracellular bacteria, which then are plated on agar and quantified by formed colonies. **(B)** Inside/outside staining is an immunofluorescent method that stepwise labels extracellular (= outside) and intracellular (= inside) bacteria separately. Outside staining is performed before cell permeabilization, whereas inside staining requires cell permeabilization.

2.2.3.10 Quantitative analysis and statistics

For quantification and analysis the software ImageJ 1.43u (National Institutes of Health, Bethesda, MD) was used. Processing of raw data as well as statistical analysis according to ANOVA were performed with Prism 5.0c (GraphPad Software, La Jolla, CA). To test significances, one-way ANOVA with Bonferroni's post-test or student's t-test were used. Results with level of significance of < 5 % ($p < 0,05$) were regarded as being significant.

3 Results

Some pathogens need to enter host cells in order to establish their intracellular niche. Virulence factors promote crossing of protective barriers and subversion of the host immune responses, thereby they have a pivotal role in pathogenicity. Many UPEC strains produce the toxin cytotoxic necrotizing factor 1 that is internalized by host cells and targets Rho GTPases in the cytosol resulting in their permanent activation. Modulation of Rho GTPases allows pathogens to disturb many cellular functions including control of the actin organization and proinflammatory signaling pathways.

This doctoral thesis examined whether RhoG was targeted by CNF1. Furthermore, this study focused on the characterization and putative functional role of CNF1-induced activation of RhoG during UPEC infections.

3.1 Identification of RhoG as a new substrate for CNF1

3.1.1 Intoxication with CNF1 induces morphological changes in HeLa cells

Recombinant CNF1 preparations were prepared and tested for activity on the human epithelial cell line, HeLa. Intoxication was assessed by observing morphological changes to the actin cytoskeleton after 2 hrs treatment with 300 ng/ml recombinant GST-CNF1. Brightfield images revealed remodeling of the cytoskeleton upon CNF1 stimulation (Figure 3.1A). In comparison to untreated cells, CNF1-intoxicated cells displayed prominent apical membrane ruffles. Moreover, confocal images of cells transfected with the green fluorescent actin marker LifeAct displaying the actin cytoskeleton revealed different toxin-enhanced actin structures including stress fibers, filopodia and membrane ruffles indicating activation of RhoA, Cdc42 and Rac1, respectively (Figure 3.1B). Thus, the activity of recombinant CNF1 in HeLa cells was demonstrated.

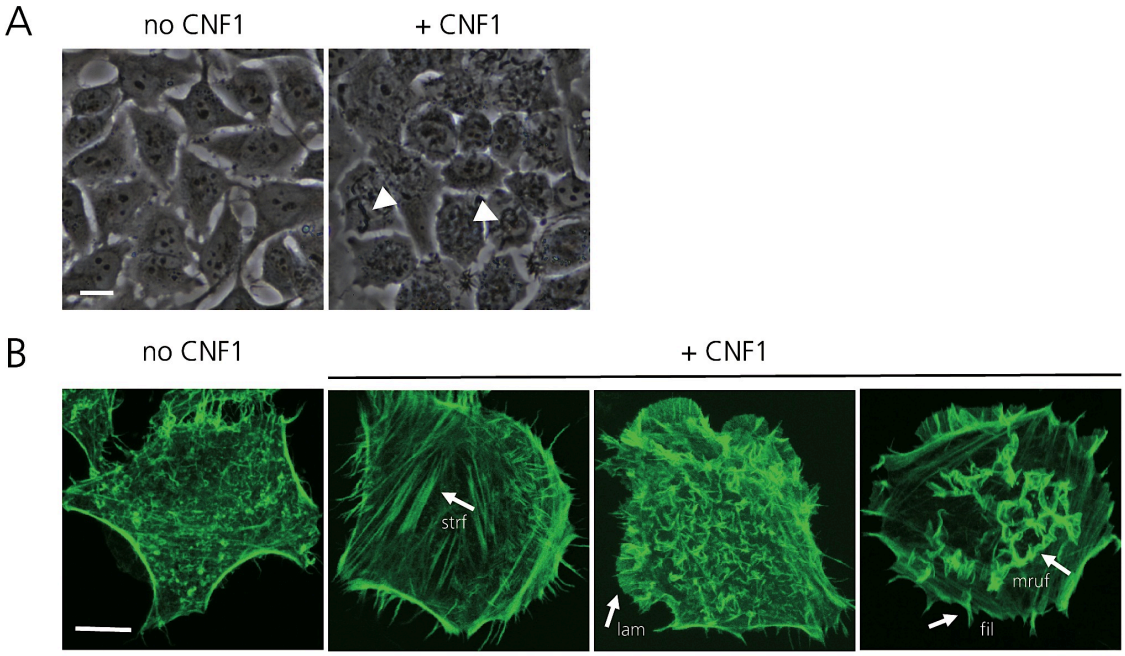

Figure 3.1: CNF1 induces prominent changes of the actin cytoskeleton.

HeLa cells were intoxicated for 2 hrs with 300 ng/ml CNF1 or left untreated. **(A)** Brightfield images were taken or **(B)** cells were transfected with LifeAct-GFP to visualize actin (green) and confocal images were processed. Arrowheads indicate actin ruffles. Arrows display prominent actin structures. Scale bars represent 20 µm **(A)** and 10 µm **(B)**. strf = stress fibers, lam = lamellipodia, fil = filopodia, mruf = membrane ruffles.

3.1.2 CNF1 induces transient activation of RhoG

Actin ruffles were the most prominent structures observed upon CNF1 intoxication. Ruffles are known to be dependent on Rac1 and/or RhoG activation (Ridley et al., 1992; Gauthier-Rouviere et al., 1998). Rac1 is a known substrate of CNF1, however, it was not known whether RhoG was a target of CNF1 activity. Therefore, activation of RhoG was measured by pulldown assays using GST-ELMO2NT. As a positive control for CNF1-induced Rho GTPase activation, activation of Rac1 was additionally quantified using pulldown assays using GST-PAK-CRIB. ELMO2NT and PAK-CRIB are effector domains that selectively bind to the GTP-bound (active) forms of RhoG and Rac1, respectively (Katoh and Negishi, 2003; Benard et al., 1999). HeLa cells were incubated with the toxin for different time periods to monitor the kinetics of Rac1 and RhoG activation. As expected, CNF1 induced Rac1 activation after 2 hrs of incubation, reaching maximal activation between 4 and 8 hrs (Figure 3.2B). Interestingly, intoxication of HeLa cells with CNF1 also led to strong activation of RhoG, following similar kinetics to Rac1 activation (Figure 3.2A). Notably, intoxication with the closely related CNFy toxin from *Y. pseudotuberculosis* did not lead to activation of RhoG, indicating that CNF1 selectively activates RhoG (Figure 3.2C). CNF1-activated Rho GTPases are reported to be subsequently targeted and degraded by the proteasome machinery resulting in a transient activation of Rho GTPases (Doye et al., 2002). Indeed, Western blotting of whole cell lysates of CNF1-stimulated cells

displayed time-dependent degradation of both RhoG and Rac1. Thus, RhoG was identified as a novel target of CNF-1-induced activation and degradation.

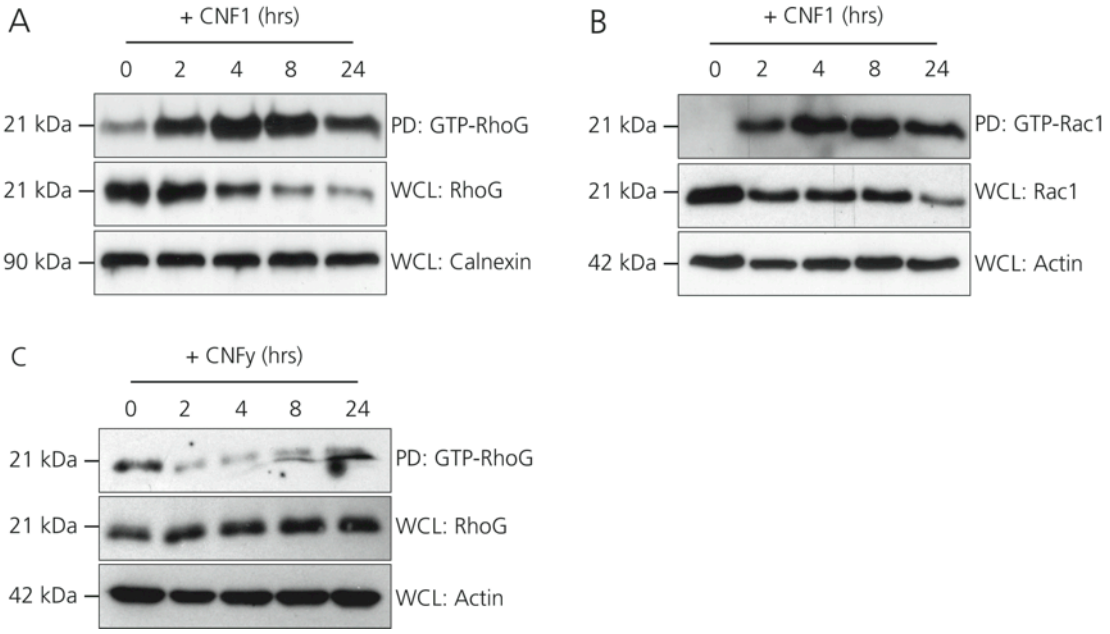

Figure 3.2: CNF1 strongly activates RhoG and causes its subsequent degradation.

HeLa cells were intoxicated with 300 ng/ml CNF1 **(A, B)** or CNFy **(C)** for indicated timepoints. Cell lysates were subjected to pulldown assays. **(A, C)** Active RhoG was precipitated with GST-ELMO2NT. **(B)** Active Rac1 was precipitated with GST-PAK-CRIB. Samples were subjected to SDS-PAGE and Western blot. Immunoblots for calnexin and actin were used as loading controls. PD = pulldown. WCL = whole cell lysates.

3.1.3 CNF1 activates RhoG via deamidation

CNF1 activates Rac1, RhoA and Cdc42 directly via deamidation of glutamine residues (Gln) at position 61 (Rac1, Cdc42) or 63 (RhoA) of the switch II region. These glutamine residues are responsible for the GTPase-activity of Rho proteins. Modification of Gln61/63 locks Rho GTPases in their GTP-bound state, leading to their permanent activation (Schmidt et al., 1997; Lerm et al., 1999). Rho GTPases share high identity of amino acids in the switch II region, and accordingly RhoG also contains glutamine at position 61 that could possibly be deamidated by CNF1 (Figure 3.3).

	51	61	71	81
Rac1	VNLGLWDTAG	**Q**EDYDRLRPL	SYPQTDVFLI	CFSLVSPA
RhoA	KQVELALWDT	AG**Q**EDYDRLR	PLSYPDTDVI	LMCFSIDS
Cdc42	YTLGLFDTAG	**Q**EDYDRLRPL	SYPQTDVFLV	CFSVVSPS
RhoG	VNLNLWDTAG	**Q**EEYDRLRTL	SYPQTNVFVI	CFSIASPP

Figure 3.3: Glutamine residues in switch II region of Rho GTPases are sites of deamidation by CNF1.

Alignment of amino acid sequences of Rac1, RhoA, Cdc42 and RhoG showing glutamine residues (Q) known to be sites of deamidation for Rac1, Cdc41 (Q61) and RhoA (Q63) and the hypothesized site of deamidation for RhoG (Q61) shown in bold and underlined.

In order to test whether CNF1 directly modifies RhoG, recombinant Rho GTPases were purified for *in vitro* reactions. The activity of the recombinant protein preparations was tested as readout for proper protein folding. Activity of the preparations, and hence proper folding, was measured by the ability to bind guanine nucleotides. Using the fluorescent GDP-analog, mant-GDP, the guanine nucleotide exchange profiles of RhoG and RhoA were determined. Addition of the Rho GTPases to mant-GDP led to an increase of fluorescence signal over time compared to the control condition in which no Rho GTPase was added (Figure 3.4), indicating the presence of mant-GDP-bound Rho GTPases in the samples. Notably, the fluorescence signal of mant-GDP-RhoG increased much slower than of mant-GDP-RhoA without reaching saturation. This indicated that RhoG and RhoA were functional, but differ in their nucleotide binding properties.

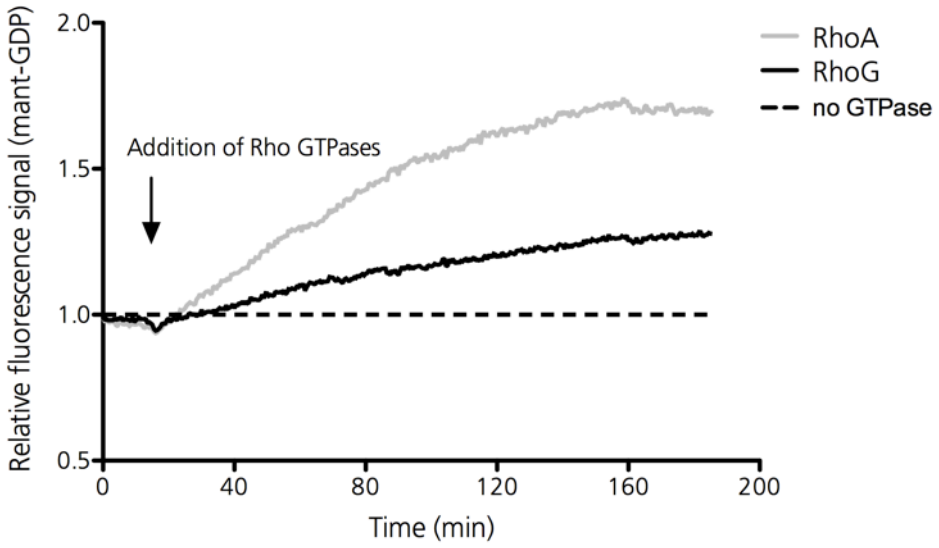

Figure 3.4: Guanine nucleotide exchange profiles of RhoA and RhoG.

The guanine nucleotide exchange was fluorimetrically measured using 0,5 µM mant-GDP. Baseline fluorescence was monitored within the first 15 min, followed by the addition of 1 µM RhoA or RhoG. Mant-GDP-bound Rho GTPases result in an increase of fluorescence signal. Values were normalized to baseline mant-GDP values. Recording settings: 25 °C, excitation 350 nm, emission 448 nm, measurement every 30 sec.

Deamidation of Gln61/63 of a Rho GTPase alters the chemical composition of the protein, resulting in a mass increment of 1 Dalton. Using mass spectrometry (MS), it was next analyzed whether RhoG is activated directly by CNF1 via deamidation. Recombinant RhoG and RhoA (as a positive control) were incubated for 4 hrs at 37 °C with recombinant GST-CNF1 at different molar ratios ranging from 5-20:1 (Rho GTPase:toxin) or left untreated. Initial experiments revealed that optimal ratio was 5:1 for RhoG and 20:1 for RhoA (data not shown). *In vitro* modified and untreated control Rho GTPases were subjected to SDS-PAGE and Coomassie staining to visualize proteins (Figure 3.5). Gel bands of relevant size (RhoA ≈ 51 kDa, RhoG ≈ 48 kDa) were excised for subsequent in-gel digestions with trypsin.

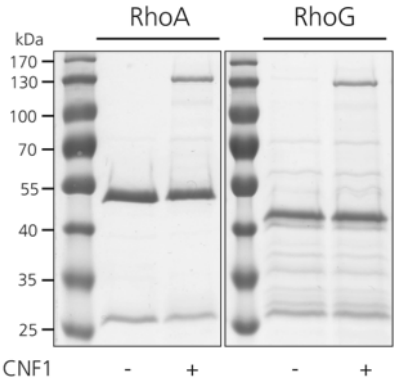

Figure 3.5: Coomassie staining of *in vitro* modified Rho GTPases.

Recombinant GST-RhoA and GST-RhoG were incubated with CNF1 (+) or left untreated (-). Samples were separated by SDS-PAGE and protein bands were visualized by Coomassie staining. Gel bands of corresponding protein size (RhoA = 51 kDa, RhoG = 48 kDa) were excised and processed for in-gel-digestion with trypsin. The additional band at 130 kDa corresponds to the size of CNF1.

The resulting tryptic peptides were analyzed by liquid chromatography/tandem mass spectrometry (LC/MS). Using reverse phase - high performance liquid chromatography (RP-HPLC), the peptides were separated according to their hydrophobicity. The chromatographic system was on-line coupled to the ion source of the mass spectrometer. In the mass spectrometer the mass/charge ratio (m/z) of the eluting peptides was determined. The mass spectrometer was operated in the positive mode, so that positively charged peptides (generally due to protonation, often two-fold or higher) could be detected. Thus, from the mass spectrometric data the elution profile for each peptide according to its mass/charge ratio can be derived (extracted ion chromatogram = EIC). However, the selective detection of a peptide and its deamidated derivative is complicated by the fact that peptides contain with a certain probability heavy isotopes (^{13}C, ^{2}H, ^{15}N), giving rise to a pattern of signals differing by a mass of 1 Da, the isotope pattern. Each molecule of a peptide containing a single heavy isotope will have the same mass as the deamidated form of the respective peptide containing no heavy isotope. Therefore, the EIC of the deamidated peptide will also display a fraction of the unmodified peptide representing all peptide molecules containing a single heavy isotope.

Figure 3.6 and Figure 3.7 summarize the MS results. Noteworthy, only samples of CNF1-intoxicated Rho GTPases are shown. Appropriate controls without CNF1-treatment were performed and are described in context. Mass spectrometric analysis of CNF1-treated recombinant RhoA identified an increase in mass in a 2009,9 Da peptide (QVELALWDTAGQEDYDR, amino acids 52 – 68, theoretical mass = 2008,9246 Da) covering the switch II region of RhoA (Figure 3.6, left). The respective ion of the peptide was detected at m/z = 1004,95 with a difference in isotope pattern of m/z = 0,5, indicating that the peptide ion was doubly charged (z = 2). Therefore, a shift of m/z = 0,5 between unmodified and modified peptide represented a mass shift of 1 Dalton that was due to deamidation of Gln63. Control experiments without toxin incubation did not lead to a mass shift of recombinant RhoA and relevant mass spectra contained isotope pattern of unmodified peptides only (data not shown). EIC of m/z = 1004,95 and m/z = 1005,452 revealed more details about the relative intensity and the isotopic composition of the relevant peptide ion (Figure 3.7, left). The EIC of m/z = 1004,95 displayed the elution property of the unmodified peptide. In contrast, at m/z = 1005,452 a second peak indicated the presence of the deamidated peptide. Due to equal mass of deamidated peptide and undeamidated peptide containing a single heavy isotope the signal appears as double peak. The relative intensity of the deamidated peptide was almost complete, indicating that CNF1 induced nearly complete deamidation of RhoA.

The mass spectra in Figure 3.6 (right) of the MS-analysis of recombinant RhoG detected a 2025,008 Da peptide, covering the region of interest in switch II (amino acids 50 – 68, theoretical mass = 2023,9355 Da) that increased in mass upon incubation with CNF1. At m/z = 1012,504 the relevant peptide ion was detected, and with a difference in isotope pattern of m/z = 0,5, the charge of this peptide was found to be 2. Indeed, a shift between unmodified and modified peptide was m/z = 0,5, representing a mass shift of 1 Dalton due to deamidation of Gln61. Control experiments without toxin incubation did not lead to a mass shift of recombinant RhoG and relevant mass spectra contained isotope pattern of unmodified peptides only (data not shown). Additionally, sequence analysis of CNF1 did not identify a 2024 Da peptide, which might mock a tryptic deamidated RhoG peptide. Figure 3.7 (right) shows the corresponding EICs of m/z = 1012,504 and m/z = 1013,007. The EIC of m/z = 1012,504 displayed the elution property of the unmodified peptide. At m/z = 1013,007 an additional peak was revealed, representing the deamidated peptide. The double peak at m/z 1013,007 results from identical masses of deamidated peptide and undeamidated peptide containing a single heavy isotope. The extent of modification is much lower compared to deamidated RhoA. Additional experiments with increasing incubation times of RhoG and toxin or various ratios of RhoG:CNF1 did not enhance the extent of deamidation (data not shown). Nevertheless, this analysis clarifies that RhoG is directly activated by CNF1 via deamidation of Gln61, but this modification occurs only partially under the experimental conditions tested.

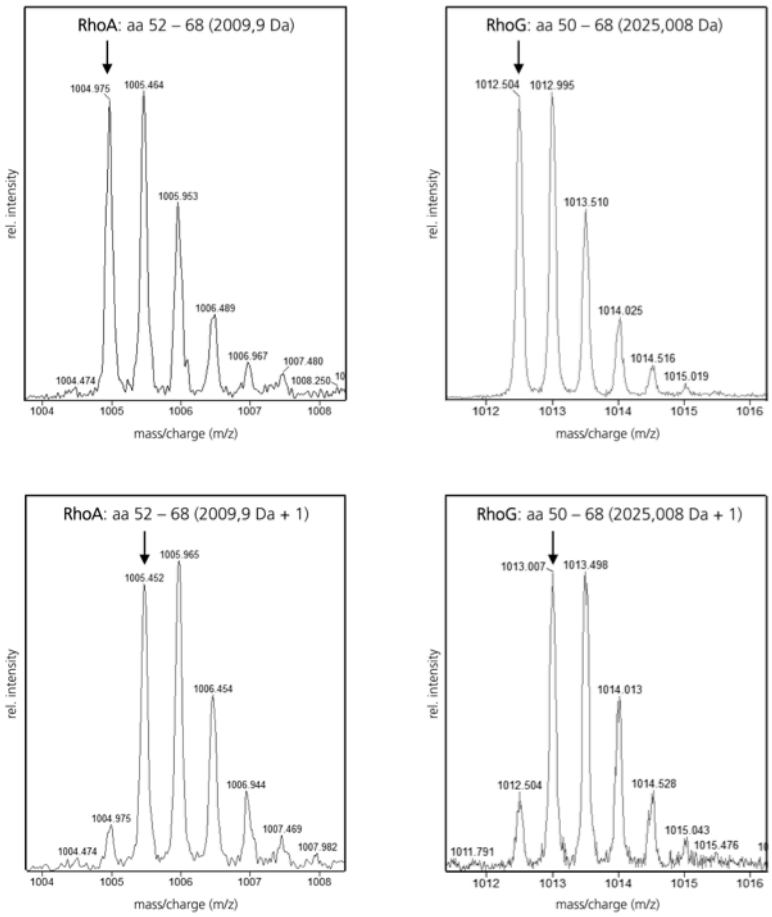

Figure 3.6: Mass spectrum reveals direct modification of RhoG by CNF1.

Purified recombinant Rho GTPases were incubated with CNF1 followed by digestion with trypsin. Tandem MS determined the masses of the tryptic peptides. Arrows indicate the monoisotopic masses of the peptides. **Top:** Mass spectra display isotope pattern of unmodified peptides of CNF1-treated recombinant RhoA and RhoG. x-axis = mass/charge ratio (m/z). y-axis = relative intensity. **Bottom:** Mass spectra display mass shift by 1 Da in isotope pattern of CNF1-treated recombinant RhoA and RhoG. x-axis = mass/charge ratio (m/z). y-axis = relative intensity.

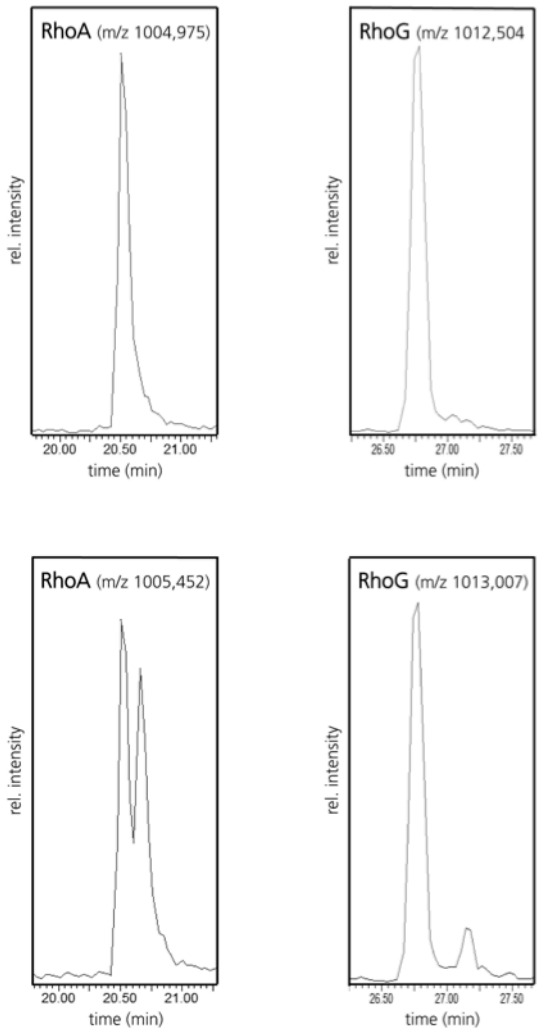

Figure 3.7: Partial deamidation of recombinant RhoG by CNF1.

Extracted ion chromatograms of LC/MC analysis of CNF1-treated recombinant RhoA and RhoG. **Top:** Extracted ion chromatograms of m/z 1004,975 and 1012,504 for RhoA and RhoG, respectively, displaying the elution property of the unmodified peptides. x-axis = retention time (minutes). y-axis = relative intensity. **Bottom**: Extracted ion chromatograms of m/z 1005,452 and 1013,007 for RhoA and RhoG, respectively. Peaks consist of 2 fractions: monoisotopic deamidated peptide and undeamidated peptide containing a single heavy isotope. x-axis = retention time (minutes). y-axis = relative intensity.

Together, RhoG was identified as a novel target of CNF-1 activation and subsequent degradation. CNF-1 activated RhoG directly through deamidation of a glutamine residue in the switch II region.

3.2 Role of RhoG in CNF1-mediated phenotypes

Next, the role of CNF1-induced RhoG activation during UPEC pathogenesis was explored. The role of RhoG was therefore investigated in several well-known CNF1-dependent cellular processes (Figure 3.8). Emphasis was primarily put on analyzing the role of CNF1-induced RhoG activation during induction of proinflammatory signaling pathways and bacterial invasion processes.

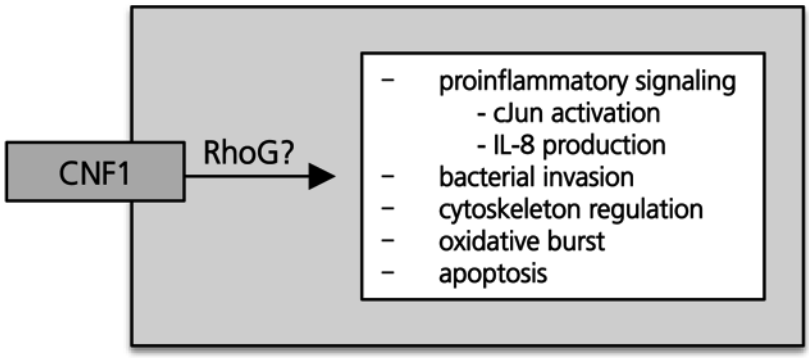

Figure 3.8: Possible RhoG-dependent CNF1 effects.

For these experiments siRNA knockdown was employed to characterize the function of RhoG and the closely related Rac1. At the protein level, up to 98% knockdown of RhoG and up to 86% knockdown of Rac1 was achieved (Figure 3.9). Furthermore, RhoG knockdown did not significantly affect the expression of Rac1 and vice versa.

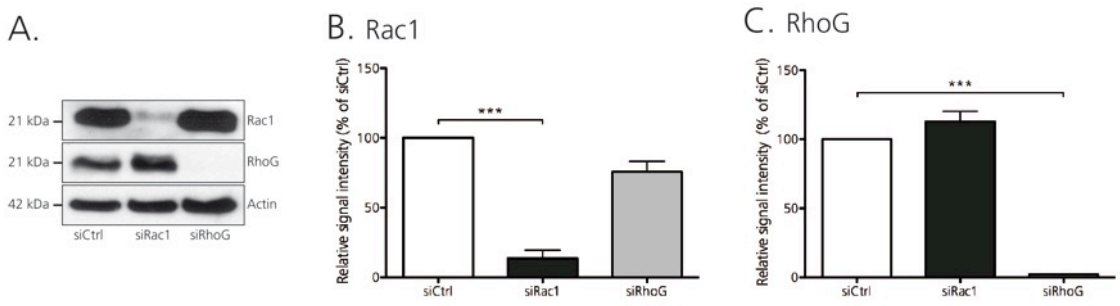

Figure 3.9: Knockdown efficiencies of Rac1 and RhoG.

HeLa cells were transfected with non-targeting (siCtrl), Rac1 (siRac1) or RhoG (siRhoG) siRNA. 72 hrs post-transfection cells were lysed and subjected to SDS-PAGE and Western blot. **(A)** Representative immunoblot with actin detection as loading control. Quantification of Rac1 **(B)** and RhoG **(C)** signal intensities were analyzed by densitometry using ImageJ software and are presented as a percentage of signal intensities of siCtrl transfected cells. Data are means ± SEM of 3 independent experiments. *** = $p < 0{,}001$. One-way ANOVA with Bonferroni's post test.

3.2.1 The role of RhoG in proinflammatory signaling

3.2.1.1 RhoG is not involved in CNF1-dependent activation of transcription factor cJun

Cells signal via different pathways in response to extracellular stimuli, including toxins. The stress-activated protein kinase (SAPK) pathway modulates gene expression in order to improve cell survival upon cellular stress. Rho GTPases relay stress signals and activate SAPKs, which in turn translocate into the nucleus. In the nucleus, the kinases phosphorylate transcription factors such as activator protein 1 (AP-1), which is a heterodimer composed of cJun and cFos, leading to specific gene expression, e.g. production of proinflammatory cytokines. In line with the impact of Rho GTPases on SAPK

activation, CNF1 is also implicated in the phosphorylation (i.e. activation) of cJun. Therefore, it was investigated whether RhoG regulates CNF1-induced activation of cJun. The nuclear phosphorylation of cJun was visualized using immunofluorescent staining of HeLa cells transfected with either control or RhoG siRNA. In the absence of CNF1 stimulation, there was not a significant accumulation of phosphorylated cJun in the nucleus of either control or RhoG knockdown cells (Figure 3.10A). However, upon stimulation with CNF1 intense nuclear phosphorylation of cJun was visible in control and RhoG knockdown cells (Figure 3.10B). Confocal images of immunostained cells were analyzed at various timepoints after stimulation with CNF1 and, at all timepoints tested, no discernible difference in CNF1-induced activation of cJun between control and RhoG knockdown cells was detected, suggesting that the phosphorylation of cJun by CNF1 was not regulated by RhoG.

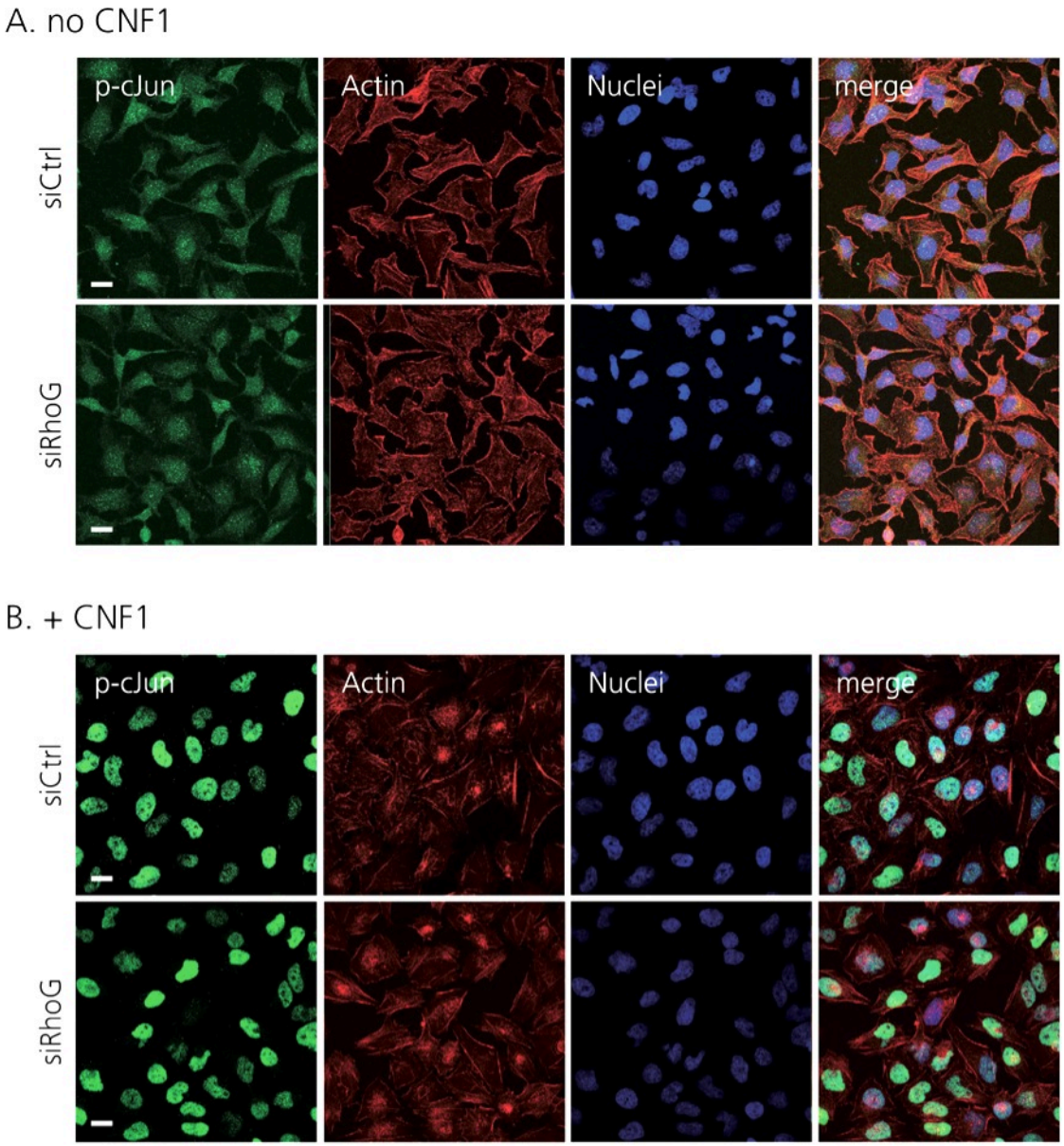

Figure 3.10: CNF1 intoxication results in RhoG-independent activation of transcription factor cJun.

HeLa cells were transfected with non-targeting (siCtrl) or RhoG (siRhoG) siRNA. 72 hrs post-transfection cells were either left untreated **(A)** or intoxicated for 2 hrs with 300 ng/ml CNF1 **(B)**. Cells were stained with phalloidin to label actin (red), DAPI to label cell nuclei (blue) and with a specific antibody against phosphorylated (activated) cJun (green). Images are en face Z-projections of confocal slices. Scale bars represent 20 µm.

In order to further assess whether RhoG played a role in CNF1-dependent cJun activation, cJun phosphorylation was also analyzed by immunoblotting (Figure 3.11).

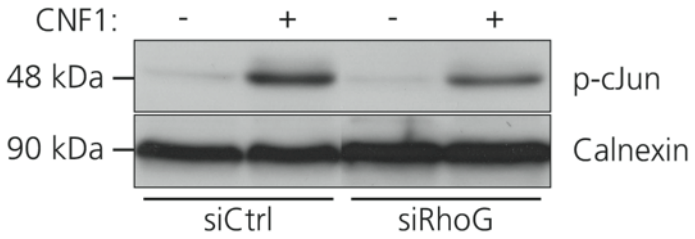

Figure 3.11: RhoG does not play a role in CNF1-mediated phosphorylation of cJun.

HeLa cells were transfected with non-targeting (siCtrl) or RhoG (siRhoG) siRNA. 72 hrs post-transfection cells were intoxicated for 2 hrs with 300 ng/ml CNF1 (+) or left untreated (-). Cells were lysed by the addition of SDS-sample buffer and subjected to SDS-PAGE and Western blot against phosphorylated cJun (p-cJun). Calnexin expression served as loading control. Western Blot analysis shown is a representative for at least 3 experiments performed.

In agreement with the immunofluorescence results presented above and previously published results (Lerm et al., 1999), CNF1 intoxication of HeLa cells resulted in phosphorylation of cJun. Significant variability in the degree of baseline cJun phosphorylation was observed between experiments, however RhoG did not influence the degree of cJun activation. Therefore, as observed via immunofluorescence and immunoblotting, CNF1-induced cJun activation is not dependent on RhoG.

3.2.1.2 RhoG is not involved in CNF1-dependent production of proinflammatory cytokine IL-8

The expression of proinflammatory cytokine interleukin 8 is regulated by the transcription factors AP-1, NF-κB and nuclear factor for IL-6 expression (NF-IL6) (Hoffmann et al., 2002). Intoxication of epithelial cells by CNF1 leads to IL-8 production, with Rac1 and Cdc42 being the main mediators (Falzano et al., 2003; Munro et al., 2004). CNF1-induced activation of cJun, which is part of the AP-1 complex, was found to be RhoG-independent, however RhoG could regulate the expression of IL-8 via alternative transcription factors. To investigate whether RhoG contributed to CNF1-induced production of IL-8, supernatants of cells exposed to CNF1 for different time periods were analyzed using ELISAs (Figure 3.12).

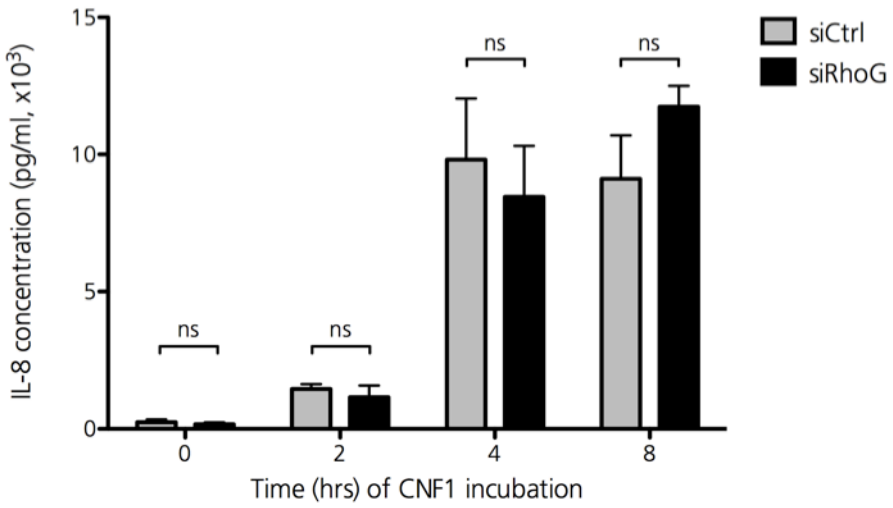

Figure 3.12: RhoG does not play a role in CNF1-induced IL-8 production.

HeLa cells were transfected with non-targeting (siCtrl) or RhoG (siRhoG) siRNA. 72 hrs post-transfection cells were intoxicated for indicated timepoints with 300 ng/ml CNF1. Thereafter, ELISAs for IL-8 were performed on culture supernatants. Data are means ± SEM of 2-4 independent experiments, each performed in duplicate. ns = not significant ($p > 0,05$). One-way ANOVA with Bonferroni's post test.

As expected, treatment of cells with CNF1 led to a significant and time-dependent increase in IL-8 secretion as compared to untreated cells. After 8 hrs of CNF1 intoxication there was slightly more IL-8 produced as compared with control cells, however this increase was not significant. At the timepoints tested, knockdown of RhoG had no significant effect on CNF1-induced IL-8 release.

Taken together, it was shown that CNF1 activates cJun and stimulates production of IL-8 by epithelial cells, but these effects are not dependent on RhoG.

3.2.2 The role of RhoG during CNF1-dependent invasion

Being a facultative intracellular pathogen, UPEC invades cells of the urinary tract to establish an intracellular niche. CNF1 is known to modulate the actin cytoskeleton and greatly enhances bacterial invasion (Figure 3.1; Lerm et al., 1999; Falzano et al., 2003) via its activation of various Rho GTPases. This study identified RhoG as a novel target of CNF1. Therefore, mechanisms involved in CNF1-dependent invasion, and more specifically, the role of RhoG, were investigated.

3.2.2.1 CNF1 increases invasion but not adherence of UPEC

First, the contribution of CNF1 to UPEC invasion into HeLa cells was examined. Cells pretreated with CNF1 were exposed to infection with UPEC strain UTI89 and invasion was determined by gentamicin protection assay that exclusively kills extracellular bacteria. CNF1 treatment of HeLa cells resulted in a significant increase in uptake of bacteria as compared to untreated cells (Figure 3.13A). Moreover, cells pretreated with GST or heat-inactivated CNF1 did not cause enhanced invasion of UPEC (Figure 3.13B). Additional adherence experiments were performed to validate that CNF1 increased bacterial entry

rather than influencing the adherence of bacteria to the cell surface. Indeed, intoxication of the cells with CNF1 did not affect the adherence, indicating that CNF1-induced invasion was not due to increased adherence (Figure 3.13C).

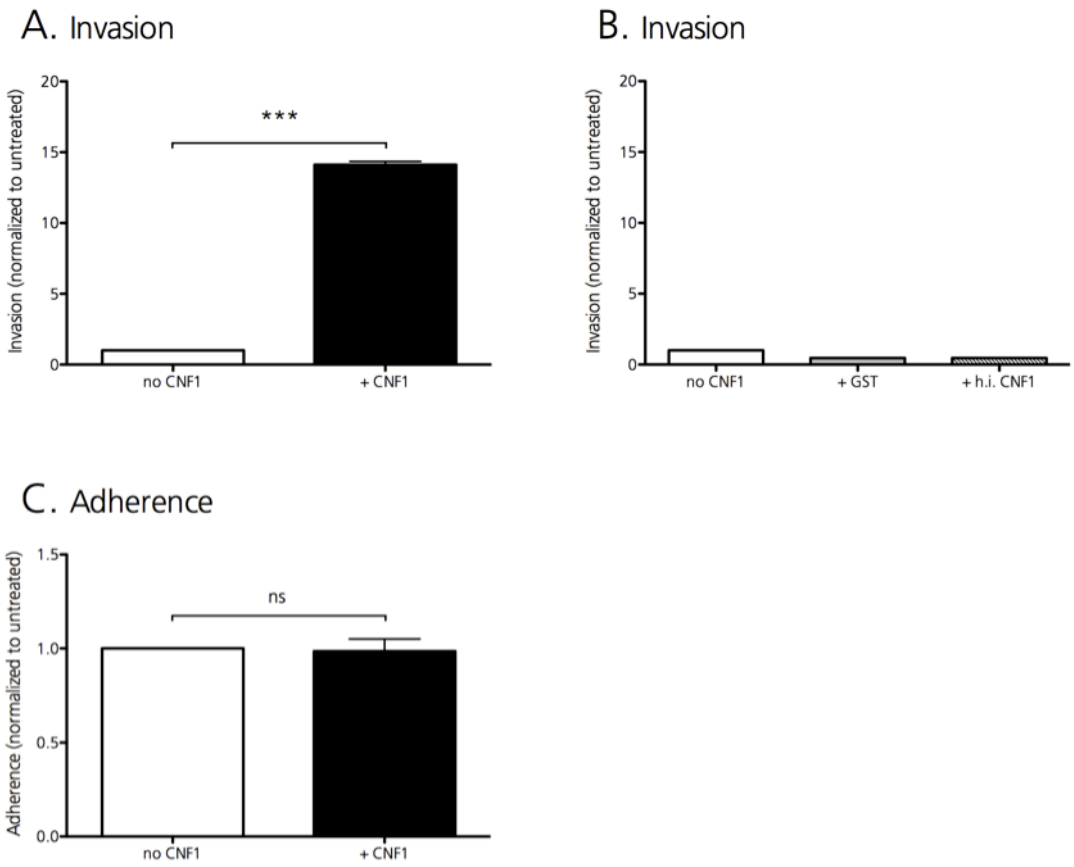

Figure 3.13: CNF1 increases UPEC invasion, but does not affect adherence.

(A) HeLa cells were preincubated for 2 hrs with 300 ng/ml CNF1 or left untreated, followed by infection with UTI89 for 1 h. Invasion was quantified using a gentamicin protection assay and normalized to invasion into untreated cells. **(B)** HeLa cells were preincubated for 2 hrs with 300 ng/ml heat-inactivated (h.i.) CNF1, GST or left untreated, followed by infection with UTI89 for 1 h. Invasion was quantified using a gentamicin protection assay and normalized to invasion into untreated cells. **(C)** HeLa cells were preincubated for 2 hrs with 300 ng/ml CNF1 or left untreated, followed by infection with UTI89 for 1 h. Adherence was quantified using an adherence assay and normalized to adherence to untreated cells. Data are means ± SEM of 1 **(B)** or 3 independent experiments **(A, C)** each performed in duplicate. ns = not significant ($p > 0,05$). *** = $p < 0,001$. Two-tailed, paired Student's t-test.

3.2.2.2 Adherence and invasion of UPEC is primarily FimH-dependent in both the presence and absence of CNF1 intoxication

UPEC express type 1 pili that mediate adherence to and invasion into host cells. The type 1 pili adhesin FimH binds mannose-containing glycoprotein receptors at the host cell surface. Expression of FimH by the UTI89 strain was confirmed by its ability to agglutinate yeast. FimH-dependent adherence was tested by antagonizing UTI89 adherence with soluble D-mannose in the presence and absence of CNF1 intoxication. In both cases, adherence of UTI89 was significantly blocked by the addition of D-mannose, confirming

the dependence of FimH for bacterial adherence (Figure 3.14A). In order to determine whether CNF1-induced invasion requires FimH or whether an alternate mechanism of uptake is employed, FimH was antagonized by the addition of D-mannose during gentamicin protection assays. Treatment of cells with mannose significantly reduced CNF1-dependent and -independent invasion relative to unblocked controls (Figure 3.14B). Despite the strong inhibition of invasion by mannose, there was a low amount of FimH-independent invasion. It is noteworthy that CNF1-mediated invasion showed a significant increase in FimH-independent invasion compared cells not intoxicated with CNF1. Collectively, in both the presence and absence of CNF1, UPEC adherence and invasion is strongly dependent on FimH expression, however in the case of CNF1-induced invasion, other uptake mechanisms might be involved.

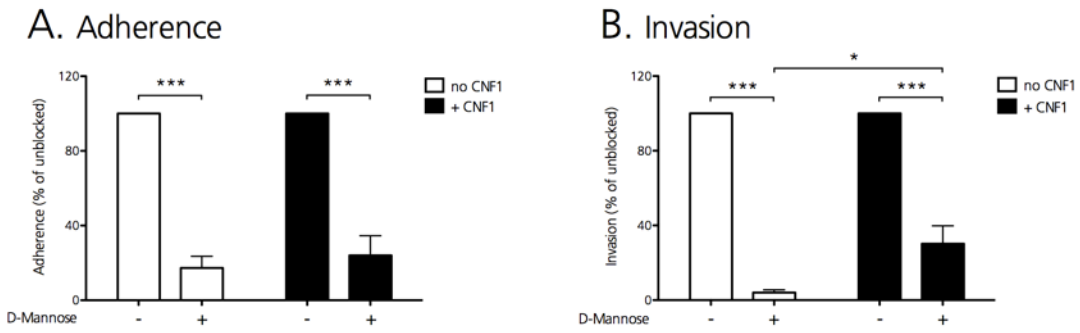

Figure 3.14: Mannose blocks bacterial adherence and invasion in both the presence and absence of CNF1.

HeLa cells were preincubated with 300 ng/ml CNF1 or left untreated in combination with (+) or without (-) addition of 2,5 % D-mannose. Thereafter, cells were infected with UTI89 for 1 h. **(A)** Adherence was quantified using an adherence assay and is presented as relative to bacterial adherence to cells not treated with mannose. **(B)** Invasion was quantified using a gentamicin protection assay and is presented as relative to bacterial invasion into cells not treated with mannose. Data are means ± SEM of 3 independent experiments, each performed in duplicate. * = $p < 0,05$. *** = $p < 0,001$. One-way ANOVA with Bonferroni's post test.

3.2.2.3 Rac1 is necessary for CNF1-dependent and -independent invasion of UPEC

The contribution of Rac1 to CNF1-induced invasion has already been established (Doye et al., 2002; Visvikis et al., 2011). Accordingly, it was confirmed that CNF1-induced bacterial uptake was significantly decreased in cells depleted of Rac1 (Figure 3.15A), indicating that the majority of the CNF1-effect on bacterial invasion was attributable to Rac1 activation. Loss of Rac1 further decreased CNF1-independent invasion (Figure 3.15A). The importance of CNF1-induced activation of Rac1 was additionally proven using gentamicin assays with wildtype Rac1 ($Rac1^{+/+}$) and Rac1 knockout ($Rac1^{-/-}$) mouse embryonic fibroblasts (MEFs). $Rac1^{+/+}$ cells displayed significant higher levels of invaded UPEC upon CNF1-stimulation than $Rac1^{-/-}$ cells (Figure 3.15B). In fact, almost no invasion of bacteria into $Rac1^{-/-}$ cells was detectable, either with or without pretreatment with CNF1. These

experiments confirmed that Rac1 is necessary for CNF1-dependent and -independent invasion of UPEC.

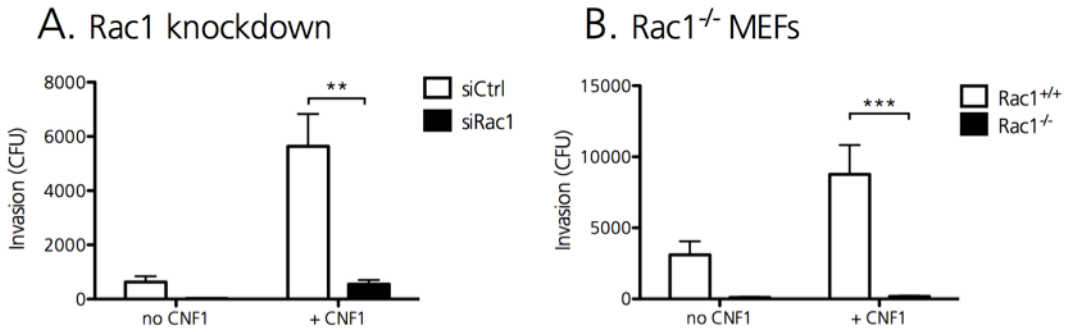

Figure 3.15: Rac1 is necessary for CNF1-dependent and -independent invasion of UPEC.

(A) HeLa cells were transfected with non-targeting (siCtrl) or Rac1 (siRac1) siRNA. 72 hrs post-transfection cells were preincubated for 2 hrs with 300 ng/ml CNF1 or left untreated, followed by infection with UTI89 for 1 h. Invasion was quantified using a gentamicin protection assay and is presented as colony forming units (CFU) per 500 µl. **(B)** $Rac1^{+/+}$ and $Rac1^{-/-}$ cells were preincubated for 2 hrs with 300 ng/ml CNF1 or left untreated, followed by infection with UTI89 for 1 h. Invasion was quantified using a gentamicin protection assay and is presented as colony forming units (CFU) per 500 µl. Data are means ± SEM of at least 3 independent experiments, each performed in duplicate. ** = $p < 0,01$. *** = $p < 0,001$. One-way ANOVA with Bonferroni's post test.

3.2.2.4 RhoG is recruited to sites of UPEC infection

To evaluate the involvement of RhoG in CNF1-induced invasion it was first investigated whether RhoG is recruited to sites of UPEC infection. Additionally, the localization of Rac1 in CNF1-intoxicated cells during infection was monitored, as its significance in bacterial entry is already known. Using immunofluorescent staining of HeLa cells transfected with Rac1-GFP and infected with UPEC strain UTI89 confirmed that Rac1 is recruited to bacterial entry sites in untreated and CNF1-intoxicated cells. Cells transfected with RhoG-GFP and infected with UTI89 revealed that RhoG is also recruited to sites of infection in untreated and CNF1-intoxicated cells (Figure 3.16). These data suggest that RhoG could play a functional role in UPEC invasion.

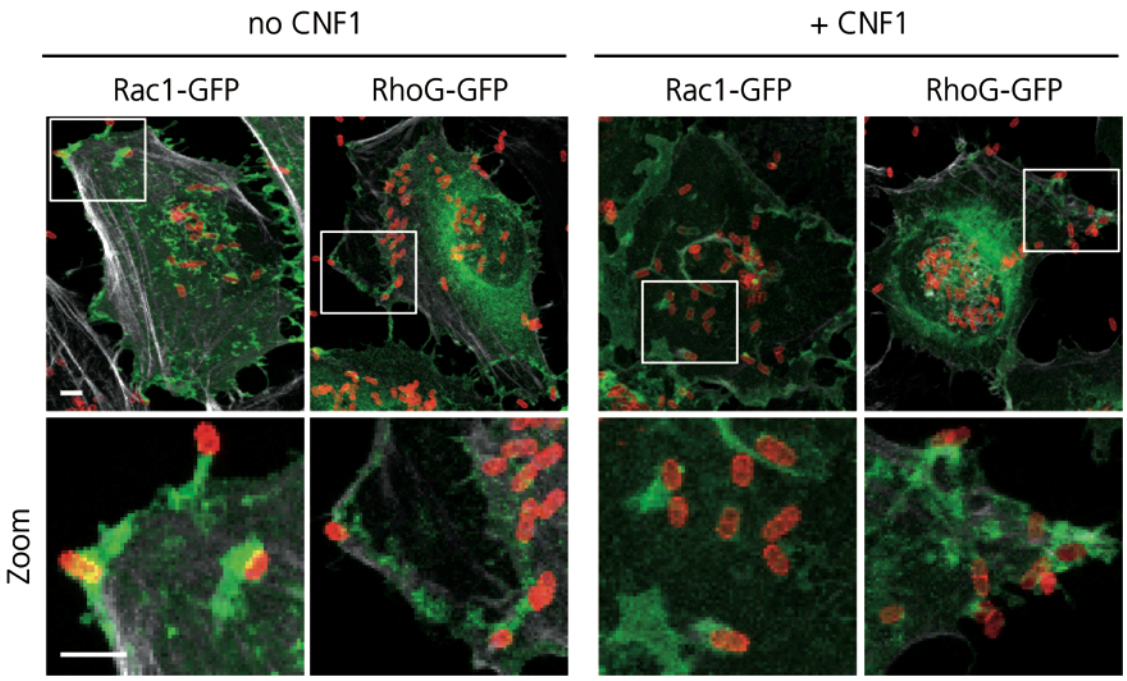

Figure 3.16: Rac1 and RhoG localize to sites of UPEC infection.

HeLa cells were transfected with wildtype Rac1-GFP or wildtype RhoG-GFP. 24 hrs post-transfection cells were incubated for 2 hrs with 300 ng/ml CNF1 or left untreated. After infection with UTI89 for 1 h cells were stained with phalloidin to label actin (grey) and an *E. coli* antiserum to label bacteria (red). Images are en face Z-projections of confocal slices. Scale bars represent 5 µm.

3.2.2.5 Knockdown of RhoG increases invasion of UPEC

CNF1-mediated UPEC invasion is primarily Rac1-dependent, however we identified RhoG as a novel target of CNF1 and observed recruitment of RhoG to sites of UPEC infection. Therefore a functional role for RhoG during CNF1-induced bacterial uptake was pursued using gentamicin protection assays with cells depleted of RhoG by siRNA knockdown. Despite the fact that RhoG was recruited to sites of UPEC infection in untreated cells (Figure 3.16), RhoG did not influence the amount of invaded bacteria (Figure 3.17A). However, in CNF1 intoxicated cells, knockdown of RhoG led to a significant increase in invasion compared to control (Figure 3.17A). In order to determine whether the observed increase in invasion of UPEC upon RhoG knockdown was due to enhanced bacterial adherence, adherence assays were performed. Adherence to RhoG knockdown cells remained unaffected independent of CNF1-preincubation of cells (Figure 3.17B). Therefore, these data suggest that RhoG indeed plays a role in CNF1-induced invasion and may act as a negative regulator of Rac1-triggered UPEC invasion.

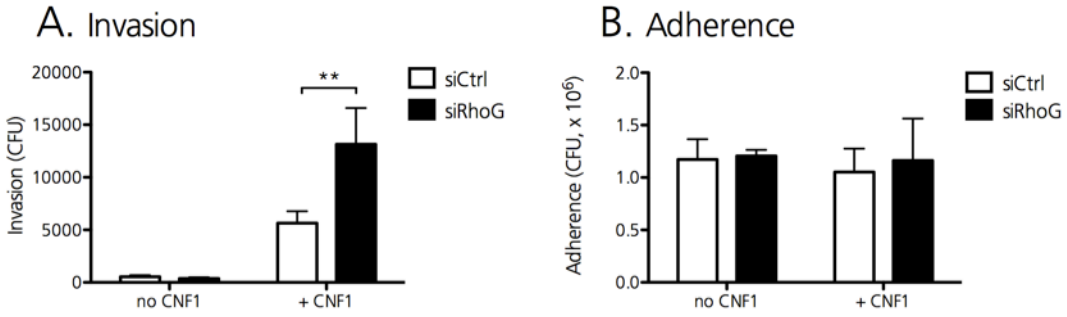

Figure 3.17: Knockdown of RhoG increases CNF1-induced invasion, but not adherence.

HeLa cells were transfected with non-targeting (siCtrl) or RhoG (siRhoG) siRNA. 72 hrs post-transfection cells were preincubated for 2 hrs with 300 ng/ml CNF1 or left untreated, followed by infection with UTI89 for 1 h. **(A)** Invasion was quantified using a gentamicin protection assay and is presented as colony forming units (CFU) per 500 µl. **(B)** Adherence was quantified using an adherence assay and presented as colony forming units (CFU) per 500 µl. Data are means ± SEM of at least 3 independent experiments, each performed in duplicate. ** = $p < 0,01$. One-way ANOVA with Bonferroni's post test.

To further strengthen and verify the inhibitory effect of RhoG on CNF1-induced invasion, immunofluorescent inside/outside staining was used to quantify intracellular bacteria. HeLa cells were depleted for either Rac1 or RhoG and preincubated with CNF1 or left untreated prior to infection with UTI89. Therefore, as already asserted with gentamicin protection assays, immunofluorescent staining confirmed that CNF1-induced invasion was decreased when Rac1 is knocked down and further increased when RhoG is depleted (Figure 3.18A). Quantitative analysis of inside/outside staining was performed and supported the findings that RhoG does not affect CNF1-independent invasion (Figure 3.18B), but significantly inhibits CNF1-induced invasion (Figure 3.18C). Compared to control cells, CNF1-independent and -dependent invasion was reduced when Rac1 was knocked down, however this decrease was not significant (Figure 3.18B, C).

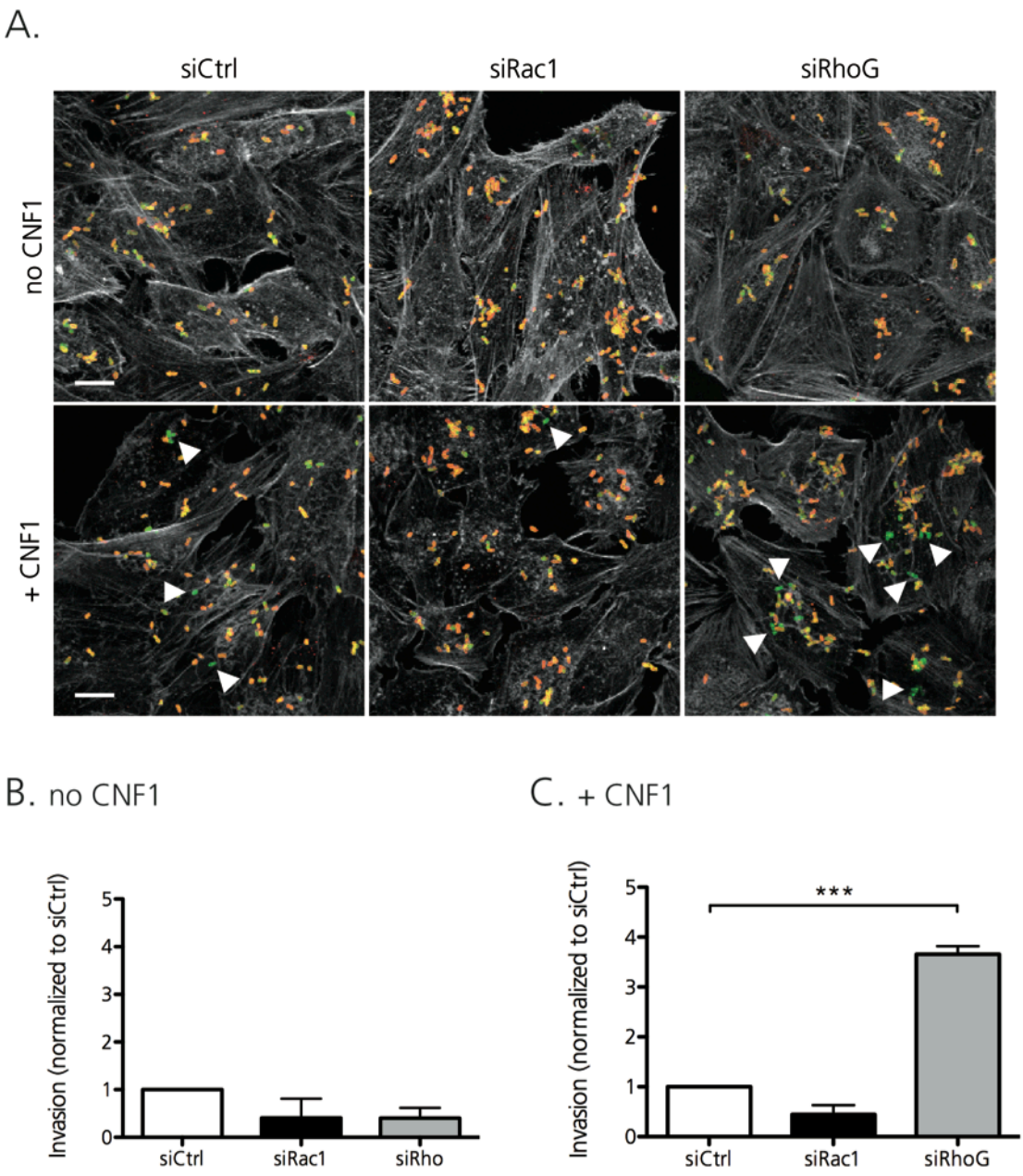

Figure 3.18: RhoG inhibits CNF1-induced invasion.

HeLa cells were transfected with non-targeting (siCtrl), Rac1 (siRac1) or RhoG (siRhoG) siRNA. 72 hrs post-transfection cells were preincubated for 2 hrs with 300 ng/ml CNF1 or left untreated, followed by infection with UTI89 for 1h. **(A)** Inside/outside staining was used to differentiate extracellular from intracellular bacteria. Extracellular bacteria appear orange while intracellular bacteria are green. Arrowheads indicate examples of internalized bacteria. Images are en face Z-projections of confocal slices and representative of 3 independent experiments. Scale bars represent 20 µm. Invasion into non-stimulated **(B)** or CNF1-intoxicated **(C)** cells was determined using inside/outside staining and is expressed as invasion normalized to invasion into siCtrl transfected cells. Data are means ± SEM of 3 independent experiments. For each experiment, at least 90 cells per condition were analyzed. *** = $p < 0{,}001$. One-way ANOVA with Bonferroni's post test.

These data collected by another method validated that in presence of CNF1, loss of RhoG further increases invasion compared to invasion into control cells.

3.2.2.6 The inhibitory effect of RhoG on UPEC invasion involves Rac1

It was shown that CNF1-stimulated invasion of UPEC is primarily mediated by Rac1 and inhibited by RhoG. Accordingly, the question then arose whether RhoG inhibits CNF1-stimulated invasion in absence of Rac1 or whether its inhibitory function is dependent on Rac1. To address this question, invasion of UTI89 was assayed using gentamicin protection assays with Rac1$^{-/-}$ fibroblasts transfected with control or RhoG siRNA. Invasion into Rac1$^{-/-}$ cells was generally very low - bordering on the level of detection of bacteria - due to the strong impact on Rac1 on invasion. Notably, invasion into Rac1 knockout cells did not significantly increase upon CNF1 stimulation, verifying that UPEC invasion is primarily Rac1-dependent (Figure 3.19A). In CNF1-intoxicated cells, knockdown of RhoG did not change the level of invaded UTI89 as compared to siCtrl transfected cells (Figure 3.19A). The knockdown efficiency of RhoG in these cells was determined by Western blotting analysis (Figure 3.19B). Together, this suggests that Rac1 is required for the inhibitory effect of RhoG on invasion and that RhoG acts in crosstalk with Rac1 to influence CNF1-dependent invasion.

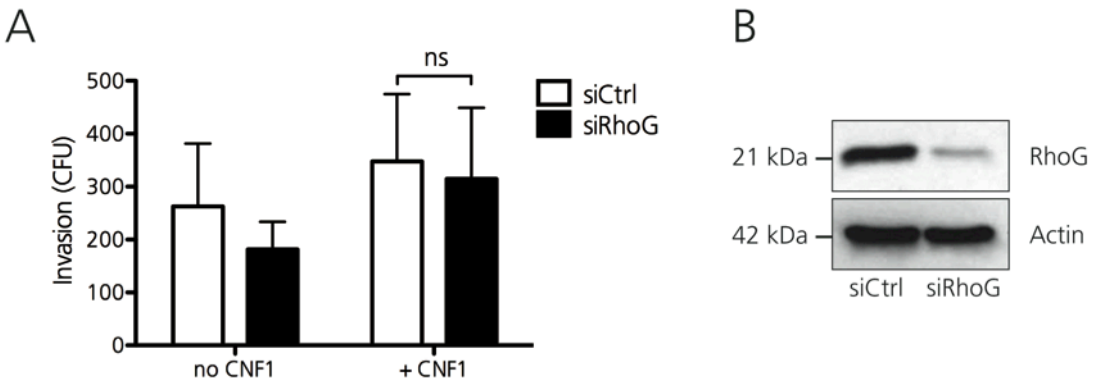

Figure 3.19: Inhibitory effect of RhoG on CNF1-stimulated invasion is dependent on Rac1.

Rac1$^{-/-}$ MEFs were transfected with non-targeting (siCtrl) or RhoG (siRhoG) siRNA. 72 hrs post-transfection cells were preincubated for 2 hrs with 300 ng/ml CNF1 or left untreated, followed by infection with UTI89 for 1 h. **(A)** Invasion was quantified using a gentamicin protection assay and is presented as colony forming units (CFU) per 500 µl. Data are means ± SEM of 4 independent experiments, each performed in duplicate. ns = not significant ($p > 0,05$). One-way ANOVA with Bonferroni's post test. **(B)** Western blot analysis of RhoG in cell lysates 72 hrs post-transfection with either siCtrl or siRhoG. Immunoblotting for actin served as a loading control.

3.2.2.7 Expression of constitutively active Rho GTPases increase invasion only in the absence of CNF1

Assuming that CNF1-induced RhoG activation inhibits invasion it was next investigated whether invasion into cells expressing constitutively active RhoG was decreased. Gentamicin protection assays were performed with HeLa cells transfected with constitutively active mutants of either Rac1 or RhoG. As expected, in the absence of CNF1, activation of Rac1 resulted in significantly enhanced levels of UTI89 invasion

compared to control transfected cells (Figure 3.20). CNF1-induced invasion was not affected by overexpression of active forms of Rac1 or RhoG (Figure 3.20).

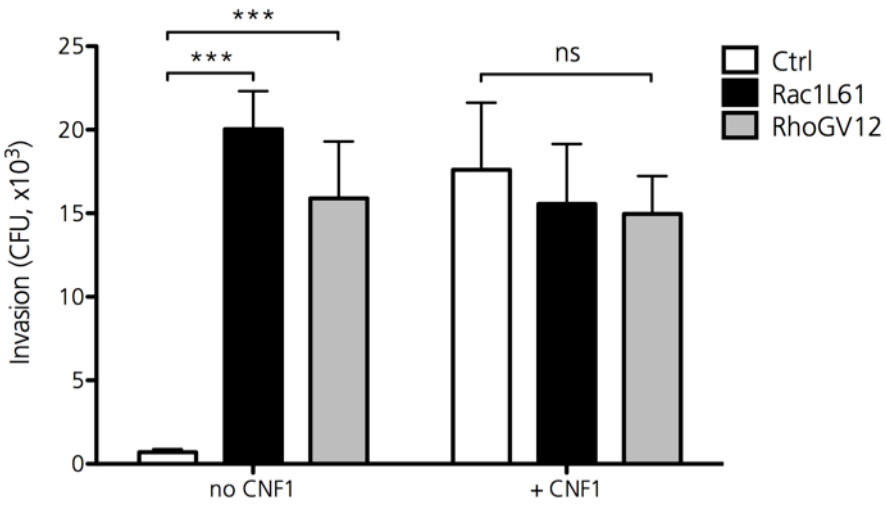

Figure 3.20: Constitutively active Rho GTPases increase invasion only in the absence of CNF1.

HeLa cells were transfected with empty control vector (Ctrl) or constitutively active mutants of Rac1 (Rac1L61) or RhoG (RhoGV12). 24 hrs post-transfection cells were preincubated for 2 hrs with 300 ng/ml CNF1 or left untreated, followed by infection with UTI89 for 1 h. Invasion was quantified using a gentamicin protection assay and is presented as colony forming units (CFU) per 500µl. Data are means ± SEM of 5 independent experiments, each performed in duplicate. *** = $p < 0{,}001$. ns = not significant ($p > 0{,}05$). One-way ANOVA with Bonferroni's post test.

As expression of constitutively active RhoG did not show inhibition of CNF1-mediated invasion as one might have expected, experiments were designed lacking CNF1 intoxication to test whether activated RhoG inhibited Rac1. In this way, additional effects of CNF1 (e.g. on GTPases or other proteins) were excluded. Simultaneous activation of Rac1 and RhoG was achieved by co-transfecting HeLa cells with a deamidation mimic of Rac1 combined with constitutively active RhoG to mimic the CNF1-effect. Invasion of UTI89 into these cells was compared to cells that were co-transfected with the deamidated mutant of Rac1 combined with wildtype RhoG. Additionally as controls, HeLa cells were singly transfected with all constructs used for these experiments.

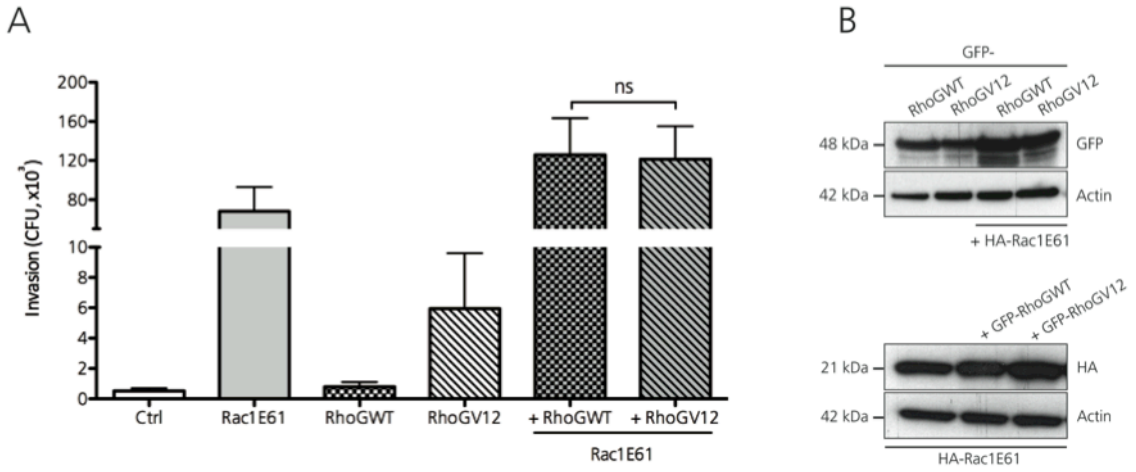

Figure 3.21: Constitutively active RhoG does not inhibit Rac1-triggered invasion in absence of CNF1.

HeLa cells were either single transfected with empty control vector (Ctrl), constitutively active Rac1 (Rac1E61), wildtype RhoG (RhoGWT) or constitutively active RhoG (RhoGV12) or cotransfected with Rac1E61 and wildtype RhoG or Rac1E61 and RhoGV12. 24 hrs post-transfection cells were infected with UTI89 for 1 h. **(A)** Invasion was quantified using a gentamicin protection assay and is presented as colony forming units (CFU) per 500µl. Data are means ± SEM of 3 independent experiments, each performed in duplicate. ns = not significant ($p > 0,05$). One-way ANOVA with Bonferroni's post test. **(B)** 24 hrs post-transfection cells were lysed and subjected to SDS-PAGE and Western blot analysis to detect expression levels of GFP- or HA-tagged Rho GTPases. Actin expression served as loading a control.

As previously shown (Figures 3.17A, 3.18B), wildtype RhoG does not influence UPEC invasion, whereas constitutively active mutants of RhoG and Rac1 increased bacterial uptake as seen in Figure 3.20. Expression of the deamidation mimic of Rac1 remarkably enhanced UTI89 invasion, however, when cotransfected with constitutively active RhoG, invasion of UTI89 was not significantly different than when cotransfected with wildtype RhoG (Figure 3.21A). Thus, constitutively active RhoG did not inhibit Rac1-dependent invasion, suggesting that constitutively active RhoG acts differently than CNF1-activated RhoG. The expression level of all constructs was determined by Western blotting analysis (Figure 3.21B).

Therefore, we have provided evidence that CNF1-activated RhoG inhibits Rac1-dependent invasion of UPEC, however, there could be additional regulatory factors that are responsible for this apparent crosstalk between Rac1 and RhoG.

3.3 Analysis of RhoG-dependent Rac1 functions

Rho GTPases are not only regulated by GEFs or GAPs, rather, there are alternative ways to modulate their activity. Regulatory mechanisms of Rho GTPase activity include subcellular localization, degradation processes and the influence of up- or downstream effectors. Moreover, there is considerable crosstalk between Rho GTPases, which can stimulate or inhibit their activation directly or indirectly. As this study revealed that RhoG plays a role in a mainly Rac1-triggered process, it was subsequently analyzed how RhoG could influence Rac1 activity, thereby leading to an inhibitory effect on CNF1-induced invasion (Figure 3.22).

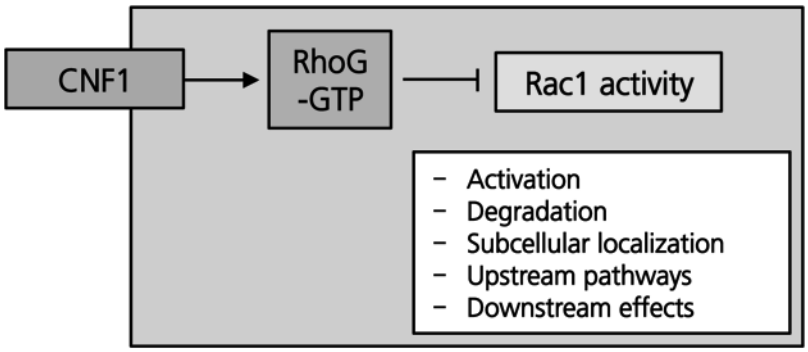

Figure 3.22: Possible mechanisms of how RhoG might modulate Rac1 activity.

3.3.1 RhoG does not influence Rac1 activation

RhoG can signal upstream or in parallel to Rac1 depending on the signaling pathway involved (Katoh et al., 2006). Therefore, the interdependence of RhoG and Rac1 activation by CNF1 was investigated. We first tested whether knockdown of RhoG enhanced CNF1-induced Rac1 activation, thereby leading to increased bacterial invasion. Pulldown assays using GST-PAK-CRIB were performed from lysates of HeLa cells depleted of RhoG by siRNA transfection and stimulated with CNF1. Western blot analysis displayed equal Rac1 activation upon CNF1-stimulation in cells depleted of RhoG and in control cells (Figure 3.23A). Quantifications of Western blot signals by densitometry confirmed that RhoG depletion did not significantly change activation of Rac1 upon CNF1 treatment (Figure 3.23B). Conversely, it was determined whether RhoG activation by CNF1 is dependent on Rac1. Rac1 was depleted by siRNA knockdown in HeLa cells and CNF1-induced RhoG activation was measured by pulldown assays using GST-ELMO2NT. Immunoblots displayed that RhoG activation after CNF1 stimulation occurred to the same extent in Rac1 knockdown cells as in control transfected cells (Figure 3.23C). This finding was quantitatively evaluated and did not show a significant difference in RhoG activation between control and Rac1 siRNA transfected cells (Figure 3.23D).

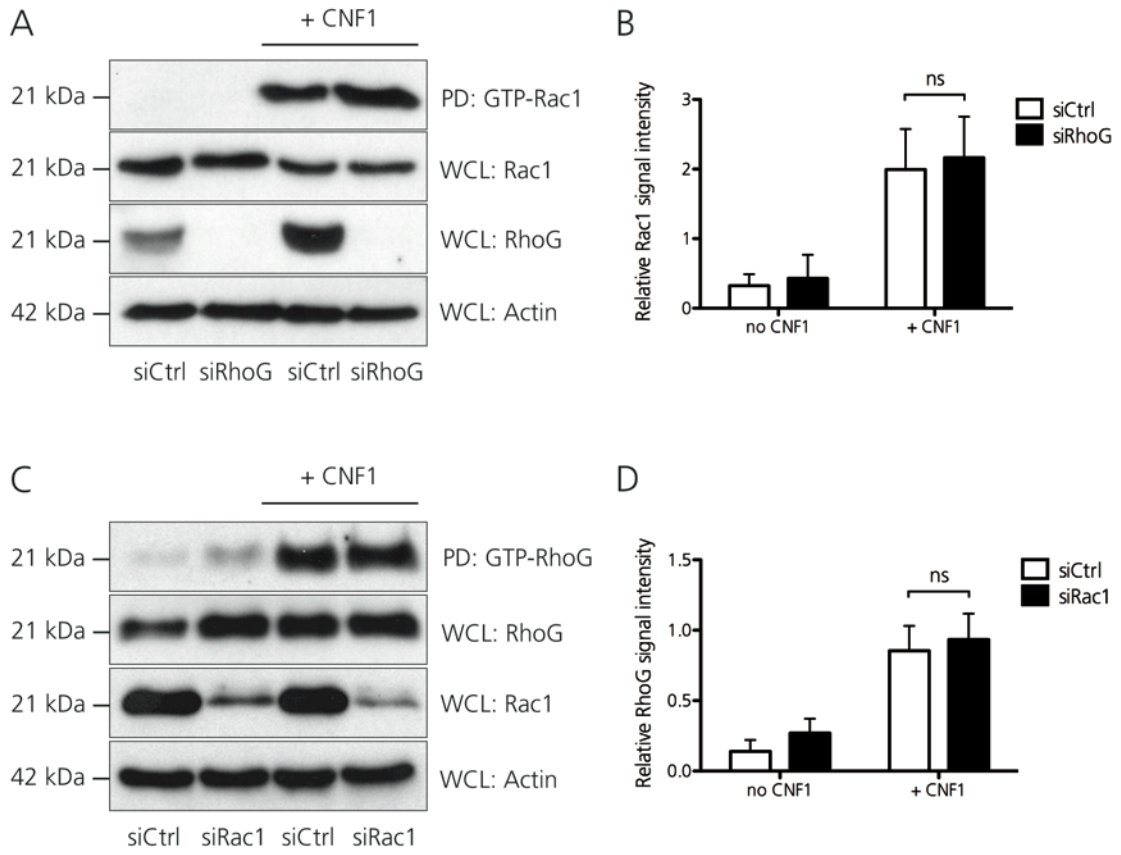

Figure 3.23: CNF1-induced activation of RhoG and Rac1 are not interdependent.

(A) HeLa cells were transfected with non-targeting (siCtrl) or RhoG (siRhoG) siRNA. 72 hrs post-transfection cells were incubated with 300 ng/ml CNF1 for 2 hrs or left untreated. Active Rac1 was precipitated with GST-PAK-CRIB from cell lysates and samples were subjected to SDS-PAGE and Western blot against Rac1 and RhoG. Actin expression served as loading control. (B) Rac1 activation was quantified by densitometry of signal intensities using ImageJ software and presented as relative signal intensities (active Rac1/total Rac1). Data are means ± SEM of 4 independent experiments. ns = not significant ($p > 0,05$). One-way ANOVA with Bonferroni's post test. (C) HeLa cells were transfected with non-targeting (siCtrl) or Rac1 (siRac1) siRNA. 72 hrs post-transfection cells were incubated with 300 ng/ml CNF1 for 2 hrs or left untreated. Active RhoG was precipitated with GST-ELMO2NT from cell lysates and samples were subjected to SDS-PAGE and Western blot against RhoG and Rac1. Actin expression served as loading control. (D) RhoG activation was quantified by densitometry of signal intensities using ImageJ software and presented as relative signal intensities (active RhoG/total RhoG). Data are means ± SEM of 2 independent experiments. ns = not significant ($p > 0,05$). One-way ANOVA with Bonferroni's post test. PD = pulldown. WCL = whole cell lysates.

These data revealed that CNF1-induced activation of Rac1 and RhoG are not interdependent and do not allude to crosstalk between each other at the level of activation. Therefore, RhoG must influence Rac1-triggered UPEC invasion by another means.

3.3.2 RhoG does not influence Rac1 localization

The activity of Rho GTPases is also regulated by their subcellular localization. Upon activation, Rho GTPases need to be localized from the cytoplasm to the plasma membrane where they regulate cytoskeleton rearrangements (Bustelo et al., 2007). Therefore it was hypothesized that upon activation by CNF1, RhoG might promote mislocation of activated Rac1 thereby compromising Rac1 function. To investigate whether RhoG plays a potential

role in subcellular localization of active Rac1 upon CNF1 stimulation, HeLa cells were depleted of RhoG by siRNA transfection and additionally transfected with Rac1-GFP. After CNF1-stimulation immunofluorescent staining was performed using phalloidin to label actin. Without CNF1 treatment, subcellular localization of Rac1-GFP was not noticeably altered in RhoG depleted cells compared to control cells (Figure 3.24A). Rac1 localized throughout the cytoplasm and was primarily absent at peripheral plasma membranes. As confocal images of xz-sections depicted (Figure 3.25A), Rac1 was distributed apically in control cells as well as in RhoG knockdown cells. CNF1 treatment induced extensive morphological changes, with cells displaying a higher content of filamentous actin. Prominent membrane protrusions like ruffles were visible to the same extent in RhoG depleted and control cells (Figure 3.24B). Furthermore, Rac1-GFP relocalized from the cytosol to the plasma membrane accumulating at sites of actin remodeling like CNF1-induced actin ruffles. As xz-sections of confocal images displayed, CNF1-activated Rac1 localized to apical membrane extensions that were highly heterogeneous structures due to their dynamic nature (Figure 3.25B). RhoG depletion did not result in any mislocation of Rac1. Hence, localization of CNF1-induced activated Rac1 was not affected by RhoG, indicating that RhoG interferes with Rac1 via an alternative mechanism.

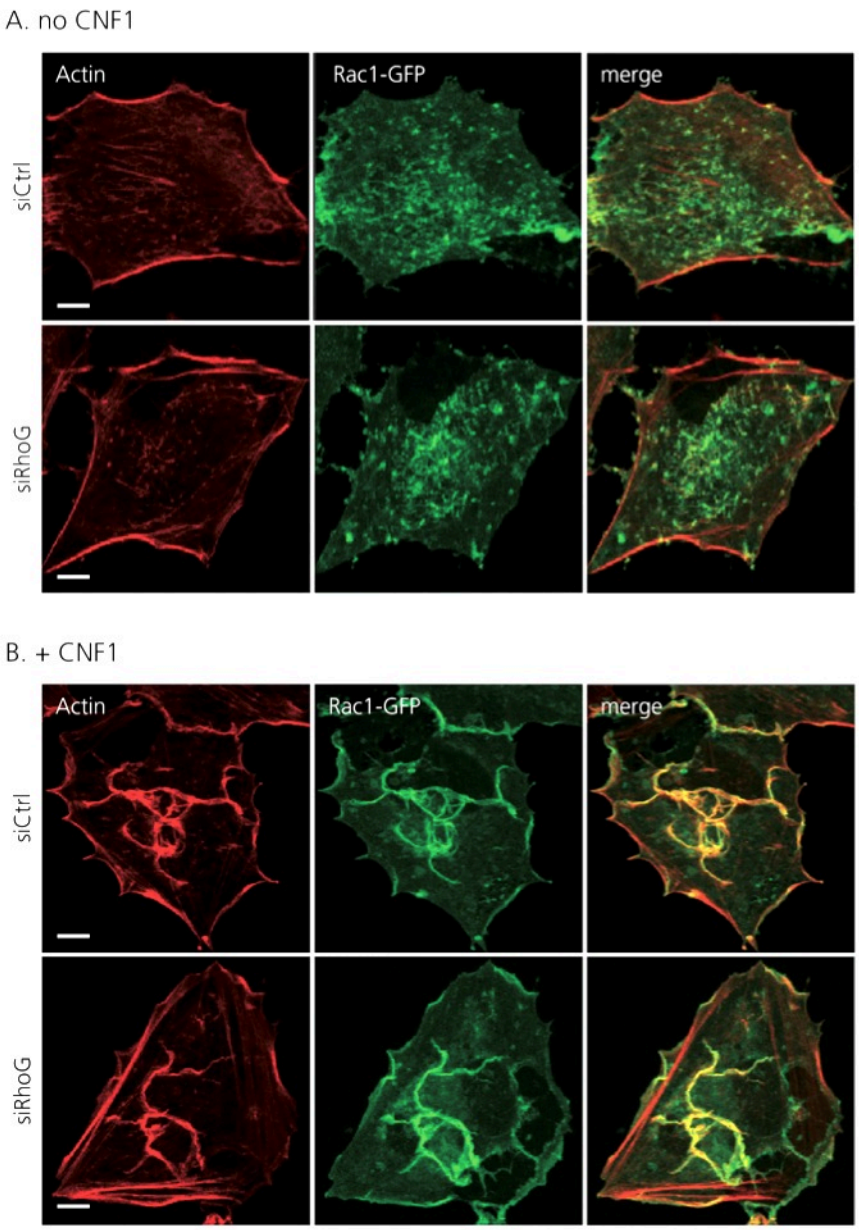

Figure 3.24: Knockdown of RhoG does not change subcellular localization of Rac1 without or with CNF1.

HeLa cells were transfected with non-targeting (siCtrl) or RhoG (siRhoG) siRNA, followed by transfection with wildtype Rac1-GFP. Cells were either left untreated **(A)** or intoxicated for 2 hrs with 300 ng/ml CNF1 **(B)**. Immunofluorescent staining labeled actin (red) using phalloidin. Images are en face Z-projections of confocal slices. Scale bars represent 10 µm.

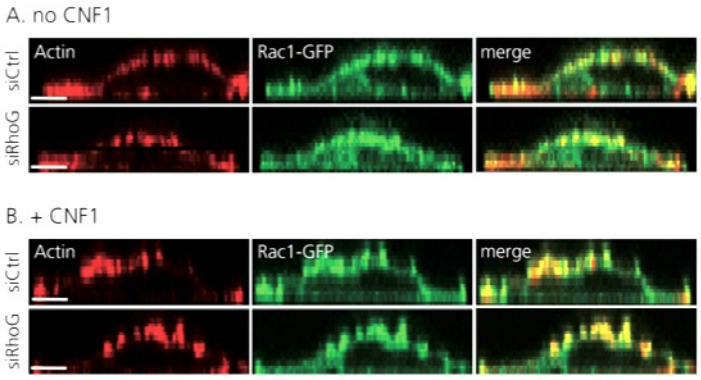

Figure 3.25: CNF1 induces Rac1 localization to actin membrane protrusions independent on RhoG.

HeLa cells were transfected with non-targeting (siCtrl) or RhoG (siRhoG) siRNA, followed by transfection with wildtype Rac1-GFP. Cells were either left untreated **(A)** or intoxicated for 2 hrs with 300 ng/ml CNF1 **(B)** and immunofluorescent staining with phalloidin was performed to label actin (red). Images are xz-sections of confocal stacks. Scale bars represent 5 µm.

3.3.3 RhoG does not play a role in CNF1-induced Rac1 degradation

CNF1 induces only a transient increase in the amount of activated Rho GTPases, as cell-mediated processes subsequently degrade activated Rho GTPases. Efficient invasion of UPEC was shown to be dependent upon both the initial activation Rac1 by CNF1 and as well as its subsequent degradation (Doye et al., 2002). This led to the question of whether RhoG's inhibitory effect on CNF1-induced invasion may be due to an inhibitory effect on Rac1 degradation. HeLa cells were depleted of RhoG by siRNA transfection and the level of Rac1 was analyzed at different timepoints after stimulation with CNF1 by immunoblotting. As already shown in Figure 3.2B, CNF1 intoxication caused a time-dependent depletion of Rac1 (Figure 3.26A). The CNF1-induced decrease in Rac1 levels in RhoG knockdown cells and control cells was quantified by densitometry. At all timepoints analyzed, the level of Rac1 degradation was not significantly different between RhoG knockdown cells and control cells (Figure 3.26B). Therefore, CNF1-induced Rac1 depletion is not dependent on RhoG.

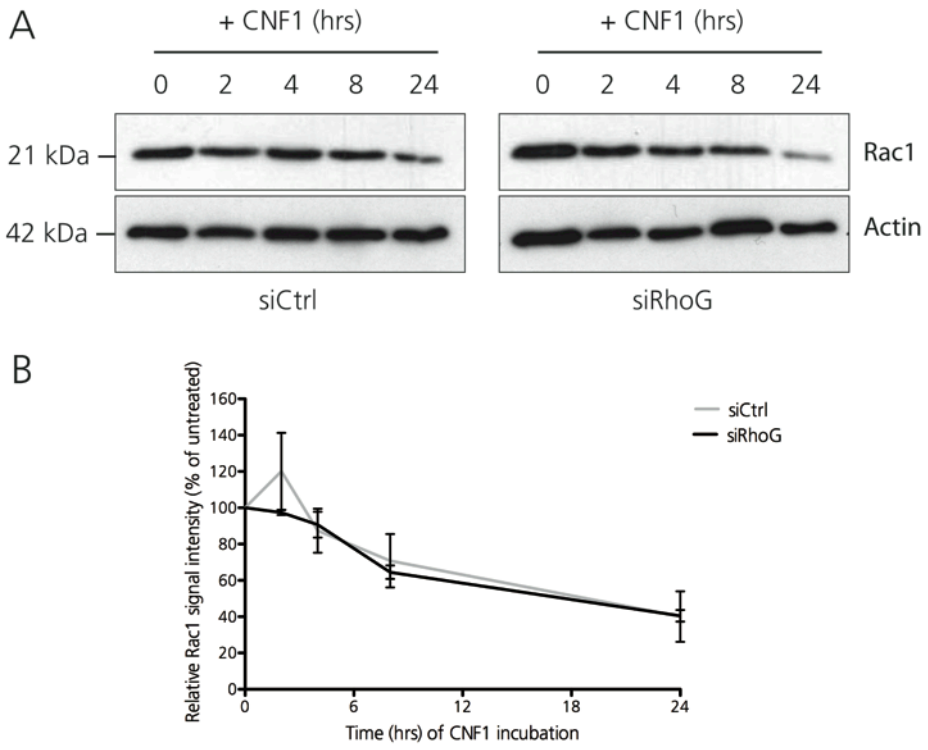

Figure 3.26: RhoG does not play a role in CNF1-induced Rac1 degradation.

HeLa cells were transfected with non-targeting (siCtrl) or RhoG (siRhoG) siRNA. 72 hrs post transfection cells were incubated with 300 ng/ml CNF1 for indicated timepoints. **(A)** Cell lysates were subjected to SDS-PAGE and Western blot against Rac1. Actin expression served as loading control. **(B)** Quantification of Rac1 signal intensities was analyzed by densitometry using ImageJ software and is presented as a percentage of signal intensities of untreated cells. Data are means ± SEM of 4 independent experiments.

4 Discussion

To date, *E. coli* CNF1 is considered to be the paradigm of bacterial cytotoxins that activate Rho GTPases, namely Rac1, RhoA and Cdc42. Modulation of these master regulators of the actin cytoskeleton provides the pathogen with control over a broad range of cell functions. The less studied Rho GTPase RhoG is implicated in various cellular processes, but the studies linking RhoG activity with bacterial pathogenesis remain few. To date, *Salmonella*, *Yersinia* and *Shigella* have been reported to utilize RhoG for their infection process. At the beginning of this project it was unknown whether CNF1 producing UPEC are able to manipulate host pathways by activation of RhoG. Therefore, this work investigated whether CNF1 targets RhoG and succeeded to identify a putative role of CNF1-activated RhoG in the virulence strategy of UPEC. Indeed, this study identified RhoG as a new target for CNF1 and additionally revealed that CNF1-activated RhoG has a negative regulatory impact on UPEC invasion. These findings enhance our current knowledge of the infection process of UPEC.

4.1 RhoG is activated via deamidation by CNF1

It has been known since the late 1990s that CNF1 activates RhoA, Rac1 and Cdc42 via deamidation of glutamine residues at position 63 for RhoA or 61 for Rac1 and Cdc42 (Schmidt et al., 1997; Flatau et al., 1997; Lerm et al., 1999). Additionally, the closely related CNFy from *Y. pseudotuberculosis* was thought to selectively activate RhoA (Hoffmann et al., 2004), however our laboratory has recently shown that CNFy also activates Rac1 and Cdc42 in intact cells (Wolters et al., 2013). Using the N-terminal domain of the specific RhoG effector ELMO, it was clearly demonstrated in this study that CNF1 activates RhoG in HeLa cells and that the kinetics of activation was similar to CNF1-induced Rac1 activation, suggesting that RhoG is a new target for CNF1 (Figure 3.2A, B). Due to a high similarity between Rac1 and RhoG in the switch II region, one could expect that CNF1 also recognizes RhoG as a target, although additional amino acids outside of the switch II region are required for sufficient substrate binding (Lerm et al., 1999). Moreover, the data revealed that the level of total RhoG decreased over time, corresponding to recent findings that CNF1-activated Rho GTPases are subsequently degraded by the proteasome machinery and further supporting the results that CNF1 activates RhoG (Doye et al., 2002). In order to prove whether depletion of CNF1-activated RhoG is catalyzed by ubiquitin-mediated proteasome degradation, one could employ an *in vivo* ubiquitylation assay using His-tagged ubiquitin (Doye et al., 2006). Interestingly, intoxication with CNFy from *Y. pseudotuberculosis* did not lead to activation of RhoG in HeLa cells (Figure 3.2C). Despite having quite homologous receptor binding domains, CNF1 and CNFy bind to different host receptors (Blumenthal et al., 2007). However, CNFy has already been shown to activate Rho GTPases in HeLa cells (Hoffmann et al., 2004), therefore the fact that CNFy did not activate RhoG could not be explained by a lack of uptake. CNF1 and CNFy share 65 % homology in amino acid sequence, including the conserved residues Cys866 and His881 in the catalytic domain that are responsible for

their activity. Thus, other residues must also contribute to the substrate specificity of CNF1 towards RhoG. Detection of such specific differences could be examined using single amino acid substitutions in CNF1, as already reported for RhoA substrate specificity of CNF1 and CNFy (Hoffmann et al., 2007). In general, specific activation of RhoG by CNF1 was clearly observed in HeLa cells, though additional experiments for CNF1-induced RhoG activation in different cells lines would verify this result. Preliminary studies of this research work used an urothelial cell line for CNF1-intoxication experiments. These cells were stimulated with CNF1 for several timepoints and displayed clear RhoG activation after 6 hrs of intoxication. Additionally, CNFy did not cause activation of RhoG in urothelial cells (personal communication with B. Roppenser). Thus, we could confirm that CNF1 induces RhoG activation in a more physiologically relevant cell line.

As already mentioned above, CNF1 modifies Rac1, RhoA and Cdc42 directly by deamidation. Deamidation of glutamine 61/63 in the switch II region results in inhibition of intrinsic and GAP-catalyzed GTP hydrolysis, and therefore, the Rho GTPase is kept in its activated state. We investigated whether CNF1 activated RhoG through deamidation. MS analysis was used to determine modifications in the amino acid sequence of recombinant RhoG and RhoA upon incubation with CNF1. Deamidation was predicted to shift the mass of the Rho GTPases by 1 Da. Corresponding to previous studies (Schmidt et al., 1997), deamidation of Gln63 of RhoA was detected in the mass spectra (Figure 3.6). The relevant peptide covering amino residues 52 to 68 (QVELALWDTAGQEDYDR) increased in mass by 1 Da, indicating deamidation. In addition to the mass spectra, our study included extracted ion chromatograms. Whereas mass spectra reveal the presence of a particular peptide, EIC display an elution profile of a given m/z value and quantitatively determines its abundance. Therefore, conclusions about the percentage of deamidating modifications can be made. Incubation with CNF1 resulted in complete deamidation of RhoA, discernible in the height of the EIC peak illustrating the deamidated peptide (Figure 3.7) Comparing tryptic peptides of unmodified and modified recombinant RhoG upon CNF1-incubation, the mass spectra revealed a mass shift of 1 Da of a peptide containing amino residues 50 to 68 (TVNLNLWDTAGQEEYDRLR), indicating deamidation of Gln61 (Figure 3.6). These data suggest that recombinant RhoG is a substrate for CNF1. Notably, the corresponding EIC peak of the relevant RhoG peptide showed that only parts of the peptides were deamidated (Figure 3.7). Changes in the incubation time of RhoG with CNF1 and variation in the ratios of RhoG:CNF1 did not influence the abundance of deamidated RhoG. Previous reports of CNF1-induced deamidation of Rho GTPases have only shown mass spectra and did not indicate whether full deamidation took place. However, assuming that CNF1 led to complete deamidation of Rho GTPases, the experimental conditions used in this study may require refinement, e.g. test proper reaction buffer conditions.

One possibility as to why we observed only incomplete deamidation was that our recombinant RhoG was not properly folded. We used the nucleotide-binding ability of RhoA and RhoG as a readout for functionality, and hence, the proper folding. In this assay, an increase in fluorescence signal corresponds to an increase of mant-GDP binding, which in turn is an indicator for the release of previously bound nucleotides. Though the preparation of recombinant RhoG displayed slower mant-GDP binding than recombinant

RhoA, the results indicated that RhoG was properly folded (Figure 3.4). However, how much of the protein was folded correctly, was not apparent from this assay. Other methods could provide more information about the percentage of correct protein folding within the sample. More conclusive evidence for correct protein folding would be spectroscopic methods such as circular dichroism (CD), which is widely used for studying the conformation of biomolecules based on their ability to absorb left- and right-handed circularly polarized light (Whitmore and Wallace, 2007). The low amount of deamidated RhoG upon CNF1 treatment could also be because the activity of RhoG itself is limited under the conditions tested. In this study, recombinant Rho GTPases were incubated with the toxin and further analyzed for modification. Another approach would be to transfect HeLa cells with tagged RhoG, intoxicate with CNF1, precipitate RhoG with an anti-tag antibody and then proceed with MS analysis. Potentially, due to more physiological conditions or the presence of required cofactors deamidation of RhoG within cells could be more effective. Comparable to that, recombinant RhoA is deamidated by CNFy very slowly *in vitro*, but in intact cells deamidation of RhoA is much faster (Hoffmann et al., 2007).

Additionally, many bacterial protein toxins have been described to modulate members of the Rho family of small GTPases by divers covalent modifications. Activation of Rac1, RhoA and Ccd42 is induced by deamidation (*E. coli/Yersinia* CNFs, *Bordetella* spp. Dnt), transglutamination (*Bordetella* spp. Dnts) or ADP-ribosylation (*P. luminescence* TccC5). Much more pathogens cause inactivation of Rac1, RhoA and Cdc42 by glycosylation (*C. difficile* toxins A and B, *C. sordellii* hemorrhagic toxin), adenylylation (*V. parahaemolyticus* VopS, *H. somni* IbpA) or proteolytic cleavage (*P. luminescence* LopT, *Yersinia* spp. YopT) (Aktories, 2011). However, bacterial toxins have never been reported to covalently modify RhoG. Thus, our finding that CNF1 is able to deamidate RhoG provokes the question whether RhoG may also be a substrate for another deamidating toxin, Dnt. Dnt was found to have an important but somewhat undefined role as virulence factor in *Bordetella* pathogenesis. Whereas it still remains unclear whether Dnt contributes to whooping cough, its contribution to atrophic rhinitis is clear (Khelef et al., 1994; Magyar et al., 2000). CNF1 and Dnt share 30 % homology in the catalytic domain and a consensus sequence, which harbors the catalytic active cysteine. Remarkably, although CNF1 and Dnt are both deamidases and transglutaminases that target the same glutamine residue in the switch II region of Rho GTPases, CNF1 preferentially acts as a deamidase, whereas Dnt primarily is a transglutaminase in presence of polyamine (Schmidt et al., 1999). It has already been shown that Rac1, RhoA and Cdc42 can be deamidated and transglutaminated by Dnt (Horiguchi et al., 1997; Masuda et al., 2000).

In conclusion, this study revealed that RhoG is a novel target of CNF1 activation and subsequent degradation, in addition to Rac1, RhoA and Cdc42. This study also demonstrates that CNF1 is capable of activating RhoG through deamidation on glutamine 61.

4.2 CNF1-induced signaling pathways are RhoG-independent

Since RhoG was found to be targeted and activated by CNF1, this study aimed to identify the role of CNF1-activated RhoG in host-pathogen interactions. The idea to study signaling pathways was motivated by the well-known impact of CNF1 on proinflammatory signaling. In response to UPEC infection, urothelial cells secrete the cytokine IL-8 (Schilling et al., 2001), which is the main chemoattractant for neutrophils (Agace, 1996). Neutrophils are an important part of the innate immune response and are the fastest, most abundant immune cell type at the site of UPEC infections. They phagocyte pathogens and produce reactive oxygen species (ROS) necessary for efficient microbial killing (Hampton et al., 1998). IL-8 expression is regulated by different transcription factors including AP-1, NF-κB and NF-IL6. These transcription factors in turn can be regulated by Rho GTPases. CNF1 is involved in IL-8 production via Rac1 and Cdc42 activation (Munro et al., 2004). CNF1 was also shown to activate cJun, which, together with cFos, forms AP-1 complex (Lerm et al., 1999). cJun can be activated by Rac1 and Cdc41 (Coso et al., 1995), however, the specific Rho GTPases involved in CNF1-dependent cJun activation were not known. We explored the possibility that RhoG was involved in CNF1-dependent proinflammatory signaling. Using different experimental techniques (immunofluorescent staining, immunoblotting) this work did not find that RhoG regulated CNF1-induced cJun activation, thus CNF1-activated RhoG does not regulate transcription factor AP-1 (Figure 3.10, Figure 3.11). Yet, AP-1 is only one transcription factor involved in expression of downstream protein IL-8. Thus, we hypothesized that CNF1-activated RhoG might regulate IL-8 expression independent of cJun. In line with other reports, we observed increased IL-8 secretion after CNF1-intoxication, however, RhoG did not significantly alter the levels of IL-8 (Figure 3.12). The CNF1 stimulation time course ran for 8 hrs and notably, at the latest timepoint there was slightly more IL-8 produced in cells depleted of RhoG compared to control cells. Although this increase was not found to be significant, it would still be interesting to determine whether CNF1-activated RhoG is implicated at later time points. Elevated levels of IL-8 from cells lacking RhoG would imply that CNF-induced RhoG activation blocks IL-8 production. Indeed, UPEC counters many host defense mechanisms and CNF1 is likely involved in some of these strategies. Munro and colleagues suggested that activation of Rho GTPases by CNF1 followed by their subsequent degradation is responsible for attenuating infection-triggered immune responses like cytokine production (Munro et al., 2004). The interaction between pathogen-associated molecular patterns (PAMPs) and host Toll-like receptors also causes the release of proinflammatory cytokines, triggering immune mobilization. Thus, modulation of Rho GTPases activity by CNF1 may limit the amplitude of host cell immune responses.

CNF1 has also been described to reduce the phagocytic activity of neutrophils and the microbicidal activity of PMNs thereby facilitating UPEC survival (Davis et al., 2005). We initially attempted to elucidate whether RhoG regulated CNF1-induced ROS production by neutrophils. In line with this hypothesis, RhoG was already identified to regulate neutrophil NADPH oxidase responsible for ROS production (Condliffe et al., 2006). Preliminary experiments with neutrophil-like HL-60 cells provided evidence that UPEC infection caused production of ROS, however, we did not find that CNF1 treatment alone stimulated oxidative burst (data not shown). One of the primary differences between our

study and that of Davis et al. is that they compared the effect of wildtype bacteria to an isogenic Δ*cnf1* mutant while we used purified CNF1 protein. The same group has more recently shown that CNF1 can be delivered by outer membrane vesicles released from the bacterial surface (Davis et al., 2006). These CNF1-containing vesicles inhibited the chemotactic responses of neutrophils while purified CNF1 did not. The authors speculate that the delivery of CNF1 via membrane vesicles target the toxin to the neutrophil membrane and possibly the cytosol more effectively than the receptor-mediated pathway previously described for CNF1. Future studies to clarify the role of RhoG in CNF1-induced ROS production should therefore employ outer membrane vesicle preparations isolated from wildtype and Δcnf1 UTI89.

As already mentioned, an inhibitory effect of CNF1 has been shown for bacterial phagocytosis. Macrophages and PMNLs display decreased bacterial phagocytosis in presence of CNF1 and the authors suggest that CNF1 mediates this inhibitory effect by blocking Rho GTPases (Hofman et al., 2000; Capo et al., 1998). Recently, a study identified RhoG to be involved in Fc gamma receptor (FcγR)- mediated and complement receptor 3 (CR3)- mediated phagocytosis (Tzircotis et al., 2011). According to that study, other Rho GTPases required for FcγR-mediated phagocytosis are Rac2 and Cdc42, whereas CR3-mediated phagocytosis involves RhoA. As RhoG activity is subverted by bacterial pathogens such as *Salmonella* and *Yersinia* during infection, one might speculate whether CNF1-induced RhoG activation might contribute to CNF1-inhibited phagocytosis (Patel and Galan et al., 2006; Mohammadi and Isberg, 2009; Roppenser et al., 2009).

4.3 RhoG and its role in CNF1-dependent invasion

Invasion into host cells is key for the pathogenesis of many pathogens, enabling bacteria to evade from the host defense machinery and to replicate intracellularly. UPEC has evolved mechanisms to gain entry into eukaryotic cells by targeting the actin cytoskeleton via manipulation of Rho GTPases, thereby resisting clearance and establishing persistence inside the urinary tract. The activation of different Rho GTPases by CNF1 stimulates bacterial uptake, with the importance of activated Rac1 on invasion having already been established (Doye et al., 2002; Visvikis et al., 2011). This work aimed to investigate the role of CNF1-induced RhoG during UPEC invasion.

Recruitment of a protein to specific site within a cell often implies it has a specific function at this site. Few bacterial pathogens recruit RhoG during invasion into host cells, whereby it is required for efficient invasion. *Salmonella* produces the effector SopB to indirectly activate RhoG via its GEF SGEF, thus provoking localized membrane ruffles and mediating bacterial entry (Patel and Galan, 2006). In addition RhoG localizes to infection sites of *Yersinia* spp. and is implicated in invasin-mediated uptake (Roppenser et al., 2009; Mohammadi et al., 2009). We demonstrated that RhoG was recruited to sites of UPEC infection either in the presence or absence of CNF1 (Figure 3.16). RhoG had not previously been implicated in UPEC host-pathogen interactions. This study revealed that RhoG plays a functional, albeit inhibitory, role in CNF1-induced bacterial invasion. Although we found that RhoG was recruited by UPEC in CNF1-independent and -dependent invasion, it did

not have a functional role during CNF1-independent invasion into host cells (Figure 3.17A, Figure 3.18B). Proteins recruited to the site of infection without any functional role at this site might be there simply due to the presence of their binding partners. Thus, in the absence of CNF1, RhoG might localize to sites of infection because of local Rac1 activation, through RhoG's ability to bind common downstream effectors of Rac1. Rac1 was also shown to be recruited to the site of UPEC entry, likely due to its role in type 1 pili/FimH mediated invasion via phosphoinositide 3-kinase and tyrosine kinase activation (Martinez and Hultgren, 2002).

To assess the role of CNF1-induced RhoG activation during UPEC invasion we primarily used the well-described and the preferentially-used gentamicin protection assay. As an alternative method we employed immunofluorescent inside/outside staining. Both techniques differ in their approach and have their own benefits and drawbacks. The gentamicin protection assay relies on the inability of the antibiotic gentamicin to cross eukaryotic cell membranes, thus intracellular bacteria remain viable and are counted as formed colonies upon host cell lysis. Invasion of bacteria into all infected cells in a given well is analyzed. There are rare reports that gentamicin is able to enter phagocytic cells via pinocytosis and kill intracellular bacteria (Drevets et al., 1994). To our knowledge there have been no such reports using non-phagocytic cells. Nonetheless, in our studies the incubation time and concentration of gentamicin was kept low, but still enough to kill extracellular bacteria. To test whether gentamicin treatment efficiently killed extracellular bacteria in our assays, the sterility of supernatants of infected and gentamicin treated HeLa cells were plated and revealed no viable bacteria. An alternative method to count intracellular bacteria is inside/outside staining, which detects individual bacteria and their localization within the host cell by fluorescent microscopy. This approach makes it possible to analyze the infection at the single cell level, but has disadvantages for extensive screening. Despite a high rate of siRNA transfection efficiency, the actual transfected cells were not visible in our inside/outside staining, thus it could not be excluded that by chance more untransfected cells were analyzed, affecting the outcome of the assay. Additionally, only a part of the total amount of cells is microscopically evaluated, often less than 0,1 %. Unequal distribution of the bacteria on a cover glass further complicates invariable, precise analysis. Finally, the staining procedure exposes the bacteria and cells to various blocking, labeling, fixation or washing steps, wherein the bacterial surface can be affected resulting in ineffective staining of the bacteria. Weighing the pros and cons of each method, we decided to use the gentamicin protection assay as standard procedure to quantify intracellular bacteria.

In line with other studies, it was determined that the adhesin FimH mainly mediated CNF1-independent UPEC invasion (Figure 3.14B) (Martinez et al., 2000). The contribution of FimH to CNF1-dependent invasion has not yet been defined. Here, we identified that CNF1-dependent UPEC invasion was also mainly mediated by FimH (Figure 3.14B). However, a significant increase of FimH-independent invasion was observed in the presence of CNF1, suggesting that additional uptake mechanisms may exist. FimH-mediated UPEC invasion requires the activation of Rac1, RhoA and Cdc42 (Martinez et al., 2000). Whether RhoG is specifically involved in FimH-dependent or an -independent uptake mechanism needs to be clarified.

This study confirmed that CNF1 contributes to UPEC invasion into epithelial cells, and that this effect is mainly dependent on Rac1 activation. Using Rac1 siRNA transfected cells and Rac1 knockout cells, it was verified that Rac1 was required for CNF1-independent and -dependent invasion (Figure 3.15A, B). Additionally, experiments with constitutively active mutants of Rac1 further revealed a role of active Rac1 in UPEC invasion (Figure 3.20, Figure 3.21A). Previous reports have already stated the high impact of Rac1 in bacterial invasion. It was shown that CNF1-independent and –dependent UPEC invasion into bladder cells requires Rac1 activation (Martinez and Hultgren, 2002; Doye et al., 2002; Visvikis et al., 2011). The invasion of meningitis causing and CNF1 expressing *E. coli* strain K1 into human brain microvascular endothelial cells is also dependent on Rac1 activation (Maruvada and Kim, 2012). Other pathogens targeting Rac1 to trigger host-cell internalization include *Yersinia*, *Streptococcus* and *Salmonella* (Alrutz et al., 2001; Shin and Kim, 2006; Criss et al., 2001).

Surprisingly, we discovered that CNF1-activated RhoG inhibits invasion, a process that is mainly dependent upon Rac1 (Figure 3.17A, Figure 3.18C). To our knowledge, this is the first time that CNF1-induced activation of a Rho GTPase is described to have an inhibitory regulatory function. For the most part, it was thought that activation of Rho GTPases by CNF1 had a beneficial effect on UPEC invasion (Doye et al., 2002; Khan et al., 2002). Perhaps the first hint that an activated Rho GTPase might be inhibitory for UPEC invasion came when it was shown that degradation of activated Rac1 was necessary for efficient invasion (Doye et al., 2002).

RhoG is also involved in remodeling of the actin cytoskeleton and subsequent uptake mechanisms into non-phagocytic cells, called macropinocytosis (Ellerbroek et al., 2004). Pathogens utilize macropinocytosis to gain entry into host cells include *Shigella*, *Salmonella* and *Legionella* (Mounier et al., 1999; Chen et al., 1996; Watari et al., 2001). The inhibitory effect of CNF1-activated RhoG could be analyzed during macropinocytosis. Thus, it could be tested whether the uptake of beads or dead bacteria is also inhibited by CNF1-induced activation of RhoG or whether CNF1-activated RhoG rather regulates uptake in an infection-dependent manner.

Although we clearly demonstrated that loss of RhoG significantly increased CNF1-dependent bacterial uptake, experiments with constitutively active RhoG could not prove that active RhoG inhibits invasion upon CNF1 stimulation (Figure 3.20, Figure 3.21A). One explanation might be that the constitutively active mutant reacts differently than the deamidated form of RhoG. In our assays we used the mutant RhoGV12, which contains an amino acid substitution in the region surrounding the switch I region. This mutation locks the Rho GTPase into its GTP-bound state, defective in its GTPase activity and thus turns it into a dominant-active mutant. Glycine 12/14 is one of a few conserved residues of Rho GTPases that are required for the GTPase activity, thus mutations at this sites modulate the GTPase activity. The posttranslational modification induced by CNF1 occurs at position 61/63, a conserved glutamine residue within the switch II region of Rho GTPases. Next to glycine 12/14, glutamine 61/63 is responsible for the hydrolysis of GTP by stabilization of the transition state during the GTP hydrolysis process (Foster et al., 1996; Garavini et al., 2002). Moreover, all known posttranslational modifications that produce activation of Rho GTPases modify an essential glutamine residue in the switch II

region (Visvikis et al., 2010). One can therefore speculate that the difference between CNF1-activated RhoG and the constitutively active mutant is due to their different sites of modification. Future experiments with a mutant that mimics deamidation of RhoG (RhoGE61) should be assessed and compare the function of deamidated RhoG versus wildtype activated RhoG.

Another possible reason why overexpression of constitutively active RhoG did not lead to a reduction of CNF1-induced invasion might be due to the lack of other cofactors or downstream effectors. The excess supply of active overexpression of constitutively active RhoG might exhaust the pool of downstream interaction partners required for the inhibitory effect of RhoG. Notably, in control transfected cells, no further increase of CNF1-induced invasion was observed when activated Rac1 mutants were expressed (Figure 3.20). This might also be due to downstream effectors being a limiting factor.

It would be interesting to further investigate whether CNF1-activated RhoG has an inhibitory effect on other Rac1-dependent processes, like membrane ruffling, apoptosis or stabilization of barrier functions. The maintenance of intestinal epithelial barrier functions was found to be regulated by Rho GTPases, in particular Rac1 and Cdc42 (Schlegel et al., 2011). Moreover, a balance of Rho GTPase activation and inactivation is crucial for optimal barrier function (Hopkins et al., 2003). It could be investigated whether CNF1-activated RhoG antagonizes the barrier stabilization function of Rac1. Upon UPEC infection the disruption of the urothelium due cell exfoliation induced by an apoptotic pathway is crucial for the pathogen to disseminate into deeper tissue layers, but also benefits the host by facilitating clearance of infection (Mulvey et al., 2000). Other toxins like B toxin from *C. difficile* directly inactivate Rac1 by glycosylation, leading to disassembly of focal adhesions and subsequent loss of cell-matrix adhesion and epithelial barrier function (Genth et al., 2008).

It was further examined whether the inhibitory effect of RhoG on invasion was dependent on Rac1 (Figure 3.19A). RhoG has already been implicated in different cellular processes, but it remained controversial whether RhoG acts via the ELMO-Dock180-Rac1 pathway or whether it can function independently on Rac1. In particular, some Rac1-independent functions of RhoG include ruffle formation and migration, macropinocytosis and phagocytosis (Meller et al., 2008; Ellerbroek et al., 2004; Tzircotis et al., 2011). Here, we found that RhoG acts as a negative regulator of UPEC invasion, a process that is dependent on Rac1. This suggests that CNF1-induced invasion is mainly promoted by activated Rho GTPases, but may be counteracted and regulated by RhoG.

4.4 RhoG as regulator or counterpart for Rac1-activity?

As orchestrators of several cellular functions, Rho GTPases often cooperate, while at other times can antagonize each other. Thus, an interaction network comprising different Rho GTPases occurs at several levels and regulates individual activities in time and space. Ridley and colleagues identified the first example of Rho GTPase crosstalk in 1992. They observed that growth factor-stimulated fibroblasts Rac1-dependent ruffle formation also lead to RhoA-like stress fibers (Ridley et al., 1992). A rising number of reports have identified different mechanisms involved in Rho GTPase crosstalk. For instance, the RhoA

effector ROCK can antagonize Rac1 activity. Suppression of ROCK prevents the formation of lysophosphatidic acid (LPA)-induced stress fibers and focal adhesions, but leads to the formation of membrane ruffles in fibroblasts (Tsuji et al., 2002). Still, there is much to learn about downstream signaling interplay between Rho GTPases and how Rho GTPases can affect each other's activity. Despite its implication in various cellular functions, many signaling pathways upstream and downstream of RhoG still remain unclear. This study revealed that RhoG is involved in a Rac1-dependent process. Despite its Rho GTPase activating activity, CNF1 converts RhoG activation into an inhibitory regulatory function. This kind of CNF1-induced regulation has not been reported before and will expand the understanding of host-pathogen interactions regarding modifications of Rho GTPases. RhoG belongs to the Rac subgroup of Rho GTPases and shares 72 % homology with Rac1. A compensatory function has already been described for closely related Rab GTPases (Wasmeier et al., 2006). Mice lacking RhoG were shown to have only mild immunological deficits and the authors speculate that members of the Rac subgroup may compensate for RhoG functions for example in cytokine production due to their structural similarity (Vigorito et al., 2004). Whether Rac1 and RhoG are able to compensate for one another is likely due to some overlapping functions and downstream effectors. Regarding crosstalk between Rac1 and RhoG, RhoG is postulated to regulate Rac1 activity via the ELMO-Dock180 pathway (Katoh et al., 2003). Thus, several effects of RhoG could be explained by its ability to activate Rac1 (Blangy et al., 2000).

Here, we systematically analyzed how CNF1-activated RhoG could influence Rac1 activity resulting in an inhibitory effect on UPEC invasion. We asked whether RhoG (1) affects the level of Rac1 activation, (2) changes the subcellular localization of activated Rac1 or (3) alters the degradation of activated Rac1.

We could exclude that RhoG regulates Rac1 activity at the level of activation. Knockdown of RhoG did not affect the extent of Rac1 activation, thus the enhanced level of CNF1-induced invasion in cells depleted of RhoG was not due to enhanced Rac1 activation (Figure 3.23A). Additionally, CNF1-mediated RhoG activation was not altered when Rac1 was depleted (Figure 3.23C). These findings revealed that in this context, Rac1 and RhoG do not compensate for one another and are not dependent on each other.

Another mechanism for regulating the activity of Rho GTPases involves their subcellular localization. Activation of Rho GTPases is followed by their transfer from the cytoplasm to the plasma membrane where they regulate cytoskeleton rearrangements and other signaling pathways (Bustelo et al., 2007). Subcellular localization of CNF1-activated Rac1 was analyzed in the presence and absence of RhoG, where we hypothesized that CNF1-activated RhoG might lead to mislocation and subsequent disfunction of activated Rac1. To analyze Rac1 localization we transfected HeLa cells with green fluorescent wildtype Rac1 and stimulated the cells with CNF1. Comparison of control and RhoG-depleted cells did not yield any differences in Rac1 localization, thus we concluded that RhoG does not influence Rac1 activity by altering its subcellular localization (Figure 3.24, Figure 3.25). These experiments could have been extended to include live-cell imaging using GFP-Rac1, thereby allowing the visualization of Rac1 dynamics during CNF1-induced actin organization. In our experiments we only determined CNF1-induced Rac1 distribution at a particular point in time, possibly overlooking differences in Rac1 localization over time.

However, even live-cell imaging would not have revealed whether membrane translocation of Rac1 was altered depending on the presence of RhoG. This could be achieved by fluorescence resonance energy transfer (FRET)-based biosensors that would have allowed visualization of spatiotemporal signaling of Rac1 (Kraynov et al., 2000; Itoh et al., 2002). And finally, active Rac1 translocates to the plasma membrane and preferentially binds to low-density, cholesterol-rich microdomains called lipid rafts (del Pozo et al., 2004). Using sucrose density gradient fractionation, lipid rafts could be isolated from CNF1-intoxicated cell lysates from control and RhoG knockdown cells and analyzed for Rac1 abundance (Jaksits et al., 2004). One could speculate that RhoG inhibits Rac1 localization to lipids rafts, thereby inhibiting Rac1-dependent UPEC invasion.

Regulation of Rho GTPases can occur at the level of protein expression and stability. At this level RhoGDI1 is often involved, stabilizing Rho GTPases and protecting them from degradation (Ho et al., 2008). In the case of CNF1 intoxication, it is already established that Rho GTPases activated by the toxin are prone to ubiquitin-mediated proteasomal degradation (Doye et al., 2002). Currently, researchers study the underlying mechanisms of the degradation process and already revealed the relevant E3-ubiquitin ligases for RhoA and Rac1, namely Smurf1 and HACE1 (Boyer et al., 2006; Torrino et al., 2011). The transient activation of Rho GTPases was reported to be important for bacterial internalization and moderate immune responses (Doye et al., 2002; Munro et al, 2004). Thus, in this study we explored whether RhoG might influence Rac1 degradation. Indeed, CNF1 intoxication caused significant Rac1 degradation, however, RhoG did not affect this process (Figure 3.26B). In line with other studies, we observed degradation after approximately 6 hrs stimulation with CNF1 (Pop et al., 2004; Munro and Lemichez, 2005). Thus, the incubation time for CNF1 used in the invasion assays was 2 hours, perhaps not long enough to see an effect of degradation on invasion into cells depleted of RhoG. Additionally, our degradation results do not support a role for RhoG in Rac1 degradation that could explain dampening late Rac1-dependent signaling events like proinflammatory cytokine production. As already mentioned, we observed slightly more IL-8 production in RhoG-depleted cells after 8 hrs CNF1-intoxication, suggesting that RhoG may inhibit late immune responses. However, this possible inhibitory effect could not be due to changes in Rac1 degradation.

RhoG was not found to antagonize Rac1 activity at the level of activation, localization, or degradation. In future, another attempt to ascertain how CNF1-activated RhoG inhibits UPEC invasion, could be to focus on possible downstream effects of Rac1 activation, namely, actin polymerization. Many intracellular pathogens hijack the host actin cytoskeleton, inducing their own uptake into cells that are normally non-phagocytic. For example, effectors injected directly into host cells by *Salmonella enterica* mimic Rho GTPase GEFs, thereby inducing massive membrane ruffling and engulfment (Friebel et al., 2001). Effectors delivered by *Shigella* activate the ELMO-Dock180 machinery, which also promotes membrane ruffles that facilitate invasion (Handa et al., 2007). Preliminary data of this study verified that CNF1-induced membrane ruffles are primarily dependent upon Rac1 activation (data not shown). It still remains unclear whether RhoG alters CNF1-induced membrane ruffles thereby making them less efficient for UPEC invasion. RhoG may be involved in Rac1-dependent modulation of the actin cytoskeleton, inhibiting a

downstream effector important for the actin dynamics involved in UPEC invasion. To further clarify this hypothesis, further experiments should include live-cell imaging of CNF1-intoxicated and infected cells. The formation of membrane ruffles and the bacterial infection process itself are highly dynamic events, making live-cell microscopy approaches appropriate tools to investigate the kinetics of actin rearrangements upon UPEC infection as a function of CNF1-activated RhoG. Moreover, it could be tested whether CNF1-activated RhoG is able to reduce invasion of other pathogens that promote membrane ruffles for their uptake, e.g. *Salmonella* or *Shigella*.

This study showed that CNF1-dependent UPEC invasion is mainly mediated by FimH (Figure 3.14B). Upon binding of FimH to host receptors several downstream signal cascades are modulated, including activation of phosphoinositide 3-kinase, focal adhesion kinase, Src family kinases, Rho GTPases and the cytoskeleton stabilizing and scaffolding complex of α-actinin and vinculin (Martinez et al., 2000; Martinez and Hultgren, 2002; Eto et al., 2007). Whether CNF1-deamdidated RhoG inhibits any members of these signaling pathways could be the subjects of future studies. In addition, whether CNF1-induced RhoG activation regulates FimH-dependent invasion pathways could be tested using UPEC lacking FimH. In general, the formation of actin ruffles is mainly driven by Rac1 and PI3-kinase signaling via the WAVE2 complex leading to Arp2/3-induced actin polymerization (Hall et al., 1998; Suetsugu et al., 2003). Due to its overlapping functions with Rac1 in cytoskeleton rearrangements, RhoG might regulate Rac1 activity in actin polymerization processes via the WAVE regulatory complex (WRC). It has been proposed that Rac1 does not solely regulate activation of the WRC, members of the Arf GTPases also play a role; however, detailed mechanisms remain unclear (Koronakis et al., 2011). In general not that many effectors of RhoG have been identified. Identification of RhoG effectors, especially those that bound to the CNF1-deamidated form of RhoG could potentially detect common effectors between Rac1 and RhoG. These common effectors would be candidates for further analysis of how CNF1-activated RhoG inhibits Rac1-dependent UPEC invasion. One standard method to identify interaction partners is the yeast two-hybrid system. A more innovative method for identifying the binding partners of deamidated RhoG would be stable isotope labeling by amino acids in cell culture (SILAC) based on mass spectrometry and applied for quantitative protein-interaction studies *in vitro* (Montani et al., 2012).

Macropinocytosis is induced by CNF1 to promote bacterial uptake into non-phagocytic cells. It was shown that a coordinate activation of Rho GTPases is involved in CNF1-induced ingestion of dead bacteria or latex beads (Falzano et al., 1993; Fiorentini et al, 2001). Interestingly, a recent, study revealed that transient activation of Rac1 is required for complete macropinosome formation (Fujii et al., 2013). Although we showed that RhoG did not influence the overall CNF1-induced activation of Rac1, in context of the internalization processes, it is possible that RhoG changes the local activation of Rac1, controlling extensive CNF1-induced uptake.

4.5 CNF1-induced RhoG activation in the virulence strategy of UPEC

Pathogens that utilize or mimic RhoG activity as a tool to facilitate invasion into non-phagocytic host cells, rather balances RhoG activation in a temporal-spatial mode. For example, during early infection phase *Salmonella* delivers effector SopB mimicking SGEF and thus leading indirectly to RhoG activation (Patel and Galan, 2006). Additionally, the effectors SopE/E2 directly activate Rac1 and Cdc42 due to their GEF activity (Friebel et al., 2001). Activation of the Rho GTPases results in actin rearrangements and bacterial internalization. After bacterial entry, the delivered effector SptP deactivates the Rho GTPases due to its function as a GAP, thereby down-regulating host cell responses (Stebbins and Galan, 2000). Another example of this "ying and yang" is reported for *Y. enterocolitica*. First, RhoG is activated by invasin-integrin interaction triggering bacterial uptake. In a later phase of infection, injected effector protein YopE acts as a Rho GAP resulting into inactivation of RhoG and Rac1 (Roppenser at al., 2009).

This study identified RhoG as a new target of CNF1 that is activated and subsequently degraded. Other Rho GTPases modulated by CNF1 follow the same mechanism of activation via deamidation and degradation. Especially the transient activation of Rac1 induced by CNF1 has been described to contribute to successful bacterial internalization and fine-tune induction of immune responses (Doye et al., 2002; Munro et al., 2004). Thus, the bacteria utilize the toxin to modulate host functions in order to survive in the face of different host responses. On the other hand, one could also argue that degradation of Rho GTPases might rather be a safety mechanism for the host, preventing undesirable cellular damage triggered by continuous activation. The cell possesses several mechanisms to regulate the activity of Rho GTPases, including degradation, membrane localization and transcription.

The finding that RhoG activation by CNF1 counteracts Rac1 activity during bacterial invasion appears to be puzzling. Rac1 and RhoG are activated by CNF1 at essentially the same time. Deamidated Rac1 facilitates invasion while deamidated RhoG inhibits the same process. Why should a pathogen want to dampen its own uptake? One idea might be that UPEC uses the inherent relative expression levels of Rac1 and RhoG to target infection to particular cell types or to a particular moment in a cell's life cycle. For example, in a cell expressing more Rac1 (and its downstream effectors) than RhoG, CNF1 intoxication would favor bacterial invasion. On the other hand, in a cell that expresses more RhoG (and its downstream effectors) than Rac1, invasion would not be favored. In this way UPEC could also fine-tune the induction of inflammatory responses. Depending on the relative abundance of intracellular Rho GTPases, CNF1 stimulation would modulate the immune responses.

This work presents for the first time a link between modulation of RhoG by uropathogenic *E. coli* via the virulence factor CNF1. Further work will help to unravel the precise function of this host-pathogen interaction.

References

Abraham, J.M., C.S. Freitag, J.R. Clements, and B.I. Eisenstein. 1985. An invertible element of DNA controls phase variation of type 1 fimbriae of Escherichia coli. *Proc Natl Acad Sci U S A*. 82:5724-5727.

Agace, W.W., S.R. Hedges, M. Ceska, and C. Svanborg. 1993. Interleukin-8 and the neutrophil response to mucosal gram-negative infection. *J Clin Invest*. 92:780-785.

Aktories, K. 2011. Bacterial protein toxins that modify host regulatory GTPases. *Nat Rev Microbiol*. 9:487-498.

Aktories, K., M. Barmann, I. Ohishi, S. Tsuyama, K.H. Jakobs, and E. Habermann. 1986. Botulinum C2 toxin ADP-ribosylates actin. *Nature*. 322:390-392.

Alrutz, M.A., A. Srivastava, K.W. Wong, C. D'Souza-Schorey, M. Tang, L.E. Ch'Ng, S.B. Snapper, and R.R. Isberg. 2001. Efficient uptake of Yersinia pseudotuberculosis via integrin receptors involves a Rac1-Arp 2/3 pathway that bypasses N-WASP function. *Mol Microbiol*. 42:689-703.

Ananias, M., and T. Yano. 2008. Serogroups and virulence genotypes of Escherichia coli isolated from patients with sepsis. *Braz J Med Biol Res*. 41:877-883.

Arnaout, M.A., B. Mahalingam, and J.P. Xiong. 2005. Integrin structure, allostery, and bidirectional signaling. *Annu Rev Cell Dev Biol*. 21:381-410.

Baorto, D.M., Z. Gao, R. Malaviya, M.L. Dustin, A. van der Merwe, D.M. Lublin, and S.N. Abraham. 1997. Survival of FimH-expressing enterobacteria in macrophages relies on glycolipid traffic. *Nature*. 389:636-639.

Birnboim, H.C., and J. Doly. 1979. A rapid alkaline extraction procedure for screening recombinant plasmid DNA. *Nucleic Acids Res*. 7:1513-1523.

Bishop, A.L., and A. Hall. 2000. Rho GTPases and their effector proteins. *Biochem J*. 348 Pt 2:241-255.

Blanco, J., M. Blanco, M.P. Alonso, J.E. Blanco, J.I. Garabal, and E.A. Gonzalez. 1992. Serogroups of Escherichia coli strains producing cytotoxic necrotizing factors CNF1 and CNF2. *FEMS Microbiol Lett*. 75:155-159.

Blangy, A., E. Vignal, S. Schmidt, A. Debant, C. Gauthier-Rouviere, and P. Fort. 2000. TrioGEF1 controls Rac- and Cdc42-dependent cell structures through the direct activation of rhoG. *J Cell Sci*. 113 (Pt 4):729-739.

Blumenthal, B., C. Hoffmann, K. Aktories, S. Backert, and G. Schmidt. 2007. The cytotoxic necrotizing factors from Yersinia pseudotuberculosis and from Escherichia coli bind to different cellular receptors but take the same route to the cytosol. *Infect Immun*. 75:3344-3353.

Boquet, P., and E. Lemichez. 2003. Bacterial virulence factors targeting Rho GTPases: parasitism or symbiosis? *Trends Cell Biol*. 13:238-246.

Boulter, E., S. Estrach, R. Garcia-Mata, and C.C. Feral. 2012. Off the beaten paths: alternative and crosstalk regulation of Rho GTPases. *Faseb J*. 26:469-479.

Boulter, E., R. Garcia-Mata, C. Guilluy, A. Dubash, G. Rossi, P.J. Brennwald, and K. Burridge. 2010. Regulation of Rho GTPase crosstalk, degradation and activity by RhoGDI1. *Nat Cell Biol*. 12:477-483.

Bourne, H.R., D.A. Sanders, and F. McCormick. 1990. The GTPase superfamily: a conserved switch for diverse cell functions. *Nature*. 348:125-132.

Bower, J.M., D.S. Eto, and M.A. Mulvey. 2005. Covert operations of uropathogenic Escherichia coli within the urinary tract. *Traffic*. 6:18-31.

Boyer, L., L. Turchi, B. Desnues, A. Doye, G. Ponzio, J.L. Mege, M. Yamashita, Y.E. Zhang, J. Bertoglio, G. Flatau, P. Boquet, and E. Lemichez. 2006. CNF1-induced ubiquitylation and proteasome destruction of activated RhoA is impaired in Smurf1-/- cells. *Mol Biol Cell*. 17:2489-2497.

Brest, P., B. Mograbi, V. Hofman, A. Loubat, B. Rossi, P. Auberger, and P. Hofman. 2003. Rho GTPase is activated by cytotoxic necrotizing factor 1 in peripheral blood T lymphocytes: potential cytotoxicity for intestinal epithelial cells. *Infect Immun*. 71:1161-1169.

Brinton, C.C., Jr. 1965. The structure, function, synthesis and genetic control of bacterial pili and a molecular model for DNA and RNA transport in gram negative bacteria. *Trans N Y Acad Sci*. 27:1003-1054.

Buchanan, K., S. Falkow, R.A. Hull, and S.I. Hull. 1985. Frequency among Enterobacteriaceae of the DNA sequences encoding type 1 pili. *J Bacteriol.* 162:799-803.

Bustelo, X.R., V. Sauzeau, and I.M. Berenjeno. 2007. GTP-binding proteins of the Rho/Rac family: regulation, effectors and functions in vivo. *Bioessays.* 29:356-370.

Capo, C., S. Meconi, M.V. Sanguedolce, N. Bardin, G. Flatau, P. Boquet, and J.L. Mege. 1998. Effect of cytotoxic necrotizing factor-1 on actin cytoskeleton in human monocytes: role in the regulation of integrin-dependent phagocytosis. *J Immunol.* 161:4301-4308.

Caprioli, A., V. Falbo, L.G. Roda, F.M. Ruggeri, and C. Zona. 1983. Partial purification and characterization of an escherichia coli toxic factor that induces morphological cell alterations. *Infect Immun.* 39:1300-1306.

Carlier, M.F. 1998. Control of actin dynamics. *Curr Opin Cell Biol.* 10:45-51.

Castillo-Lluva, S., M.H. Tatham, R.C. Jones, E.G. Jaffray, R.D. Edmondson, R.T. Hay, and A. Malliri. 2010. SUMOylation of the GTPase Rac1 is required for optimal cell migration. *Nat Cell Biol.* 12:1078-1085.

Chen, L.M., S. Hobbie, and J.E. Galan. 1996. Requirement of CDC42 for Salmonella-induced cytoskeletal and nuclear responses. *Science.* 274:2115-2118.

Chen, Y., Z. Yang, M. Meng, Y. Zhao, N. Dong, H. Yan, L. Liu, M. Ding, H.B. Peng, and F. Shao. 2009. Cullin mediates degradation of RhoA through evolutionarily conserved BTB adaptors to control actin cytoskeleton structure and cell movement. *Mol Cell.* 35:841-855.

Chromek, M., Z. Slamova, P. Bergman, L. Kovacs, L. Podracka, I. Ehren, T. Hokfelt, G.H. Gudmundsson, R.L. Gallo, B. Agerberth, and A. Brauner. 2006. The antimicrobial peptide cathelicidin protects the urinary tract against invasive bacterial infection. *Nat Med.* 12:636-641.

Chung, J.W., S.J. Hong, K.J. Kim, D. Goti, M.F. Stins, S. Shin, V.L. Dawson, T.M. Dawson, and K.S. Kim. 2003. 37-kDa laminin receptor precursor modulates cytotoxic necrotizing factor 1-mediated RhoA activation and bacterial uptake. *J Biol Chem.* 278:16857-16862.

Condliffe, A.M., L.M. Webb, G.J. Ferguson, K. Davidson, M. Turner, E. Vigorito, M. Manifava, E.R. Chilvers, L.R. Stephens, and P.T. Hawkins. 2006. RhoG regulates the neutrophil NADPH oxidase. *J Immunol.* 176:5314-5320.

Contamin, S., A. Galmiche, A. Doye, G. Flatau, A. Benmerah, and P. Boquet. 2000. The p21 Rho-activating toxin cytotoxic necrotizing factor 1 is endocytosed by a clathrin-independent mechanism and enters the cytosol by an acidic-dependent membrane translocation step. *Mol Biol Cell.* 11:1775-1787.

Coso, O.A., M. Chiariello, J.C. Yu, H. Teramoto, P. Crespo, N. Xu, T. Miki, and J.S. Gutkind. 1995. The small GTP-binding proteins Rac1 and Cdc42 regulate the activity of the JNK/SAPK signaling pathway. *Cell.* 81:1137-1146.

Criss, A.K., D.M. Ahlgren, T.S. Jou, B.A. McCormick, and J.E. Casanova. 2001. The GTPase Rac1 selectively regulates Salmonella invasion at the apical plasma membrane of polarized epithelial cells. *J Cell Sci.* 114:1331-1341.

Czuchra, A., X. Wu, H. Meyer, J. van Hengel, T. Schroeder, R. Geffers, K. Rottner, and C. Brakebusch. 2005. Cdc42 is not essential for filopodium formation, directed migration, cell polarization, and mitosis in fibroblastoid cells. *Mol Biol Cell.* 16:4473-4484.

Davis, J.M., H.M. Carvalho, S.B. Rasmussen, and A.D. O'Brien. 2006. Cytotoxic necrotizing factor type 1 delivered by outer membrane vesicles of uropathogenic Escherichia coli attenuates polymorphonuclear leukocyte antimicrobial activity and chemotaxis. *Infect Immun.* 74:4401-4408.

Davis, J.M., S.B. Rasmussen, and A.D. O'Brien. 2005. Cytotoxic necrotizing factor type 1 production by uropathogenic Escherichia coli modulates polymorphonuclear leukocyte function. *Infect Immun.* 73:5301-5310.

de Curtis, I., and J. Meldolesi. 2012. Cell surface dynamics - how Rho GTPases orchestrate the interplay between the plasma membrane and the cortical cytoskeleton. *J Cell Sci.* 125:4435-4444.

De Rycke, J., A. Milon, and E. Oswald. 1999. Necrotoxic Escherichia coli (NTEC): two emerging categories of human and animal pathogens. *Vet Res.* 30:221-233.

deBakker, C.D., L.B. Haney, J.M. Kinchen, C. Grimsley, M. Lu, D. Klingele, P.K. Hsu, B.K. Chou, L.C. Cheng, A. Blangy, J. Sondek, M.O. Hengartner, Y.C. Wu, and K.S. Ravichandran. 2004. Phagocytosis of apoptotic cells is regulated by a UNC-73/TRIO-MIG-2/RhoG signaling module and armadillo repeats of CED-12/ELMO. *Curr Biol.* 14:2208-2216.

del Pozo, M.A., N.B. Alderson, W.B. Kiosses, H.H. Chiang, R.G. Anderson, and M.A. Schwartz. 2004. Integrins regulate Rac targeting by internalization of membrane domains. *Science.* 303:839-842.

Dhakal, B.K., R.R. Kulesus, and M.A. Mulvey. 2008. Mechanisms and consequences of bladder cell invasion by uropathogenic Escherichia coli. *Eur J Clin Invest.* 38 Suppl 2:2-11.

Dhakal, B.K., and M.A. Mulvey. 2012. The UPEC pore-forming toxin alpha-hemolysin triggers proteolysis of host proteins to disrupt cell adhesion, inflammatory, and survival pathways. *Cell Host Microbe*. 11:58-69.

Disanza, A., S. Mantoani, M. Hertzog, S. Gerboth, E. Frittoli, A. Steffen, K. Berhoerster, H.J. Kreienkamp, F. Milanesi, P.P. Di Fiore, A. Ciliberto, T.E. Stradal, and G. Scita. 2006. Regulation of cell shape by Cdc42 is mediated by the synergic actin-bundling activity of the Eps8-IRSp53 complex. *Nat Cell Biol*. 8:1337-1347.

Dovas, A., and J.R. Couchman. 2005. RhoGDI: multiple functions in the regulation of Rho family GTPase activities. *Biochem J*. 390:1-9.

Doye, A., L. Boyer, A. Mettouchi, and E. Lemichez. 2006. Ubiquitin-mediated proteasomal degradation of Rho proteins by the CNF1 toxin. *Methods Enzymol*. 406:447-456.

Doye, A., A. Mettouchi, G. Bossis, R. Clement, C. Buisson-Touati, G. Flatau, L. Gagnoux, M. Piechaczyk, P. Boquet, and E. Lemichez. 2002. CNF1 exploits the ubiquitin-proteasome machinery to restrict Rho GTPase activation for bacterial host cell invasion. *Cell*. 111:553-564.

Drevets, D.A., B.P. Canono, P.J. Leenen, and P.A. Campbell. 1994. Gentamicin kills intracellular Listeria monocytogenes. *Infect Immun*. 62:2222-2228.

Eden, S., R. Rohatgi, A.V. Podtelejnikov, M. Mann, and M.W. Kirschner. 2002. Mechanism of regulation of WAVE1-induced actin nucleation by Rac1 and Nck. *Nature*. 418:790-793.

Elfenbein, A., J.M. Rhodes, J. Meller, M.A. Schwartz, M. Matsuda, and M. Simons. 2009. Suppression of RhoG activity is mediated by a syndecan 4-synectin-RhoGDI1 complex and is reversed by PKCalpha in a Rac1 activation pathway. *J Cell Biol*. 186:75-83.

Ellerbroek, S.M., K. Wennerberg, W.T. Arthur, J.M. Dunty, D.R. Bowman, K.A. DeMali, C. Der, and K. Burridge. 2004. SGEF, a RhoG guanine nucleotide exchange factor that stimulates macropinocytosis. *Mol Biol Cell*. 15:3309-3319.

Erdem, A.L., F. Avelino, J. Xicohtencatl-Cortes, and J.A. Giron. 2007. Host protein binding and adhesive properties of H6 and H7 flagella of attaching and effacing Escherichia coli. *J Bacteriol*. 189:7426-7435.

Essler, M., S. Linder, B. Schell, K. Hufner, A. Wiedemann, K. Randhahn, J.M. Staddon, and M. Aepfelbacher. 2003. Cytotoxic necrotizing factor 1 of Escherichia coli stimulates Rho/Rho-kinase-dependent myosin light-chain phosphorylation without inactivating myosin light-chain phosphatase in endothelial cells. *Infect Immun*. 71:5188-5193.

Eto, D.S., T.A. Jones, J.L. Sundsbak, and M.A. Mulvey. 2007. Integrin-mediated host cell invasion by type 1-piliated uropathogenic Escherichia coli. *PLoS Pathog*. 3:e100.

Eto, D.S., J.L. Sundsbak, and M.A. Mulvey. 2006. Actin-gated intracellular growth and resurgence of uropathogenic Escherichia coli. *Cell Microbiol*. 8:704-717.

Falbo, V., T. Pace, L. Picci, E. Pizzi, and A. Caprioli. 1993. Isolation and nucleotide sequence of the gene encoding cytotoxic necrotizing factor 1 of Escherichia coli. *Infect Immun*. 61:4909-4914.

Falzano, L., C. Fiorentini, G. Donelli, E. Michel, C. Kocks, P. Cossart, L. Cabanie, E. Oswald, and P. Boquet. 1993. Induction of phagocytic behaviour in human epithelial cells by Escherichia coli cytotoxic necrotizing factor type 1. *Mol Microbiol*. 9:1247-1254.

Falzano, L., M.G. Quaranta, S. Travaglione, P. Filippini, A. Fabbri, M. Viora, G. Donelli, and C. Fiorentini. 2003. Cytotoxic necrotizing factor 1 enhances reactive oxygen species-dependent transcription and secretion of proinflammatory cytokines in human uroepithelial cells. *Infect Immun*. 71:4178-4181.

Feig, L.A. 1999. Tools of the trade: use of dominant-inhibitory mutants of Ras-family GTPases. *Nat Cell Biol*. 1:E25-27.

Fiorentini, C., L. Falzano, A. Fabbri, A. Stringaro, M. Logozzi, S. Travaglione, S. Contamin, G. Arancia, W. Malorni, and S. Fais. 2001. Activation of rho GTPases by cytotoxic necrotizing factor 1 induces macropinocytosis and scavenging activity in epithelial cells. *Mol Biol Cell*. 12:2061-2073.

Flatau, G., E. Lemichez, M. Gauthier, P. Chardin, S. Paris, C. Fiorentini, and P. Boquet. 1997. Toxin-induced activation of the G protein p21 Rho by deamidation of glutamine. *Nature*. 387:729-733.

Foster, R., K.Q. Hu, Y. Lu, K.M. Nolan, J. Thissen, and J. Settleman. 1996. Identification of a novel human Rho protein with unusual properties: GTPase deficiency and in vivo farnesylation. *Mol Cell Biol*. 16:2689-2699.

Foxman, B. 2002. Epidemiology of urinary tract infections: incidence, morbidity, and economic costs. *Am J Med*. 113 Suppl 1A:5S-13S.

Foxman, B., R. Barlow, H. D'Arcy, B. Gillespie, and J.D. Sobel. 2000. Urinary tract infection: self-reported incidence and associated costs. *Ann Epidemiol*. 10:509-515.

Francis, C.L., T.A. Ryan, B.D. Jones, S.J. Smith, and S. Falkow. 1993. Ruffles induced by Salmonella and other stimuli direct macropinocytosis of bacteria. *Nature*. 364:639-642.

Franke, K., W. Otto, S. Johannes, J. Baumgart, R. Nitsch, and S. Schumacher. 2012. miR-124-regulated RhoG reduces neuronal process complexity via ELMO/Dock180/Rac1 and Cdc42 signalling. *Embo J*. 31:2908-2921.

Friebel, A., H. Ilchmann, M. Aepfelbacher, K. Ehrbar, W. Machleidt, and W.D. Hardt. 2001. SopE and SopE2 from Salmonella typhimurium activate different sets of RhoGTPases of the host cell. *J Biol Chem*. 276:34035-34040.

Fujii, M., K. Kawai, Y. Egami, and N. Araki. 2013. Dissecting the roles of Rac1 activation and deactivation in macropinocytosis using microscopic photo-manipulation. *Sci Rep*. 3:2385.

Fujimoto, S., M. Negishi, and H. Katoh. 2009. RhoG promotes neural progenitor cell proliferation in mouse cerebral cortex. *Mol Biol Cell*. 20:4941-4950.

Garavini, H., K. Riento, J.P. Phelan, M.S. McAlister, A.J. Ridley, and N.H. Keep. 2002. Crystal structure of the core domain of RhoE/Rnd3: a constitutively activated small G protein. *Biochemistry*. 41:6303-6310.

Garcia-Mata, R., E. Boulter, and K. Burridge. 2011. The 'invisible hand': regulation of RHO GTPases by RHOGDIs. *Nat Rev Mol Cell Biol*. 12:493-504.

Garcia-Mata, R., and K. Burridge. 2007. Catching a GEF by its tail. *Trends Cell Biol*. 17:36-43.

Gauthier-Rouviere, C., E. Vignal, M. Meriane, P. Roux, P. Montcourier, and P. Fort. 1998. RhoG GTPase controls a pathway that independently activates Rac1 and Cdc42Hs. *Mol Biol Cell*. 9:1379-1394.

Genth, H., K. Aktories, and I. Just. 1999. Monoglucosylation of RhoA at threonine 37 blocks cytosol-membrane cycling. *J Biol Chem*. 274:29050-29056.

Genth, H., R. Gerhard, A. Maeda, M. Amano, K. Kaibuchi, K. Aktories, and I. Just. 2003. Entrapment of Rho ADP-ribosylated by Clostridium botulinum C3 exoenzyme in the Rho-guanine nucleotide dissociation inhibitor-1 complex. *J Biol Chem*. 278:28523-28527.

Ghosh, S., M.J. May, and E.B. Kopp. 1998. NF-kappa B and Rel proteins: evolutionarily conserved mediators of immune responses. *Annu Rev Immunol*. 16:225-260.

Goode, B.L., and M.J. Eck. 2007. Mechanism and function of formins in the control of actin assembly. *Annu Rev Biochem*. 76:593-627.

Hakoshima, T., T. Shimizu, and R. Maesaki. 2003. Structural basis of the Rho GTPase signaling. *J Biochem*. 134:327-331.

Hall, A. 1998. Rho GTPases and the actin cytoskeleton. *Science*. 279:509-514.

Hampton, M.B., A.J. Kettle, and C.C. Winterbourn. 1998. Inside the neutrophil phagosome: oxidants, myeloperoxidase, and bacterial killing. *Blood*. 92:3007-3017.

Hancock, J.F., H. Paterson, and C.J. Marshall. 1990. A polybasic domain or palmitoylation is required in addition to the CAAX motif to localize p21ras to the plasma membrane. *Cell*. 63:133-139.

Handa, Y., M. Suzuki, K. Ohya, H. Iwai, N. Ishijima, A.J. Koleske, Y. Fukui, and C. Sasakawa. 2007. Shigella IpgB1 promotes bacterial entry through the ELMO-Dock180 machinery. *Nat Cell Biol*. 9:121-128.

Hanein, D., P. Matsudaira, and D.J. DeRosier. 1997. Evidence for a conformational change in actin induced by fimbrin (N375) binding. *J Cell Biol*. 139:387-396.

Haraoka, M., L. Hang, B. Frendeus, G. Godaly, M. Burdick, R. Strieter, and C. Svanborg. 1999. Neutrophil recruitment and resistance to urinary tract infection. *J Infect Dis*. 180:1220-1229.

Heo, J., and S.L. Campbell. 2005. Mechanism of redox-mediated guanine nucleotide exchange on redox-active Rho GTPases. *J Biol Chem*. 280:31003-31010.

Ho, T.T., S.D. Merajver, C.M. Lapiere, B.V. Nusgens, and C.F. Deroanne. 2008. RhoA-GDP regulates RhoB protein stability. Potential involvement of RhoGDIalpha. *J Biol Chem*. 283:21588-21598.

Hoffmann, C., K. Aktories, and G. Schmidt. 2007. Change in substrate specificity of cytotoxic necrotizing factor unmasks proteasome-independent down-regulation of constitutively active RhoA. *J Biol Chem*. 282:10826-10832.

Hoffmann, C., M. Pop, J. Leemhuis, J. Schirmer, K. Aktories, and G. Schmidt. 2004. The Yersinia pseudotuberculosis cytotoxic necrotizing factor (CNFY) selectively activates RhoA. *J Biol Chem*. 279:16026-16032.

Hoffmann, E., O. Dittrich-Breiholz, H. Holtmann, and M. Kracht. 2002. Multiple control of interleukin-8 gene expression. *J Leukoc Biol*. 72:847-855.

Hofman, P., G. Le Negrate, B. Mograbi, V. Hofman, P. Brest, A. Alliana-Schmid, G. Flatau, P. Boquet, and B. Rossi. 2000. Escherichia coli cytotoxic necrotizing factor-1 (CNF-1) increases the adherence to epithelia and the oxidative burst of human polymorphonuclear leukocytes but decreases bacteria phagocytosis. *J Leukoc Biol.* 68:522-528.

Holden, N.J., and D.L. Gally. 2004. Switches, cross-talk and memory in Escherichia coli adherence. *J Med Microbiol.* 53:585-593.

Hopkins, A.M., S.V. Walsh, P. Verkade, P. Boquet, and A. Nusrat. 2003. Constitutive activation of Rho proteins by CNF-1 influences tight junction structure and epithelial barrier function. *J Cell Sci.* 116:725-742.

Hung, C.S., J. Bouckaert, D. Hung, J. Pinkner, C. Widberg, A. DeFusco, C.G. Auguste, R. Strouse, S. Langermann, G. Waksman, and S.J. Hultgren. 2002. Structural basis of tropism of Escherichia coli to the bladder during urinary tract infection. *Mol Microbiol.* 44:903-915.

Hurst, R.E. 1994. Structure, function, and pathology of proteoglycans and glycosaminoglycans in the urinary tract. *World J Urol.* 12:3-10.

Ismail, A.M., S.B. Padrick, B. Chen, J. Umetani, and M.K. Rosen. 2009. The WAVE regulatory complex is inhibited. *Nat Struct Mol Biol.* 16:561-563.

Itoh, R.E., K. Kurokawa, Y. Ohba, H. Yoshizaki, N. Mochizuki, and M. Matsuda. 2002. Activation of rac and cdc42 video imaged by fluorescent resonance energy transfer-based single-molecule probes in the membrane of living cells. *Mol Cell Biol.* 22:6582-6591.

Jaffe, A.B., and A. Hall. 2005. Rho GTPases: biochemistry and biology. *Annu Rev Cell Dev Biol.* 21:247-269.

Jaksits, S., W. Bauer, E. Kriehuber, M. Zeyda, T.M. Stulnig, G. Stingl, E. Fiebiger, and D. Maurer. 2004. Lipid raft-associated GTPase signaling controls morphology and CD8+ T cell stimulatory capacity of human dendritic cells. *J Immunol.* 173:1628-1639.

Johnson, J.R. 1991. Virulence factors in Escherichia coli urinary tract infection. *Clin Microbiol Rev.* 4:80-128.

Jones, C.H., J.S. Pinkner, R. Roth, J. Heuser, A.V. Nicholes, S.N. Abraham, and S.J. Hultgren. 1995. FimH adhesin of type 1 pili is assembled into a fibrillar tip structure in the Enterobacteriaceae. *Proc Natl Acad Sci U S A.* 92:2081-2085.

Just, I., J. Selzer, M. Wilm, C. von Eichel-Streiber, M. Mann, and K. Aktories. 1995. Glucosylation of Rho proteins by Clostridium difficile toxin B. *Nature.* 375:500-503.

Kaper, J.B., J.P. Nataro, and H.L. Mobley. 2004. Pathogenic Escherichia coli. *Nat Rev Microbiol.* 2:123-140.

Katoh, H., K. Hiramoto, and M. Negishi. 2006. Activation of Rac1 by RhoG regulates cell migration. *J Cell Sci.* 119:56-65.

Katoh, H., and M. Negishi. 2003. RhoG activates Rac1 by direct interaction with the Dock180-binding protein Elmo. *Nature.* 424:461-464.

Katoh, H., H. Yasui, Y. Yamaguchi, J. Aoki, H. Fujita, K. Mori, and M. Negishi. 2000. Small GTPase RhoG is a key regulator for neurite outgrowth in PC12 cells. *Mol Cell Biol.* 20:7378-7387.

Khan, N.A., Y. Wang, K.J. Kim, J.W. Chung, C.A. Wass, and K.S. Kim. 2002. Cytotoxic necrotizing factor-1 contributes to Escherichia coli K1 invasion of the central nervous system. *J Biol Chem.* 277:15607-15612.

Khelef, N., C.M. Bachelet, B.B. Vargaftig, and N. Guiso. 1994. Characterization of murine lung inflammation after infection with parental Bordetella pertussis and mutants deficient in adhesins or toxins. *Infect Immun.* 62:2893-2900.

Kim, K.J., J.W. Chung, and K.S. Kim. 2005. 67-kDa laminin receptor promotes internalization of cytotoxic necrotizing factor 1-expressing Escherichia coli K1 into human brain microvascular endothelial cells. *J Biol Chem.* 280:1360-1368.

Klumpp, D.J., A.C. Weiser, S. Sengupta, S.G. Forrestal, R.A. Batler, and A.J. Schaeffer. 2001. Uropathogenic Escherichia coli potentiates type 1 pilus-induced apoptosis by suppressing NF-kappaB. *Infect Immun.* 69:6689-6695.

Knust, Z., B. Blumenthal, K. Aktories, and G. Schmidt. 2009. Cleavage of Escherichia coli cytotoxic necrotizing factor 1 is required for full biologic activity. *Infect Immun.* 77:1835-1841.

Knust, Z., and G. Schmidt. 2010. Cytotoxic Necrotizing Factors (CNFs)-A Growing Toxin Family. *Toxins (Basel).* 2:116-127.

Koronakis, V., P.J. Hume, D. Humphreys, T. Liu, O. Horning, O.N. Jensen, and E.J. McGhie. 2011. WAVE regulatory complex activation by cooperating GTPases Arf and Rac1. *Proc Natl Acad Sci U S A.* 108:14449-14454.

Korotkova, N., E. Cota, Y. Lebedin, S. Monpouet, J. Guignot, A.L. Servin, S. Matthews, and S.L. Moseley. 2006. A subfamily of Dr adhesins of Escherichia coli bind independently to decay-accelerating factor and the N-domain of carcinoembryonic antigen. *J Biol Chem.* 281:29120-29130.

Kouokam, J.C., S.N. Wai, M. Fallman, U. Dobrindt, J. Hacker, and B.E. Uhlin. 2006. Active cytotoxic necrotizing factor 1 associated with outer membrane vesicles from uropathogenic Escherichia coli. *Infect Immun.* 74:2022-2030.

Kovacic, H.N., K. Irani, and P.J. Goldschmidt-Clermont. 2001. Redox regulation of human Rac1 stability by the proteasome in human aortic endothelial cells. *J Biol Chem.* 276:45856-45861.

Kraynov, V.S., C. Chamberlain, G.M. Bokoch, M.A. Schwartz, S. Slabaugh, and K.M. Hahn. 2000. Localized Rac activation dynamics visualized in living cells. *Science.* 290:333-337.

Kukkonen, M., T. Raunio, R. Virkola, K. Lahteenmaki, P.H. Makela, P. Klemm, S. Clegg, and T.K. Korhonen. 1993. Basement membrane carbohydrate as a target for bacterial adhesion: binding of type I fimbriae of Salmonella enterica and Escherichia coli to laminin. *Mol Microbiol.* 7:229-237.

Kwiatkowska, A., S. Didier, S. Fortin, Y. Chuang, T. White, M.E. Berens, E. Rushing, J. Eschbacher, N.L. Tran, A. Chan, and M. Symons. 2012. The small GTPase RhoG mediates glioblastoma cell invasion. *Mol Cancer.* 11:65.

Lane, M.C., C.J. Alteri, S.N. Smith, and H.L. Mobley. 2007. Expression of flagella is coincident with uropathogenic Escherichia coli ascension to the upper urinary tract. *Proc Natl Acad Sci U S A.* 104:16669-16674.

Lane, M.C., A.N. Simms, and H.L. Mobley. 2007. complex interplay between type 1 fimbrial expression and flagellum-mediated motility of uropathogenic Escherichia coli. *J Bacteriol.* 189:5523-5533.

Lang, P., F. Gesbert, M. Delespine-Carmagnat, R. Stancou, M. Pouchelet, and J. Bertoglio. 1996. Protein kinase A phosphorylation of RhoA mediates the morphological and functional effects of cyclic AMP in cytotoxic lymphocytes. *Embo J.* 15:510-519.

Lemichez, E., G. Flatau, M. Bruzzone, P. Boquet, and M. Gauthier. 1997. Molecular localization of the Escherichia coli cytotoxic necrotizing factor CNF1 cell-binding and catalytic domains. *Mol Microbiol.* 24:1061-1070.

Lerm, M., M. Pop, G. Fritz, K. Aktories, and G. Schmidt. 2002. Proteasomal degradation of cytotoxic necrotizing factor 1-activated rac. *Infect Immun.* 70:4053-4058.

Lerm, M., G. Schmidt, U.M. Goehring, J. Schirmer, and K. Aktories. 1999. Identification of the region of rho involved in substrate recognition by Escherichia coli cytotoxic necrotizing factor 1 (CNF1). *J Biol Chem.* 274:28999-29004.

Lerm, M., J. Selzer, A. Hoffmeyer, U.R. Rapp, K. Aktories, and G. Schmidt. 1999. Deamidation of Cdc42 and Rac by Escherichia coli cytotoxic necrotizing factor 1: activation of c-Jun N-terminal kinase in HeLa cells. *Infect Immun.* 67:496-503.

Leusch, H.G., Z. Drzeniek, Z. Markos-Pusztai, and C. Wagener. 1991. Binding of Escherichia coli and Salmonella strains to members of the carcinoembryonic antigen family: differential binding inhibition by aromatic alpha-glycosides of mannose. *Infect Immun.* 59:2051-2057.

Lockman, H.A., R.A. Gillespie, B.D. Baker, and E. Shakhnovich. 2002. Yersinia pseudotuberculosis produces a cytotoxic necrotizing factor. *Infect Immun.* 70:2708-2714.

Magyar, T., R. Glavits, G.D. Pullinger, and A.J. Lax. 2000. The pathological effect of the Bordetella dermonecrotic toxin in mice. *Acta Vet Hung.* 48:397-406.

Makeyev, E.V., J. Zhang, M.A. Carrasco, and T. Maniatis. 2007. The MicroRNA miR-124 promotes neuronal differentiation by triggering brain-specific alternative pre-mRNA splicing. *Mol Cell.* 27:435-448.

Malorni, W., and C. Fiorentini. 2006. Is the Rac GTPase-activating toxin CNF1 a smart hijacker of host cell fate? *Faseb J.* 20:606-609.

Manges, A.R., J.R. Johnson, B. Foxman, T.T. O'Bryan, K.E. Fullerton, and L.W. Riley. 2001. Widespread distribution of urinary tract infections caused by a multidrug-resistant Escherichia coli clonal group. *N Engl J Med.* 345:1007-1013.

Martinez, J.J., and S.J. Hultgren. 2002. Requirement of Rho-family GTPases in the invasion of Type 1-piliated uropathogenic Escherichia coli. *Cell Microbiol.* 4:19-28.

Martinez, J.J., M.A. Mulvey, J.D. Schilling, J.S. Pinkner, and S.J. Hultgren. 2000. Type 1 pilus-mediated bacterial invasion of bladder epithelial cells. *Embo J.* 19:2803-2812.

Martinez-Martin, N., E. Fernandez-Arenas, S. Cemerski, P. Delgado, M. Turner, J. Heuser, D.J. Irvine, B. Huang, X.R. Bustelo, A. Shaw, and B. Alarcon. 2011. T cell receptor internalization from the immunological synapse is mediated by TC21 and RhoG GTPase-dependent phagocytosis. *Immunity.* 35:208-222.

Maruvada, R., and K.S. Kim. 2012. IbeA and OmpA of Escherichia coli K1 exploit Rac1 activation for invasion of human brain microvascular endothelial cells. *Infect Immun.* 80:2035-2041.

Masuda, M., L. Betancourt, T. Matsuzawa, T. Kashimoto, T. Takao, Y. Shimonishi, and Y. Horiguchi. 2000. Activation of rho through a cross-link with polyamines catalyzed by Bordetella dermonecrotizing toxin. *Embo J.* 19:521-530.

Mathur, R., H. Oh, D. Zhang, S.G. Park, J. Seo, A. Koblansky, M.S. Hayden, and S. Ghosh. 2012. A mouse model of Salmonella typhi infection. *Cell.* 151:590-602.

Mattila, P.K., and P. Lappalainen. 2008. Filopodia: molecular architecture and cellular functions. *Nat Rev Mol Cell Biol.* 9:446-454.

Mazur, A.J., D. Gremm, T. Dansranjavin, M. Litwin, B.M. Jockusch, A. Wegner, A.G. Weeds, and H.G. Mannherz. 2010. Modulation of actin filament dynamics by actin-binding proteins residing in lamellipodia. *Eur J Cell Biol.* 89:402-413.

Meller, J., L. Vidali, and M.A. Schwartz. 2008. Endogenous RhoG is dispensable for integrin-mediated cell spreading but contributes to Rac-independent migration. *J Cell Sci.* 121:1981-1989.

Michaelson, D., J. Silletti, G. Murphy, P. D'Eustachio, M. Rush, and M.R. Philips. 2001. Differential localization of Rho GTPases in live cells: regulation by hypervariable regions and RhoGDI binding. *J Cell Biol.* 152:111-126.

Miki, H., H. Yamaguchi, S. Suetsugu, and T. Takenawa. 2000. IRSp53 is an essential intermediate between Rac and WAVE in the regulation of membrane ruffling. *Nature.* 408:732-735.

Millard, T.H., S.J. Sharp, and L.M. Machesky. 2004. Signalling to actin assembly via the WASP (Wiskott-Aldrich syndrome protein)-family proteins and the Arp2/3 complex. *Biochem J.* 380:1-17.

Mills, M., K.C. Meysick, and A.D. O'Brien. 2000. Cytotoxic necrotizing factor type 1 of uropathogenic Escherichia coli kills cultured human uroepithelial 5637 cells by an apoptotic mechanism. *Infect Immun.* 68:5869-5880.

Mohammadi, S., and R.R. Isberg. 2009. Yersinia pseudotuberculosis virulence determinants invasin, YopE, and YopT modulate RhoG activity and localization. *Infect Immun.* 77:4771-4782.

Montani, L., D. Bausch-Fluck, A.F. Domingues, B. Wollscheid, and J.B. Relvas. 2012. Identification of new interacting partners for atypical Rho GTPases: a SILAC-based approach. *Methods Mol Biol.* 827:305-317.

Morschhauser, J., H. Hoschutzky, K. Jann, and J. Hacker. 1990. Functional analysis of the sialic acid-binding adhesin SfaS of pathogenic Escherichia coli by site-specific mutagenesis. *Infect Immun.* 58:2133-2138.

Mounier, J., V. Laurent, A. Hall, P. Fort, M.F. Carlier, P.J. Sansonetti, and C. Egile. 1999. Rho family GTPases control entry of Shigella flexneri into epithelial cells but not intracellular motility. *J Cell Sci.* 112 (Pt 13):2069-2080.

Mulvey, M.A., Y.S. Lopez-Boado, C.L. Wilson, R. Roth, W.C. Parks, J. Heuser, and S.J. Hultgren. 1998. Induction and evasion of host defenses by type 1-piliated uropathogenic Escherichia coli. *Science.* 282:1494-1497.

Mulvey, M.A., J.D. Schilling, and S.J. Hultgren. 2001. Establishment of a persistent Escherichia coli reservoir during the acute phase of a bladder infection. *Infect Immun.* 69:4572-4579.

Mulvey, M.A., J.D. Schilling, J.J. Martinez, and S.J. Hultgren. 2000. Bad bugs and beleaguered bladders: interplay between uropathogenic Escherichia coli and innate host defenses. *Proc Natl Acad Sci U S A.* 97:8829-8835.

Munro, P., G. Flatau, A. Doye, L. Boyer, O. Oregioni, J.L. Mege, L. Landraud, and E. Lemichez. 2004. Activation and proteasomal degradation of rho GTPases by cytotoxic necrotizing factor-1 elicit a controlled inflammatory response. *J Biol Chem.* 279:35849-35857.

Munro, P., and E. Lemichez. 2005. Bacterial toxins activating Rho GTPases. *Curr Top Microbiol Immunol.* 291:177-190.

Murga, C., M. Zohar, H. Teramoto, and J.S. Gutkind. 2002. Rac1 and RhoG promote cell survival by the activation of PI3K and Akt, independently of their ability to stimulate JNK and NF-kappaB. *Oncogene.* 21:207-216.

Mysorekar, I.U., M.A. Mulvey, S.J. Hultgren, and J.I. Gordon. 2002. Molecular regulation of urothelial renewal and host defenses during infection with uropathogenic Escherichia coli. *J Biol Chem.* 277:7412-7419.

Naumanen, P., P. Lappalainen, and P. Hotulainen. 2008. Mechanisms of actin stress fibre assembly. *J Microsc.* 231:446-454.

Nethe, M., and P.L. Hordijk. 2010. The role of ubiquitylation and degradation in RhoGTPase signalling. *J Cell Sci.* 123:4011-4018.

Nowicki, B., R. Selvarangan, and S. Nowicki. 2001. Family of Escherichia coli Dr adhesins: decay-accelerating factor receptor recognition and invasiveness. *J Infect Dis.* 183 Suppl 1:S24-27.

Olofsson, B. 1999. Rho guanine dissociation inhibitors: pivotal molecules in cellular signalling. *Cell Signal.* 11:545-554.

Orden, J.A., G. Dominguez-Bernal, S. Martinez-Pulgarin, M. Blanco, J.E. Blanco, A. Mora, J. Blanco, and R. de la Fuente. 2007. Necrotoxigenic Escherichia coli from sheep and goats produce a new type of cytotoxic necrotizing factor (CNF3) associated with the eae and ehxA genes. *Int Microbiol.* 10:47-55.

Oswald, E., and J. De Rycke. 1990. A single protein of 110 kDa is associated with the multinucleating and necrotizing activity coded by the Vir plasmid of Escherichia coli. *FEMS Microbiol Lett.* 56:279-284.

Parkkinen, J., J. Hacker, and T.K. Korhonen. 1991. Enhancement of tissue plasminogen activator-catalyzed plasminogen activation by Escherichia coli S fimbriae associated with neonatal septicaemia and meningitis. *Thromb Haemost.* 65:483-486.

Patel, J.C., and J.E. Galan. 2006. Differential activation and function of Rho GTPases during Salmonella-host cell interactions. *J Cell Biol.* 175:453-463.

Pellegrin, S., and H. Mellor. 2007. Actin stress fibres. *J Cell Sci.* 120:3491-3499.

Peng, J., B.J. Wallar, A. Flanders, P.J. Swiatek, and A.S. Alberts. 2003. Disruption of the Diaphanous-related formin Drf1 gene encoding mDia1 reveals a role for Drf3 as an effector for Cdc42. *Curr Biol.* 13:534-545.

Petkovsek, Z., K. Elersic, M. Gubina, D. Zgur-Bertok, and M. Starcic Erjavec. 2009. Virulence potential of Escherichia coli isolates from skin and soft tissue infections. *J Clin Microbiol.* 47:1811-1817.

Pop, M., K. Aktories, and G. Schmidt. 2004. Isotype-specific degradation of Rac activated by the cytotoxic necrotizing factor 1. *J Biol Chem.* 279:35840-35848.

Pouttu, R., T. Puustinen, R. Virkola, J. Hacker, P. Klemm, and T.K. Korhonen. 1999. Amino acid residue Ala-62 in the FimH fimbrial adhesin is critical for the adhesiveness of meningitis-associated Escherichia coli to collagens. *Mol Microbiol.* 31:1747-1757.

Prasadarao, N.V., C.A. Wass, J. Hacker, K. Jann, and K.S. Kim. 1993. Adhesion of S-fimbriated Escherichia coli to brain glycolipids mediated by sfaA gene-encoded protein of S-fimbriae. *J Biol Chem.* 268:10356-10363.

Prieto-Sanchez, R.M., I.M. Berenjeno, and X.R. Bustelo. 2006. Involvement of the Rho/Rac family member RhoG in caveolar endocytosis. *Oncogene.* 25:2961-2973

Remaut, H., C. Tang, N.S. Henderson, J.S. Pinkner, T. Wang, S.J. Hultgren, D.G. Thanassi, G. Waksman, and H. Li. 2008. Fiber formation across the bacterial outer membrane by the chaperone/usher pathway. *Cell.* 133:640-652.

Ridley, A.J., H.F. Paterson, C.L. Johnston, D. Diekmann, and A. Hall. 1992. The small GTP-binding protein rac regulates growth factor-induced membrane ruffling. *Cell.* 70:401-410.

Riento, K., and A.J. Ridley. 2003. Rocks: multifunctional kinases in cell behaviour. *Nat Rev Mol Cell Biol.* 4:446-456.

Rippere-Lampe, K.E., A.D. O'Brien, R. Conran, and H.A. Lockman. 2001. Mutation of the gene encoding cytotoxic necrotizing factor type 1 (cnf1) attenuates the virulence of uropathogenic Escherichia coli. *Infect Immun.* 69:3954-3964.

Roberts, J.A., B.I. Marklund, D. Ilver, D. Haslam, M.B. Kaack, G. Baskin, M. Louis, R. Mollby, J. Winberg, and S. Normark. 1994. The Gal(alpha 1-4)Gal-specific tip adhesin of Escherichia coli P-fimbriae is needed for pyelonephritis to occur in the normal urinary tract. *Proc Natl Acad Sci U S A.* 91:11889-11893.

Rolli-Derkinderen, M., G. Toumaniantz, P. Pacaud, and G. Loirand. 2010. RhoA phosphorylation induces Rac1 release from guanine dissociation inhibitor alpha and stimulation of vascular smooth muscle cell migration. *Mol Cell Biol.* 30:4786-4796.

Roppenser, B., A. Roder, M. Hentschke, K. Ruckdeschel, and M. Aepfelbacher. 2009. Yersinia enterocolitica differentially modulates RhoG activity in host cells. *J Cell Sci.* 122:696-705.

Rottner, K., and T.E. Stradal. 2011. Actin dynamics and turnover in cell motility. *Curr Opin Cell Biol.* 23:569-578.

Rubin, E.J., D.M. Gill, P. Boquet, and M.R. Popoff. 1988. Functional modification of a 21-kilodalton G protein when ADP-ribosylated by exoenzyme C3 of Clostridium botulinum. *Mol Cell Biol.* 8:418-426.

Russo, T.A., A. Stapleton, S. Wenderoth, T.M. Hooton, and W.E. Stamm. 1995. Chromosomal restriction fragment length polymorphism analysis of Escherichia coli strains causing recurrent urinary tract infections in young women. *J Infect Dis.* 172:440-445.

Samson, T., C. Welch, E. Monaghan-Benson, K.M. Hahn, and K. Burridge. 2010. Endogenous RhoG is rapidly activated after epidermal growth factor stimulation through multiple guanine-nucleotide exchange factors. *Mol Biol Cell.* 21:1629-1642.

Sander, E.E., J.P. ten Klooster, S. van Delft, R.A. van der Kammen, and J.G. Collard. 1999. Rac downregulates Rho activity: reciprocal balance between both GTPases determines cellular morphology and migratory behavior. *J Cell Biol.* 147:1009-1022.

Sander, E.E., S. van Delft, J.P. ten Klooster, T. Reid, R.A. van der Kammen, F. Michiels, and J.G. Collard. 1998. Matrix-dependent Tiam1/Rac signaling in epithelial cells promotes either cell-cell adhesion or cell migration and is regulated by phosphatidylinositol 3-kinase. *J Cell Biol.* 143:1385-1398.

Scheffzek, K., M.R. Ahmadian, and A. Wittinghofer. 1998. GTPase-activating proteins: helping hands to complement an active site. *Trends Biochem Sci.* 23:257-262.

Schilling, J.D., S.M. Martin, C.S. Hung, R.G. Lorenz, and S.J. Hultgren. 2003. Toll-like receptor 4 on stromal and hematopoietic cells mediates innate resistance to uropathogenic Escherichia coli. *Proc Natl Acad Sci U S A.* 100:4203-4208.

Schilling, J.D., M.A. Mulvey, C.D. Vincent, R.G. Lorenz, and S.J. Hultgren. 2001. Bacterial invasion augments epithelial cytokine responses to Escherichia coli through a lipopolysaccharide-dependent mechanism. *J Immunol.* 166:1148-1155.

Schlegel, N., M. Meir, V. Spindler, C.T. Germer, and J. Waschke. 2011. Differential role of Rho GTPases in intestinal epithelial barrier regulation in vitro. *J Cell Physiol.* 226:1196-1203.

Schmidt, G., P. Sehr, M. Wilm, J. Selzer, M. Mann, and K. Aktories. 1997. Gln 63 of Rho is deamidated by Escherichia coli cytotoxic necrotizing factor-1. *Nature.* 387:725-729.

Schwartz, M. 2004. Rho signalling at a glance. *J Cell Sci.* 117:5457-5458.

Sehr, P., G. Joseph, H. Genth, I. Just, E. Pick, and K. Aktories. 1998. Glucosylation and ADP ribosylation of rho proteins: effects on nucleotide binding, GTPase activity, and effector coupling. *Biochemistry.* 37:5296-5304.

Shin, S., and K.S. Kim. 2006. RhoA and Rac1 contribute to type III group B streptococcal invasion of human brain microvascular endothelial cells. *Biochem Biophys Res Commun.* 345:538-542.

Silva, J.C., R. Denny, C.A. Dorschel, M. Gorenstein, I.J. Kass, G.Z. Li, T. McKenna, M.J. Nold, K. Richardson, P. Young, and S. Geromanos. 2005. Quantitative proteomic analysis by accurate mass retention time pairs. *Anal Chem.* 77:2187-2200.

Skaar, E.P. 2010. The battle for iron between bacterial pathogens and their vertebrate hosts. *PLoS Pathog.* 6:e1000949.

Small, J.V., T. Stradal, E. Vignal, and K. Rottner. 2002. The lamellipodium: where motility begins. *Trends Cell Biol.* 12:112-120.

Smith, Y.C., K.K. Grande, S.B. Rasmussen, and A.D. O'Brien. 2006. Novel three-dimensional organoid model for evaluation of the interaction of uropathogenic Escherichia coli with terminally differentiated human urothelial cells. *Infect Immun.* 74:750-757.

Snyder, J.A., B.J. Haugen, C.V. Lockatell, N. Maroncle, E.C. Hagan, D.E. Johnson, R.A. Welch, and H.L. Mobley. 2005. Coordinate expression of fimbriae in uropathogenic Escherichia coli. *Infect Immun.* 73:7588-7596.

Sokurenko, E.V., H.S. Courtney, S.N. Abraham, P. Klemm, and D.L. Hasty. 1992. Functional heterogeneity of type 1 fimbriae of Escherichia coli. *Infect Immun.* 60:4709-4719.

Stebbins, C.E., and J.E. Galan. 2000. Modulation of host signaling by a bacterial mimic: structure of the Salmonella effector SptP bound to Rac1. *Mol Cell.* 6:1449-1460.

Steffen, A., M. Ladwein, G.A. Dimchev, A. Hein, L. Schwenkmezger, S. Arens, K.I. Ladwein, J.M. Holleboom, F. Schur, J.V. Small, J. Schwarz, R. Gerhard, J. Faix, T.E. Stradal, C. Brakebusch, and K. Rottner. 2013. Rac function is critical for cell migration but not required for spreading and focal adhesion formation. *J Cell Sci.*

Stradal, T.E., and G. Scita. 2006. Protein complexes regulating Arp2/3-mediated actin assembly. *Curr Opin Cell Biol.* 18:4-10.

Suetsugu, S., D. Yamazaki, S. Kurisu, and T. Takenawa. 2003. Differential roles of WAVE1 and WAVE2 in dorsal and peripheral ruffle formation for fibroblast cell migration. *Dev Cell.* 5:595-609.

Tkachenko, E., M. Sabouri-Ghomi, O. Pertz, C. Kim, E. Gutierrez, M. Machacek, A. Groisman, G. Danuser, and M.H. Ginsberg. 2011. Protein kinase A governs a RhoA-RhoGDI protrusion-retraction pacemaker in migrating cells. *Nat Cell Biol.* 13:660-667.

Torrino, S., O. Visvikis, A. Doye, L. Boyer, C. Stefani, P. Munro, J. Bertoglio, G. Gacon, A. Mettouchi, and E. Lemichez. 2011. The E3 ubiquitin-ligase HACE1 catalyzes the ubiquitylation of active Rac1. *Dev Cell.* 21:959-965.

Tsuji, T., T. Ishizaki, M. Okamoto, C. Higashida, K. Kimura, T. Furuyashiki, Y. Arakawa, R.B. Birge, T. Nakamoto, H. Hirai, and S. Narumiya. 2002. ROCK and mDia1 antagonize in Rho-dependent Rac activation in Swiss 3T3 fibroblasts. *J Cell Biol.* 157:819-830.

Tzircotis, G., V.M. Braga, and E. Caron. 2011. RhoG is required for both FcgammaR- and CR3-mediated phagocytosis. *J Cell Sci.* 124:2897-2902.

Valencia, A., P. Chardin, A. Wittinghofer, and C. Sander. 1991. The ras protein family: evolutionary tree and role of conserved amino acids. *Biochemistry.* 30:4637-4648.

Valore, E.V., C.H. Park, A.J. Quayle, K.R. Wiles, P.B. McCray, Jr., and T. Ganz. 1998. Human beta-defensin-1: an antimicrobial peptide of urogenital tissues. *J Clin Invest.* 101:1633-1642.

van Buul, J.D., M.J. Allingham, T. Samson, J. Meller, E. Boulter, R. Garcia-Mata, and K. Burridge. 2007. RhoG regulates endothelial apical cup assembly downstream from ICAM1 engagement and is involved in leukocyte trans-endothelial migration. *J Cell Biol.* 178:1279-1293.

Vetter, I.R., and A. Wittinghofer. 2001. The guanine nucleotide-binding switch in three dimensions. *Science.* 294:1299-1304.

Vignal, E., A. Blangy, M. Martin, C. Gauthier-Rouviere, and P. Fort. 2001. Kinectin is a key effector of RhoG microtubule-dependent cellular activity. *Mol Cell Biol.* 21:8022-8034.

Vigorito, E., S. Bell, B.J. Hebeis, H. Reynolds, S. McAdam, P.C. Emson, A. McKenzie, and M. Turner. 2004. Immunological function in mice lacking the Rac-related GTPase RhoG. *Mol Cell Biol.* 24:719-729.

Vincent, S., P. Jeanteur, and P. Fort. 1992. Growth-regulated expression of rhoG, a new member of the ras homolog gene family. *Mol Cell Biol.* 12:3138-3148.

Visvikis, O., L. Boyer, S. Torrino, A. Doye, M. Lemonnier, P. Lores, M. Rolando, G. Flatau, A. Mettouchi, D. Bouvard, E. Veiga, G. Gacon, P. Cossart, and E. Lemichez. 2011. Escherichia coli producing CNF1 toxin hijacks Tollip to trigger Rac1-dependent cell invasion. *Traffic.* 12:579-590.

Visvikis, O., M.P. Maddugoda, and E. Lemichez. 2010. Direct modifications of Rho proteins: deconstructing GTPase regulation. *Biol Cell.* 102:377-389.

Wang, H.R., Y. Zhang, B. Ozdamar, A.A. Ogunjimi, E. Alexandrova, G.H. Thomsen, and J.L. Wrana. 2003. Regulation of cell polarity and protrusion formation by targeting RhoA for degradation. *Science.* 302:1775-1779.

Wasmeier, C., M. Romao, L. Plowright, D.C. Bennett, G. Raposo, and M.C. Seabra. 2006. Rab38 and Rab32 control post-Golgi trafficking of melanogenic enzymes. *J Cell Biol.* 175:271-281.

Watarai, M., I. Derre, J. Kirby, J.D. Growney, W.F. Dietrich, and R.R. Isberg. 2001. Legionella pneumophila is internalized by a macropinocytotic uptake pathway controlled by the Dot/Icm system and the mouse Lgn1 locus. *J Exp Med.* 194:1081-1096.

Weissman, A.M. 2001. Themes and variations on ubiquitylation. *Nat Rev Mol Cell Biol.* 2:169-178.

Wennerberg, K., S.M. Ellerbroek, R.Y. Liu, A.E. Karnoub, K. Burridge, and C.J. Der. 2002. RhoG signals in parallel with Rac1 and Cdc42. *J Biol Chem.* 277:47810-47817.

Wennerberg, K., K.L. Rossman, and C.J. Der. 2005. The Ras superfamily at a glance. *J Cell Sci.* 118:843-846.

Whitmore, L., and B.A. Wallace. 2008. Protein secondary structure analyses from circular dichroism spectroscopy: methods and reference databases. *Biopolymers.* 89:392-400.

Wiles, T.J., B.K. Dhakal, D.S. Eto, and M.A. Mulvey. 2008. Inactivation of host Akt/protein kinase B signaling by bacterial pore-forming toxins. *Mol Biol Cell.* 19:1427-1438.

Wiles, T.J., R.R. Kulesus, and M.A. Mulvey. 2008. Origins and virulence mechanisms of uropathogenic Escherichia coli. *Exp Mol Pathol.* 85:11-19.

Wolters, M., E.C. Boyle, K. Lardong, K. Trulzsch, A. Steffen, K. Rottner, K. Ruckdeschel, and M. Aepfelbacher. 2013. Cytotoxic necrotizing factor-y boosts yersinia effector translocation by activating rac protein. *J Biol Chem.* 288:23543-23553.

Worby, C.A., S. Mattoo, R.P. Kruger, L.B. Corbeil, A. Koller, J.C. Mendez, B. Zekarias, C. Lazar, and J.E. Dixon. 2009. The fic domain: regulation of cell signaling by adenylylation. *Mol Cell.* 34:93-103.

Xiao, B., Z. Liu, B.S. Li, B. Tang, W. Li, G. Guo, Y. Shi, F. Wang, Y. Wu, W.D. Tong, H. Guo, X.H. Mao, and Q.M. Zou. 2009. Induction of microRNA-155 during Helicobacter pylori infection and its negative regulatory role in the inflammatory response. *J Infect Dis.* 200:916-925.

Yamaki, N., M. Negishi, and H. Katoh. 2007. RhoG regulates anoikis through a phosphatidylinositol 3-kinase-dependent mechanism. *Exp Cell Res.* 313:2821-2832.

Yamamoto, M., H.H. Wu, H. Momose, A. Rademaker, and R. Oyasu. 1992. Marked enhancement of rat urinary bladder carcinogenesis by heat-killed Escherichia coli. *Cancer Res.* 52:5329-5333.

Yarbrough, M.L., Y. Li, L.N. Kinch, N.V. Grishin, H.L. Ball, and K. Orth. 2009. AMPylation of Rho GTPases by Vibrio VopS disrupts effector binding and downstream signaling. *Science.* 323:269-272.

Yu, H., and K.S. Kim. 2010. Ferredoxin is involved in secretion of cytotoxic necrotizing factor 1 across the cytoplasmic membrane in Escherichia coli K1. *Infect Immun.* 78:838-844.

Zhang, D., G. Zhang, M.S. Hayden, M.B. Greenblatt, C. Bussey, R.A. Flavell, and S. Ghosh. 2004. A toll-like receptor that prevents infection by uropathogenic bacteria. *Science.* 303:1522-1526.

Zhou, G., W.J. Mo, P. Sebbel, G. Min, T.A. Neubert, R. Glockshuber, X.R. Wu, T.T. Sun, and X.P. Kong.

2001. Uroplakin Ia is the urothelial receptor for uropathogenic Escherichia coli: evidence from in vitro FimH binding. *J Cell Sci.* 114:4095-4103.

Declaration

I hereby declare, on oath, that I have written the present dissertation by my own and have not used other than the acknowledged resources and aids.

Hamburg, June 2014